Aus der Klinik für Kardiologie, Pneumologie und Angiologie
der Heinrich-Heine-Universität Düsseldorf
Univ.-Prof. Dr. med. Malte Kelm

eNOS Signaling Pathway in Red Blood Cells Contributes to Deformability and ATP Release

Dissertation

zur Erlangung des Grades eines Doktors der Medizin
der Medizinischen Fakultät der Heinrich-Heine-Universität Düsseldorf

vorgelegt von

Maximilian Johannes Ziegler

aus Nürnberg, Deutschland

Düsseldorf, September 2017

Als Inauguraldissertation gedruckt mit der Genehmigung der

medizinischen Fakultät der Heinrich-Heine-Universität Düsseldorf

gez.:

Dekan: Herr Univ.-Prof. Dr. med. Nikolaj Klöcker

Erstgutachterin: Frau Prof. Dr. rer. nat. Dr. Cortese-Krott

Zweitgutachter: Herr Prof. Dr. rer. nat. Suschek

This dissertation I dedicate to my mother

who made me who I am

and who always supported me.

Abstract

Background The development and progression of cardiovascular diseases is correlated to endothelial dysfunction. Decreased nitric oxide (NO) bioavailability is considered to be both a characteristic and a cause of endothelial dysfunction. NO is produced by a group of NO synthases (NOS). Recently it was shown that red blood cells (RBCs) carry an active endothelial NOS (eNOS), which contributes to the vasculature´s NO pool. In patients who suffer from endothelial dysfunction the activity of RBC-eNOS is significantly impaired compared to healthy controls. The exact role of RBC-eNOS remains uncertain.

Aims The aim of this work is to identify soluble guanylate cyclase (sGC) and protein kinase G1 (PRKG1) in mature human RBCs. Both proteins are part of the eNOS signaling pathway, which is known from the vasculature. Additionally the work investigates the function of sGC and PRKG1 with regard to RBC deformability and influence on pannexin 1 (pnx1), which is an adenosine triphosphate (ATP) gating channel in RBCs.

Methods The detection of sGC and PRKG1 in RBCs was performed using western blot analyses. Western blot analyses were also used to investigate the influence of coronary artery disease (CAD) and hypertension on protein quantities in RBCs. Measurement of PRKG1 activity in RBCs was assessed by an enzyme-linked immunosorband assay (ELISA). Deformability was analyzed by Laser assisted optical rotational red cell analyzer (LORRCA) at different levels of shear stress. The influence of eNOS, sGC and PRKG1 on deformability was assessed as elongation index (EI) after different treatments. A combination of flowcytometric and ectacytometric analyses has been established to investigate the influence of deformation on RBC-eNOS activity. Flowcytometric measurements were established to elucidate the role of eNOS signaling with regard to pnx1.

Results Western blot results show that mature human RBCs carry a sGC and PRKG1. The analysis of protein quantities does not reveal significant differences between healthy test persons and patients who suffer from CAD and hypertension. ELISA reveals that an active PRKG can be found in RBCs. The results of ectacytometric measurements show that activation of the eNOS/ sGC/ PRKG1-signaling cascade in RBCs with SperNO and 8-bromo-cGMP significantly contributes to improved deformability. In contrast inhibition with DT2 and ODQ significantly decreases the ability of RBCs to deform. Flowcytometric measurements adduce evidence that eNOS/ sGC/ PRKG1-signaling is involved in the regulation of pnx1 in RBCs. Carbenoxolone, which is an inhibitor of pnx1, significantly increases the fluorescent signal within RBCs. Inhibition of NOS and PRKG1 mimic the effect of carbenoxolone. The treatment of RBCs with 8-bromo-cGMP significantly decreases the fluorescent signals within RBCs in a dose dependent manner.

Summary The present work reveals that adult, human RBCs carry a sGC and a PRKG1. Both proteins are an integral part of the eNOS signaling cascade within RBCs. They significantly contribute to deformability at low levels of shear stress. Furthermore results presented here provide evidence that eNOS signaling is involved in the regulation of pnx1 in RBCs.

Zusammenfassung

Hintergrund Die Entwicklung und das Voranschreiten kardiovaskulärer Erkrankungen stehen mit endothelialer Dysfunktion in Verbindung. Herabgesetzte Bioverfügbarkeit von Stickstoffmonoxid (NO) wird sowohl als Auslöser als auch Charakteristikum endothelialer Dysfunktion angesehen. Kürzlich konnte gezeigt werden, dass Erythrozyten eine aktive endotheliale NO-Synthase (eNOS) besitzen. Diese trägt zum vaskulären NO-Pool bei. Bei Patienten, die unter endothelialer Dysfunktion leiden, ist die Funktion der erythrozytären eNOS signifikant eingeschränkt. Die exakte Rolle der eNOS in Erythrozyten ist unklar.
Ziel Das Ziel dieser Arbeit besteht darin, *soluble guanylate cyclase* (sGC) und *protein kinase G1* (PRKG1) in adulten, humanen Erythrozyten zu identifizieren. Beide Proteine sind Bestandteil der eNOS Signalkaskade, die aus dem Gefäßsystem bekannt ist. Zusätzlich untersucht die Arbeit die Funktion von sGC und PRKG1 im Hinblick auf Verformbarkeit und Einfluss auf Pannexin 1 Kanäle (Pnx1) in Erythrozyten, die Adenosintriphosphat (ATP)-Freisetzung erlauben.
Methoden Die Identifizierung der Proteine erfolgt mittels *Western Blot* Analysen. Die Auswirkung kardiovaskulärer Erkrankung und Hypertonie auf den Proteingehalt von Erythrozyten wird ebenfalls mittels *Western Blot* untersucht. Die Messung der PRKG1 Aktivität wurde mittels *enzyme-linked immunosorband assay* (ELISA) durchgeführt. Bei verschiedenen Scherkräften wurde die Deformierbarkeit von Erythrozyten mit einem Ektazytometer gemessen. Der Einfluss von sGC und PRKG1 auf erythrozytäre Verformbarkeit wurde als Elongationsindex (EI) nach verschiedenen Behandlungen untersucht. Eine Kombination aus Durchfluss- und Ektazytometrie wurde etabliert, um den Einfluss erythrozytärer Verformung auf eNOS-Aktivierung zu untersuchen. Eine weitere durchflusszytometrische Methodik wurde etabliert, um die Rolle der eNOS-Signalkaskade mit Blick auf Pnx1 zu klären.
Ergebnisse Die Western Blot Ergebnisse zeigen, dass adulte, humane Erythrozyten eine sGC und PRKG1 tragen. Die Analyse der Proteinmengen zwischen gesunden Testpersonen und Patienten, die unter koronarer Herzerkrankung (KHK) und Hypertonie leiden, weisen keine signifikanten Unterschiede auf. Die Ergebnisse der ELISA ergeben, dass die PRKG in Erythrozyten aktiv ist. Ektazytometrische Messungen zeigen, dass die Aktivierung der eNOS/ sGC/ PRKG1-Signalkaskade mittels SperNO und 8-bromo cGMP die Verformbarkeit signifikant verbessert. Im Gegensatz dazu verringern die Inhibitoren DT2 und ODQ die Verformbarkeit signifikant. Durchflusszytometrische Messungen deuten darauf hin, dass eNOS, sGC und PRKG1 an der Regulation von Pnx1 beteiligt sind. Der Pnx1-Inhibitor Carbenoxolone verringert signifikant das Fluoreszenzsignal innerhalb von Erythrozyten. Inhibierung von NOS und PRKG1 führen ebenfalls zu signifikant erhöhter intrazellulärer Fluoreszenz. Die Behandlung von Erythrozyten mit 8-bromo-cGMP verringert dosisabhängig signifikant das Fluoreszenzsignal.
Zusammenfassung Die vorliegende Arbeit zeigt, dass reife, humane Erythrozyten eine sGC und eine PRKG1 tragen. Beide Proteine sind fester Bestandteil der eNOS-Signalkaskade innerhalb von Erythrozyten. Sie führen zu einer signifikanten Steigerung der Verformbarkeit bei niedrigem Scherstress. Zusätzlich zeigen die Ergebnisse dieser Arbeit erstmals, dass die eNOS-Signalkaskade an der Regulation von Pnx1 beteiligt ist.

Abbreviation panel

Ab	Antibody
AC	Adenylate cyclase
ATP	Adenosine triphosphate
BD	Becton, Dickinson biosciences
BH4	Tetrahydrobiopterin
BKcs	Big potassium channels
BSA	Bovine serum albumin
CAD	Coronary artery disease
cAMP	3',5'-Cyclic adenosine monophosphate
CF-DA	Carboxyfluorescein diacetate
CFTR	Cystic fibrosis transmembrane regulator
cGMP	3′,5′-Cyclic guanosine monophosphate
CNX	Connexin
CO	Carbon monoxide
CTRL	Control
DAF-FM-DA	4-Amino-5-methylamino-2,7-difluorescein-diacetate
DT2	DT2-trifluoracetate salt
FhlA	Formate hydrogen lyase activator (transcriptional factor)
EI	Elongation index
ELISA	Enzyme linked immunosorband assay
eNOS	Endothelial NO synthase
FACS	fluorescence-activated cell sorting
G	Gravitational force
Gi	Inhibitory subunit of guanosine binding protein
Gs	Stimulating subunit of guanosine binding protein

GTP	Guanosine triphosphate
HRP	Horse radish peroxidase
IP	Immunoprecipitation
IU	International unit
kDa	Kilo dalton
KO	Knock out
L-Arg	L-Arginine
LC MS	Liquid chromatography-mass spectrometry
LDL	Low density lipoprotein
LDS	Lithium dodecyl sulfate
L-NAME	N^G-Nitro-L-arginine-methyl ester. HCl
LORRCA	Laser optimized rotational red cell analyzer
MI	Myocardial infarction
MLCK	Myosin light chain kinase
NaCl	Sodium chloride
NADP	Nicotinamide adenine dinucleotide phosphate
NO	Nitric oxide
O_2	Oxygen
ODQ	1H-[1,2,4]oxadiazolo[4,3-a] quinoxalin-1-one
PBS	Phosphate buffer saline
PDE	Phosphodiesterase
Pnx	Pannexin
PRKG	cGMP dependent protein kinase
PSS	Physiological salt solution
PVP	Polyvinylpyrrolidone
RBC	Red blood cell
RIPA Buffer	Radio immunoprecipitation assay buffer
ROS	Reactive oxygen species

SD	Standard deviation
SDS PAGE	Sodium dodecyl polyacrylamite gel electrophoresis
sGC	Soluble guanylate cyclase
SMC	Smooth muscle cells
SperNO	Spermine NONOate
TA	Tris acetate
TBS	Tris buffer saline
VSMC	Vascular smooth muscle cells
WHO	World health organization

Contents

Figure index

Table index

1 Introduction

1.1 Cardiovascular disease and endothelial dysfunction

The term cardiovascular disease describes a variety of diseases, such as coronary artery disease (CAD), cerebrovascular disease or peripheral arterial occlusive disease. Myocardial infarction (MI) and strokes can be taken as most severe and acute results of cardiovascular disease. The global status report on noncommunicable diseases from 2014 revealed that cardiovascular disease caused 17.5 million deaths (WHO, 2014). This makes cardiovascular disease responsible for 46% of deaths amongst noncommunicable diseases. By 2030 the estimated number of cardiovascular disease related deaths is going to rise up to 52 million (WHO, 2010).

The key trigger for cardiovascular disease is arteriosclerosis. It describes the affection of the arterial vascular system. In the progress of arteriosclerosis lipids, connective tissue and calcium are being stored in the artery wall. This causes thickening of the artery wall and at final stages might occlude the concerning vessels. An enduring imbalance in endothelial homeostasis, which can be referred to as endothelial dysfunction induces or aggravates an existing arteriosclerosis. It results in impaired regulation of vascular tone, platelet activity, leukocyte adhesion and angiogenesis (Chen and Walterscheid, 2006). Reasons for this imbalance are turbulent blood flow (Prado et al., 2008), increased free radicals that occur during cigarette smoking (Michael Pittilo, 2000), hypertension and diabetes mellitus (Sowers et al., 2001), elevated and modified low density lipoproteins (LDL) (Mitra et al., 2011) and elevated plasma homocysteine concentrations (Boers, 2000; Wierzbicki, 2007).

In all of these events nitric oxide (NO) and its bioavailability in vasculature plays an important role. Studies revealed a positive correlation between endothelial dysfunction and impaired NO/ cyclic guanosine monophosphate (cGMP) signaling (Heiss et al., 2006; Evgenov et al., 2006; Neunteufl et al., 2000; Schächinger et al., 2000). In vasculature NO, a short lived radical gas, is produced by endothelial nitric oxide synthase (eNOS). Already prior to macroscopic or even microscopic structural changes of vasculature, impaired NO signaling in endothelium can be observed (Napoli and Ignarro, 2009). Accordingly our group revealed a lower

concentration of eNOS in RBCs and microparticles in patients who suffer from endothelial dysfunction (Cortese-Krott et al., 2012b; Horn et al., 2013).

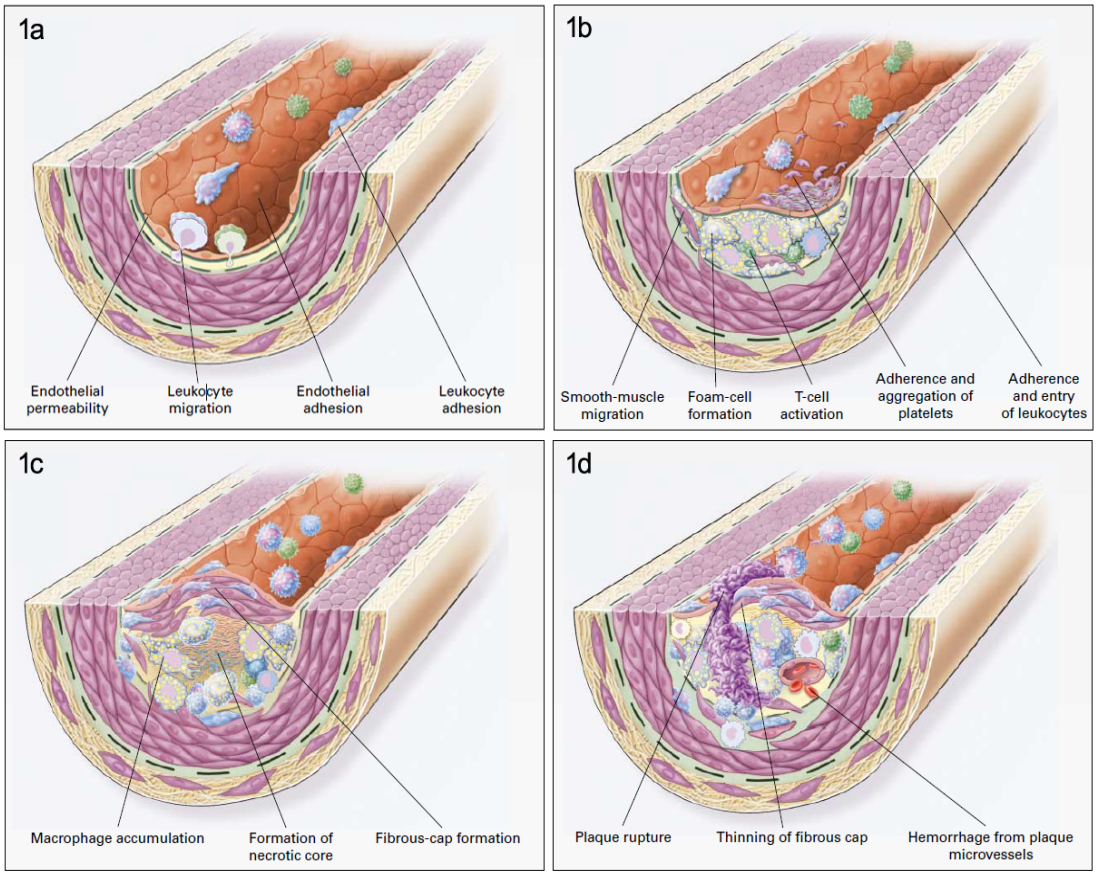

Figure 1: Development of arteriosclerosis (Ross et al., 1999)

The image illustrates the progress of arteriosclerosis. Impaired NO-homeostasis is thought to cause increased epithelial permeability and adhesion of leucocytes and platelets. In the progress of arteriosclerosis cytokines and growth factors cause the diapedesis of more defending cells, which form fatty streaks and later arteriosclerotic plaques. Rising pressure within the plaque might cause rupture and occlusion of the vessel.

In the course of arteriosclerotic development impaired NO bioavailability is followed by different steps of pathophysiological remodeling. In general these adaptations can be described as chronic artery inflammation. First microscopic changes that can be observed are increased vascular permeability and increased adherence of platelets and leukocytes to the endothelial wall (Springer and Cybulsky, 1995; Fig. 1). Increased permeability is likely to be caused by an altered intercellular communication and lack of gap junction proteins like connexin 40 (cnx40) and cnx43. (Chadjichristos et al., 2010; Saliez et al., 2008). Adhesion of leukocytes and platelets is provoked by cytokines and ends up in the formation of

fatty streaks, which initially consist of lipid-laden monocytes and macrophages (Fig. 1). Growth factors released by platelets stimulate the proliferation of smooth muscle cells (Bornfeldt et al., 1994; Ross and Glomset, 1973). Ongoing release of growth factors and cytokines results in the progress from fatty streaks to intermediate and advanced lesions (Fig. 1).

These lesions tend to form a fibrotic cover that protects the lesion from the vascular lumen. Below the fibrotic cover a mixture of leukocytes, lipid, and debris might form a necrotic core. Continuing activation and diapedesis of macrophages below the stiff fibrotic cover causes a thinning and therefore instability of the whole fibrous plaque. In addition the release of proteolytic enzymes might cause bleeding into the plaque from vasa vasorum. Consequently the rising pressure aggravates the instability of the plaque. Rupture or ulceration of the fibrous plaque are the end points in this pathogenesis and can rapidly lead to thrombosis and occlusion of the vessel (Fig. 1). Depending on the location of a ruptured plaque CAD, cerebrovascular disease or peripheral arterial occlusive disease might occur.

1.2 eNOS/ sGC/ PRKG1 signaling

1.2.1 eNOS

NO is a short lived gas, which is critically involved in a variety of physiological and pathological processes (Moncada et al., 1991). It is produced by a protein family of NOS (EC number 1.14.13.39, Dioxygenase), which can be found in different tissues. Next to eNOS (Gene ID: 4846), inducible NOS (iNOS; Gene ID 4843) and neuronal NOS (nNOS; Gene ID 4842) are also part of this protein family. All NOS are encoded by different genes on different chromosomes.

As participant of the body's defense system iNOS produces large amounts of NO. iNOS can be found in macrophages and monocytes (Siedlar et al., 1999). nNOS is present in certain neurons where it takes part in neuronal signaling (Rothe et al., 2005).

In endothelial cells NO is produced in response to shear stress or receptor mediated. It targets the prosthetic heme group of soluble guanylate cyclase and increases the generation of cGMP by a 200 fold. cGMP activates protein kinase G1, which phosphorylates different target proteins. In vasculature eNOS/ sGC/

PRKG1 signaling is involved in relaxation of smooth muscle cells (SMCs; Ignarro et al., 1986), smooth muscle growth (Garg and Hassid, 1989), leukocyte adhesion (Kubes et al., 1991) and platelet aggregation.

eNOS is involved in the regulation of blood pressure and vasodilation (O W Griffith and Stuehr, 1995). It is expressed in endothelial cells (Palmer and Moncada, 1989) and the corpus cavernosum (Rajfer et al., 1992).

The presence of eNOS within RBCs has been shown by Cortese-Krott et al. in 2012. LC-MS/MS proofed that not only endothelial cells but also RBCs contain a functional type3 isoform of eNOS (Cortese-Krott et al., 2012b). RBC-eNOS consistently forms NO and citrulline from L-arginine and molecular oxygen (O_2) (Chen and Mehta, 1998). Proper formation of NO requires the presence of L-Arginin, tetrahydrobiopterin (BH_4) and Ca^{2+} (Heinzel et al., 1992; Vasquez-Vivar et al., 1998, Knowles et al., 1989).

The effects of NO on RBCs include the regulation of lifespan and deformability (Kleinbongard et al., 2006; Horn et al., 2011). Additionally NO formation within RBCs inhibits platelet aggregation and effect velocity and blood flow, which gave new insides into blood homeostasis (Chen and Mehta, 1998; Kleinbongard et al., 2006).

In endothelium eNOS can be activated by shear forces created by the blood stream across the surface of endothelial cells. Ulker et al. suggested a similar activation of eNOS within RBCs. They reported about an increased activation of RBC-eNOS at low levels of shear stress ranging from 0.013Pa to 0.1Pa (Ulker et al., 2011). Depending on the bloods viscosity and shear rates different shear stresses can be found in vasculature. Physiological shear rates in vasculature range from 130 s^{-1} in the descending aorta, to 1250 s^{-1} in capillaries and 8000 s^{-1} in arterioles (Vennemann et al., 2007, Papaioannou and Stefanadis, 2005). According to data by Lipowsky et al. those shear rates lead to shear stresses between 0.1 and 5.5 Pa (Fig. 2). The highest shear stress can be found in the smallest vessels, which demand strongest deformation from RBCs. The activation of RBC-eNOS due to higher shear stress, which can be found in arterioles and capillaries, still needs to be enlightened.

Additionally it is uncertain whether RBC-eNOS is involved in intracellular signaling of RBCs. sGC, PRKG 1 and phosphodiesterase 5 (PDE5) are possible candidates

that might subsequently be induced by an active RBC-eNOS. Yet the presence of sGC and PRKG1 has not been illustrated in mature human RBCs.

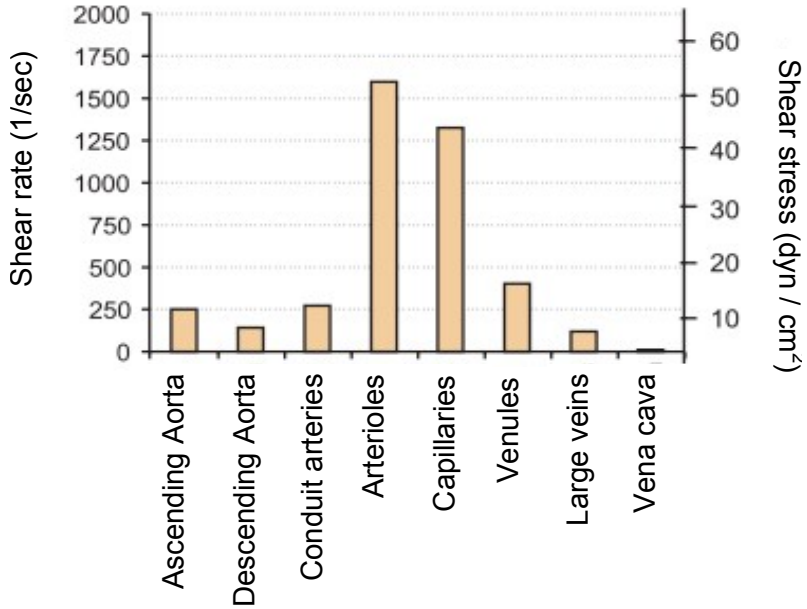

Figure 2: Shear stress values with regard to shear rates in different vessels

The image by Papaionnou and Stefanadis with data from Lipowksy et al. demonstrates the relationship between physiological shear rates and shear stress in different vessels. Shear stress ranges from 0.1 Pa to about 5.5 Pa. Highest shear stress can be found in arterioles and capillaries (Papaioannou and Stefanadis, 2005, Lipowsky et al., 1978, Lipowsky et al., 1980;
10 dyn/cm² = 1Pa).

1.2.2 sGC

sGC is an important component of cellular signaling. It is a key signal-transduction enzyme, which can be activated by NO (Arnold et al., 1977; Böhme et al., 1978; Schultz et al., 1977) and carbon monoxide (CO) (Ramos et al., 1989; Brüne and Ullrich, 1987; Brüne et al., 1990). It is typically composed of a large α-subunit and a small β-subunit forming a heterodimer. To this date four human sGC subunits have been identified: α_1, α_2, β_1 and β_2 (Zabel et al., 1998). A catalytically active sGC has only been found after heterodimer formation of an α- and a β- subunit (Winger and Marletta, 2005). The smaller β-subunit contains a prosthetic ferrous heme, which is crucial for activation of sGC (Stasch et al., 2011). Reduced iron

(Fe^{2+}) is the target of NO and causes a 200 fold activation of the catalytic domain (Ignarro et al., 1982). The loss or oxidation of iron (Fe^{3+}) in sGC results in the loss of sGC´s NO sensor and hence causes inactivation of the protein (Roy et al., 2008; Stasch et al., 2002; Schmidt et al., 2003). An active sGC produces cGMP from guanosine triphosphate (GTP) (Ignarro et al., 1982). cGMP is an important second messenger, which activates PRKG1. Additionally binding of cGMP to the GAF-A region of PDE5 causes a 10-15 fold activation of PDE5. In situations of increased levels of cGMP this feed forward mechanism regulates hydrolyses of cGMP.

Different pathophysiological states, like hypertension, heart failure, ischemic reperfusion or arteriosclerosis, are linked to increased levels of reactive oxygen species (ROS). ROS are likely to oxidize sGC. Consequently these diseases may disable NO-signaling (Fig. 3).

NO-signaling in endothelial and smooth muscle cells is well investigated. The description of an active RBC-eNOS in mature, human RBCs and the influence of NO on deformability and life span of RBCs bring up the thought of a NO-signaling pathway within RBCs. Yet the presence of sGC in mature human RBCs has not been illustrated.

Ikuta et al. have investigated the effects of NO and cGMP on erythroid progenitor cells during differentiation. The treatment of erythroid progenitor cells with NO and hydroxyurea causes increased levels of cGMP in erythroid progenitor cells. Furthermore they were able to show that cGMP levels influence the expression of gamma globin in erythroid progenitor cells and therefore underline the importance of sGC during erythropoiesis.

The same group also performed northern blot analyses on erythroid progenitor cells, which revealed the expression of alpha and beta subunits of sGC (Ikuta et al., 2001). The results of Ikuta et al. were performed on early stages of erythroid cells and demonstrate the presence of sGC by northern blot analyses. Since sGC can be found in erythroid progenitor cells it seems likely that mature human RBCs also carry a sGC. Conran et al. measured cGMP levels in mature RBCs from healthy individuals and in RBCs from patients who suffer from sickle cell disease. They detected increased levels of cGMP in the sickle cell group after incubation with 3-Isobutyl-1-methylxanthin (IBMX), which is a PDE inhibitor. (Conran et al., 2004). This result points towards the existence of a protein with a sGC like

function. The mere protein that produces cGMP in adult human RBCs has not yet been identified.

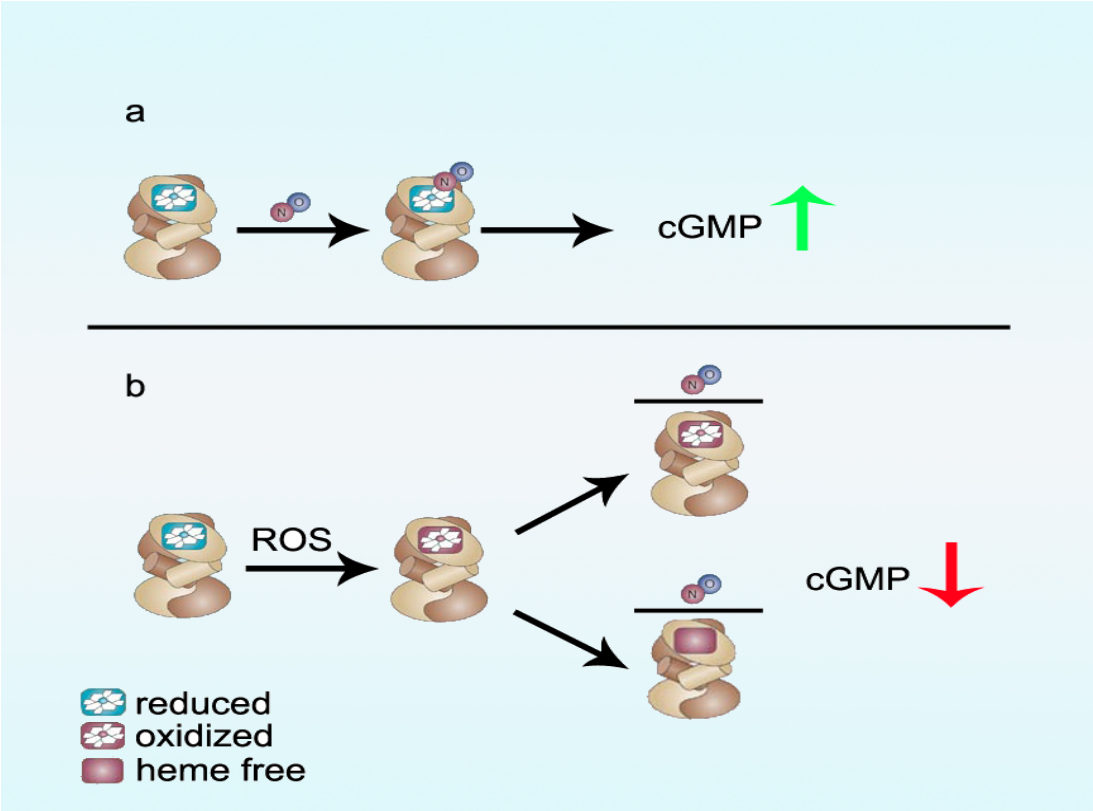

Figure 3: Effects of ROS on sGC functionality

The image (modified from Evgenov et al., 2006) illustrates different redox states of sGC. The first part of the image illustrates the normal state of sGC that can be found physiologically (a). The second part shows that increased levels of ROS can cause oxidation of heme in sGC. NO is not able to bind to oxidized heme. In addition oxidization loosens the binding between heme and sGC, which might cause the loss of heme. Both loss and oxidation of heme result in decreased levels of cGMP (b). Cyclic guanosine monophosphate = cGMP, reactive oxygen species = ROS, nitric oxide = NO)

1.2.3 PRKG1

PRKGs are important cell signaling kinases. They can be activated by cGMP, which is produced by sGC. Activation of PRKG ends up in phosphorylation of serines and threonines of different substrate proteins like ion channels or enzymes. In vasculature PRKG1 influences SMC relaxation. It also seems to be

involved in the generation of arteriosclerotic plaques and the growth of vascular SMCs within these plaques (Joshi et al., 2011).

In eukaryotes two genes have been identified that encode for PRKGs. One gene encodes for PRKG2, which is a particulate form of PRKG. It is bound to the cell membrane and has a molecular weight of around 85kDa. PRKG1 is a soluble enzyme, which can be found in the cytosol. It is composed of two identical subunits with three domains, which form a homodimer. The subunits have a molecular weight of 75kDa. Alternate splicing creates two isoforms of PRKG1, PRKG1 alpha and beta. Referring to the alpha splice variant, differences of both splice variants can only be found in amino acids 2-89 of the N-terminal domain (Tamura et al., 1996). The difference explains presumably their specificity for interaction with different target substrates. The differences may also explain a tenfold higher affinity of PRKG1 alpha to cGMP (Butt et al., 1993; Lee et al., 2011). The N-terminal domain is needed for homodimerization and autoinhibitory effects. The catalytic and regulatory domains of both subunits are identical. PRKG1 can be found in hippocampus, cerebellum, lung, platelets, aorta and heart (Tamura et al., 1996; Butt et al., 1993).

The function of PRKG1 on SMC relaxation is well examined. PRKG1 knock out (KO) mice response insufficiently to NO/ sodium nitroprusside (SNP) induced vasodilatation (Koeppen et al., 2004; Pfeifer et al., 1998; Sausbier et al., 2000). PRKG1 regulates SMC relaxation on different levels. It activates myosin light chain phosphatase (MLCP) (Wooldridge et al., 2004), which ends up in dephosphorylation of myosin light chains (MLC) and Ca^{2+}-independent SMC relaxation. PRKG1 also lowers intracellular Ca^{2+} levels. It lowers Ca^{2+} release from the sarcoplasmic reticulum and regulates big potassium channels (BKcs). This causes hyperpolarization by closing voltage dependent Ca^{2+} channels of the membrane (Sausbier et al., 2000; Robertson et al., 1993). Ca^{2+} is needed for the activation of myosin light chain kinase (MLCK) via calmodulin. The influence of PRKG1 makes it a possible target for medication concerning high or low blood pressure.

Similar to sGC, PRKG1 is an integral part of NO-signaling in vasculature. The presence of an active eNOS in adult RBCs also makes PRKG1 a possible target of eNOS-signaling within mature RBCs. Studies by different groups suggest that PRKG1 can also be found in erythroid progenitor cells and adult RBCs. Ikuta et al.

were able to give insight on the influence of cGMP on gene expression of K562B cells, which is a cell line representing an early stage of erythropoetic cells. In these erythroid progenitor cells high levels of bromo-cGMP influence the expression of gamma globin (Ikuta et al., 2001). cGMP effects the expression of gamma globin either directly or via activation of PRKG1. In 2008 Feil et al. compared PRKG1 KO mice to control animals with regard to RBC survival. They found that the number of RBCs, hematocrit and hemoglobin were significantly reduced in KO mice. Their analyses provide evidence that the reasons for these changes can be found within mature RBCs. Due to those results it seems reasonable that an active PRKG1 can be found in adult mice RBCs (Föller et al., 2008). The presence of PRKG1 in adult human RBCs still needs to be illustrated.

1.2.4 PDE5

PDEs belong to an enzymatic family of phosphohydrolases that until now include eleven different proteins. Inactivation of cyclic nucleotides is an equivalent function of all PDEs. Yet they differ in regulating modes, specificity for cyclic nucleotides and inhibitory stimuli and genetic loci (Bender and Beavo, 2006). PDE5 is an integral part of the eNOS/ sGC/ PRKG1 signaling pathway. It specifically catalyzes the hydrolysis of cyclic GMP to 5'GMP at low substrate concentrations and therefore is able to control cGMP levels in cells.

PDE5 has first been described in platelets (Coquil et al., 1980; Hamet and Coquil, 1978). Meanwhile PDE5 has for example been detected in the cerebellum, corpus cavernosum, SMCs and RBCs (Shimizu-Albergine et al., 2003, Ballard et al., 1998, Adderley et al., 2011, p. 5).

One gene encodes for PDE5. Due to posttranscriptional modification three different PDE5 isoforms can be found in humans (PDE5A1, PDE5A2, PDE5A3). PDE5A1 has a molecular weight of 99 kDa and consists of 875 aminoacids (AA). It contains a phosphorylation site, a catalytic domain and two GAF domains. GAF domains were first described in three different proteins, which they are named after. These proteins were c**G**MP-specific PDEs, **A**Cs and formate hydrogen lyase Activator (**F**hlA)**.** Binding of cGMP to GAF A results in a 9-11 fold increased activation of PDE5 (Rybalkin et al., 2003). This way PDE5 is involved in a feed forward mechanism initiated by sGC. The production of cGMP on the one hand

activates PRKG1 and on the other hand is involved in its own hydrolysis. Phosphorylation of PDE5 by PRKG near GAF A increases the bonding capacity of GAF A to cGMP (Francis et al., 2002). Although PRKG is likely to be the main kinase involved in phosphorylation of PDE5, PKA might also phosphorylate PDE5, which is bound to GAF A (Corbin et al., 2000).

As a member of the eNOS signaling pathway, PDE5 is an important regulator of muscle tone in SMCs. In this context PDE5 is the target of drugs used in the treatment for erectile dysfunction or pulmonary artery hypertension (Goldstein et al., 1998, Weimann et al., 2000). In 2011 Adderley et al. found that RBCs carry PDE5 and that PDE5 regulates cGMP levels in RBCs (Adderley et al., 2011). The function of PDE5 as a member of the eNOS/sGC/PRKG1-signaling pathway in mature human RBCs still remains uncertain.

1.3 Properties of RBCs

RBCs represent the largest cell population in blood. Adult RBCs evolve from myelopoetic stem cells in red bone marrow. Following a life cycle of around 120 days in circulation the spleen´s reticular system removes old and impaired RBCs from the blood. RBCs have a diameter of around 7.4 µm and a height of 2.5 µm at the thickest point. The shape of RBCs can be described as biconcave disk with a flattened center. This shape is established throughout the connection of lipid bilayer and a complex membrane skeleton. It allows RBCs to undergo strong cell deformation without destruction. Deformability is an important factor for the maintenance of physiological microcirculation.

The exchange of O_2, carbon dioxide (CO_2) and nutrients takes place in microcirculation. The microcirculatory system consists of distal arterioles, the capillary system and proximal venules. The diameter of capillaries is significantly smaller than the diameter of RBCs. Hence the proper ability to deform is crucial for the passage through capillaries and maintenance of microcirculation (Parthasarathi and Lipowsky, 1999, Lipowsky et al., 1993; Shiga et al., 1990). Impaired RBC deformability is closely linked to different diseases, such as diabetes, renal function loss and cardiovascular disease (McMillan et al., 1978, Brown et al., 2005, Keymel et al., 2011). Deformability of RBCs decisively

depends on intracellular viscosity (1), the cellular metabolic state (2) and membrane fluidity (3).

1] Intracellular viscosity depends on the cytoplasmatic concentration of hemoglobin. In humans the mean corpuscular hemoglobin concentration (MCHC) ranges between 32 and 36 g/dl. Hemoglobin concentrations above 37 g/dl induce a steep increase in viscosity and hinder the red cells to recover their normal cell shape after deformation (Evans et al., 1984).

2] The metabolic state of RBCs is another factor, which influences intracellular viscosity. Na-K-ATPases regulate the osmotic balance and hence cell volume and cytoplasmatic viscosity (Stengelin and Hoffman, 1997; Inaba and Maede, 1986; Koc et al., 2003). The cellular metabolic state also controls intracellular Ca^{2+} concentrations, which are essential for eNOS activity and affect RBC deformability (Alderton et al., 2001, Murakami et al., 1986, Oonishi et al., 1997).

3] Membrane properties arise from the composition of a lipid bilayer, which is connected to a two dimensional membrane skeleton (Fig. 4). It allows the cells to undergo large reversible deformations while still maintaining its physiological properties during its 120 days of lifetime in circulation.

The lipid bilayer is composed of symmetrically distributed proportions of cholesterol and asymmetrically distributed proportions of phospholipids between the inside and the outside lipid layer (Seigneuret and Devaux, 1984). This specific composition grants RBCs a certain membrane fluidity, which is needed for modulation of cell functions and rheological behavior (Chabanel et al., 1983). The loss of asymmetrically distribution of phospholipids and therefore loss of membrane fluidity seems to be involved in the aging and destruction process of RBCs in spleen´s reticuloendothelial system.

Reduced membrane fluidity of RBCs can be found in patients with essential hypertension. Tsuda et al. suggested that abnormal microviscosity of the cell membranes might contribute to blood pressure elevation. (K. Tsuda et al., 2000, Tsuda et al., 1987). In 2000 Tsuda et al. positively correlated membrane fluidity and NO bioavailability. Incubation of RBCs with S-nitroso-N-acetylpenicillamine (SNAP), a NO donor, significantly increases membrane fluidity. The influence of SNAP on membrane fluidity was the greatest in patients who suffer from primary hypertension (Kazushi Tsuda et al., 2000). This result indicates a lack of NO

bioavailability in patients who suffer from primary hypertension, which is being restored by NO-donators. Lately it has been reported that RBCs carry an active eNOS. Interestingly, 2012 Cortese-Krott et al. were able to reveal an impaired function of eNOS within RBCs of patients who suffer from CVD (Cortese-Krott et al., 2012b). Taken together, these results adduce evidence that intracellular derived NO plays an important role in the maintenance of RBC membrane fluidity. Yet the exact mechanisms of how NO influences membrane fluidity remain unclear.

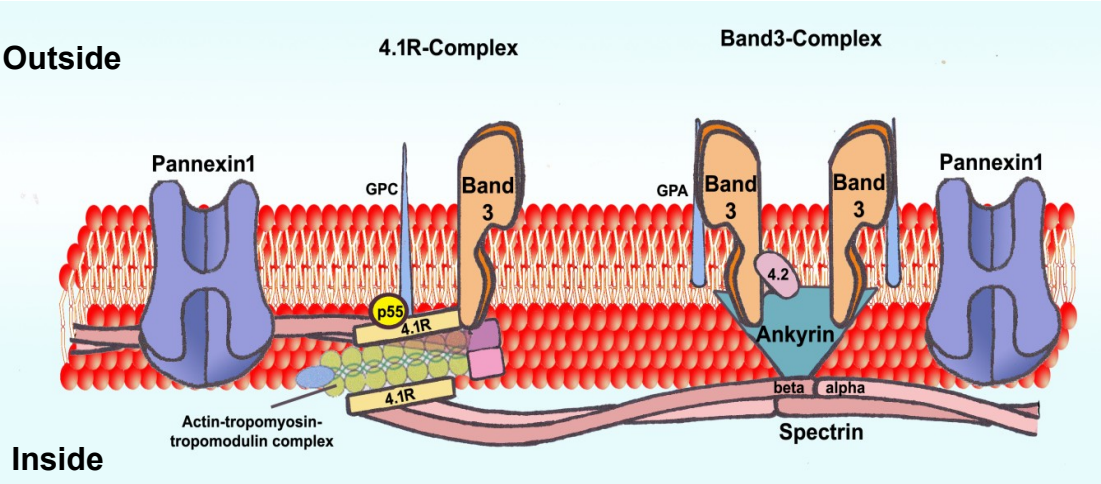

Figure 4: RBC membrane

Modified image by (Salomao et al., 2008). The image illustrates the cooperation between RBC lipid bilayer and membrane skeleton, which accords for RBCs unique mechanical properties. Pnx1, GPC, GPA and band3 are proteins that span through the membrane. Ankyrin and 4.1R connect the membrane skeleton to these membrane proteins. Pnx1 is an ATP conducting channel in RBCs. Red blood cell = RBC, pannexin 1 = pnx1, adenosine triphosphate = ATP, glycophorins A = GPA, glycophorins C =GPC.

The membrane composition is crossed by a number of transport and structural proteins like pnx1, band3 or glycophorins. Pnx1 is thought to be involved in ATP release while band3 and glycophorins are necessary for the connection of the lipid bilayer to the membrane skeleton. The membrane skeleton is a two dimensional layer of interconnecting structural proteins that span below the whole lipid bilayer. Spectrin, actin and protein 4.1R are most prominent in this network (Dort et al., 2001). The two components of the membrane are connected by bridging proteins like ankyrin or 4.1R (An et al., 2004; Rybicki et al., 1988; Fig. 4). Although both the

lipid bilayer and the membrane skeleton influence deformability, the physical properties of the membrane skeleton are believed to be the main parameter for elastic characteristics of the membrane (Shiga et al., 1990). Oonishi et al. suggested that intracellular Ca^{2+} and cAMP signaling ends up in phosphorylation of the membrane skeleton and that phosphorylation effects RBC filterability (Oonishi et al., 1997).

Especially spectrin determines the membrane skeleton´s role. Without structural damage spectrin can be expanded from 37 nm up to 200% of its original length or contract down to 40% (Byers and Branton, 1985; Lee et al., 1999; Evans and Celle, 1975). Spectrin contributes to elasticity of normal RBCs due to repeated amino acid sequences (Johnson et al., 2007). Hereditary, structural changes in the composition of the membrane skeleton, that can be found in spherocytosis, elliptocytosis or stomatocytosis, go along with a shortened half life of RBCs (Fukushima et al., 1990; Lux et al., 1990; Barcellini et al., 2011). Increased splenic sequestration due to reduced deformability accounts for these changes and goes along with splenomegaly.

The ability to deform in response to outer forces is not just a passive function of RBCs. Deformability measurement techniques allow the investigation of single RBCs or the investigation of rheological behavior of a whole red cell population. Single cell techniques include micropipette aspiration, atomic force microscopy or optical tweezers. Rheological observations can be performed with ectacytometers, filtration tests or microfluidic devices. The usage of laser optimized rotational red cell analyzer (LORRCA), an ectacytometer, is a commonly used and evaluated method for the analysis of RBC deformability. Investigations concerning RBCs revealed that a variety of stimuli can improve or worsen deformability.

Different groups were able to establish a link between NO bioavailability in RBCs and RBC deformability. Treatment of RBCs with a superoxide anion producing system decreases RBC deformability (Baskurt et al., 1998). Therefore, these results for the first time indicated that the loss of NO bioavailability causes a decrease in deformability (Baskurt et al., 1998). In 2003 Baskurt et al. used LORRCA to show that eNOS signaling effects RBC deformability. Treatment with a NO donor causes an increase in deformability. Inhibition of NOS with N omega-nitro-L-arginine (LNNA) and sGC with ODQ causes a decrease in RBC deformability (Bor-Kucukatay et al., 2003). This group also showed that chronic

inhibition of eNOS in rats causes a decrease in deformability and aggregation of RBCs (Bor-Kucukatay et al., 2000). These results gave new insight into intracellular homeostasis of RBCs.

In 2006 Kleinbongard et al. were able to provide new evidence for the presence of an active NO production within RBCs (Kleinbongard et al., 2006). The comparison of NO production within different blood cells reveals the highest NO production in monocytes, followed by neutrophile granulocytes, lymphocytes and RBCs. Yet RBCs represent bloods largest cell population and therefore the biggest source of NO in the circulation (Cortese-Krott et al., 2010). Paracrine secreted NO by RBCs might be sufficient to influence vascular tone (Baskurt et al., 2011). Bor-Kucukatay et al. investigated deformability of RBCs at 1.58Pa. The results reveal that administration of NG-Nitro-L-arginine-methyl ester HCl (L-NAME) and oxadiazolo-quinoxalin (ODQ) to RBCs decreases deformability significantly. Administration of NO-donors increases deformability at 1.58Pa (Bor-Kucukatay et al., 2003). In vasculature shear stress ranges from 0.1 Pa to about 5.5 Pa. Highest shear stress can be found in arterioles and capillaries (Papaioannou and Stefanadis, 2005, Lipowsky et al., 1978, Lipowsky et al., 1980) The influence of higher shear forces and the role of PRKG1 with regard to deformability of RBCs have not been investigated so far.

1.4 ATP release from RBCs

ATP is an important energy source and modulator of cell functions. In vasculature binding of ATP to P2Y receptors of endothelial cells results in smooth muscle relaxation (Buvinic et al., 2002, Ellsworth et al., 1995) and influences platelet aggregation (Birk et al., 2002). The ability to relax or exert tension is a crucial function of SMCs in vasculature. It allows the body to react to different physiological stresses by regulation of blood flow and blood pressure. This makes ATP an important regulator of vascular homeostasis.

Recently RBCs have been shown to be an important source of ATP in the vasculature. Different studies were able to show that RBCs carry large amounts of ATP and that ATP released by RBCs can be sufficient to interact with endothelial P2Y receptors (Ellsworth et al., 1995; Sprague et al., 2003).

Impaired ATP release from RBCs has been linked to primary pulmonary hypertension (PPH) and diabetes type 2, which is closely linked to an increased risk of arteriosclerosis.

In 2001 Sprague et al. postulated that impaired release of ATP causes an imbalance in NO signaling in the vasculature which leads to PPH. The lack of ATP release in patients who suffer from PPH causes an impaired relaxation of vessels in terminal vessels of the lung. This leads to increased vascular resistance and increased pulmonary blood pressure (Sprague et al., 2001b). The same group investigated ATP release from RBCs in patients who suffer from type 2 diabetes (DM2). Incubation of RBCs with mastopran, a stimulator of the inhibitory subunit of guanosine binding protein (Gi), causes an increase of ATP release from RBCs in healthy test persons. An impaired release of ATP from RBCs in response to mastopran can be observed in patients who suffer from DM2. The group also inversely correlated increased levels of HbA1c with decreased ATP release from RBCs (Sprague et al., 2006). High levels of HbA1c increase the risk of arteriosclerosis in vasculature. These findings may point towards an important role of ATP release from RBCs with regard to vascular homeostasis. Several groups have investigated the mechanisms contributing to ATP release from RBCs. Since ATP is a charged molecule, it cannot cross the cell membrane via concentration induced diffusion. Subsequently RBCs need to posses transport mechanisms or channels that enable ATP release. In general, candidates for ATP release from cells are vesicular transport, cystic fibrosis transmembrane conductance regulator (CFTR), cnx and pnx. Vesicular ATP release from cells is well documented (Sawada et al., 2008). However, in 2003 Tarashi et al. where able to show that RBC cannot perform vesicular transport under physiological conditions (Taraschi et al., 2003).

Investigations concerning CFTR revealed that the presence of CFTR is necessary for ATP release from RBCs. Accordingly, deformation triggered ATP release from RBCs cannot be observed in patients who suffer from cystic fibrosis (Sprague et al., 1998). Braunstein et al. were able to show that CFTR accelerates ATP release from cells but at the same time ruled out the idea that CFTR is the ATP conduit itself. Thus, lipid bilayers containing only CFTR channels are not able to transport ATP (Braunstein et al., 2001).

Cnx represent a family of hemi channels in different tissues. In glial cells cnx43 has been shown to be associated with ATP release and cell to cell communication (Kang et al., 2008, p. 43). In 2006, however, Locovei et al. could not find evidence for the presence of cnx43 in RBC membranes. Simultaneously, this group reported that pnx1 can be detected on the surface of RBCs (Locovei et al., 2006a).

Pnx represent a newly discovered family of hemi channels in vertebrates. To this date three different types of pannexins have been described (Litvin et al., 2006). At first glance pnx seem to be related to cnx, which also form hemi channels. Despite the outer similarity, pnx and cnx do not show any sequence homology. However, some of the functions of pnx and cnx seem to be alike. Namely pnx hemi channels were investigated regarding ATP release from different cell types, including RBCs (Bao et al., 2004; Huang et al., 2007; Ransford et al., 2009; Locovei et al., 2006a).

Different physiological and pharmacological stimuli end up in ATP release from RBCs into vasculature. However, the exact intracellular signaling cascades that control pnx1 remain uncertain. Known triggers that cause ATP release are cell deformation (Sprague et al., 1998), low O_2 tension (Bergfeld and Forrester, 1992), prostacyclins (Sprague et al., 2008), depolarization and increased concentrations of intracellular calcium (Locovei et al., 2006b, Huang et al., 2007). Previously it has been reported that RBCs contain the functional heterotrimeric G-Proteins Gs and Gi. Activation of both proteins is required for ATP release in response to low O_2 tension or prostacyclin analogs. Furthermore, data presented by Sprague et al. show that the second messenger cyclic adenosine monophosphate (cAMP) is involved in intracellular signaling, which leads to ATP release. The heterotrimeric G proteins Gs and Gi activate adenylate cyclase (AC) and accumulation of cAMP is accompanied by increased ATP release (Sprague et al., 2005, 2001a). Cell deformation and intracellular Ca^{2+} concentrations are linked to both eNOS activity and ATP release. Therefore, it seems likely that eNOS signaling might also influence ATP release from RBCs. Yet the influence of eNOS signaling with regard to pnx1 has not been investigated.

1.5 Aims of the dissertation

The development and progression of cardiovascular diseases is correlated to endothelial dysfunction. Decreased NO bioavailability is considered to be both a characteristic and a cause of endothelial dysfunction. NO is produced by a group of NOS. Recently it was shown that RBCs carry an active eNOS, which contributes to the vasculature´s NO pool. In patients who suffer from endothelial dysfunction the activity of eNOS in RBCs is significantly impaired, compared to healthy controls. The exact role of eNOS in RBCs still has to be elucidated. Accumulating data support the idea that eNOS signaling within RBCs affects deformability. The treatment of RBCs with a NO donor enhances deformability while NOS inhibition with L-NAME decreases deformability. Deformation of RBCs in turn initiates a mechanotransductive process, which leads to significant ATP release. The relationship between deformability and deformation triggered ATP release presumes that both functions are linked together. Accordingly eNOS signaling might also contribute to ATP release from RBCs. sGC and PRKG1 are key enzymes of NO signaling. The presence of a full and functioning eNOS/ sGC/ PRKG1 signaling pathway in mature human RBCs has not been demonstrated so far.

This work aims to investigate the presence of full eNOS/ sGC/ PRKG1 signaling pathway in mature human RBCs by raising the following questions: 1) Do mature human RBCs contain sGC and PRKG1? 2) Is PRKG1 active in mature human RBCs? 3) Are sGC and PRKG1 part of an eNOS signaling cascade that influences deformability and ATP release via pannexin 1 from RBCs? 4) Do arterial hypertension and CAD influence the presence of sGC, PRKG1 or PDE5 in RBCs?

To supply evidence for the presence of sGC and PRKG1 western blot analyses will be performed. An enzyme linked immunosorband assay (ELISA) will be used to investigate the activity of PRKG1 in RBCs. Deformability was analyzed by Laser assisted optical rotational cell analyzer (LORRCA) at different levels of shear stress. The influence of eNOS, sGC and PRKG1 on deformability was assessed as elongation index (EI) after different treatments. A combination of flowcytometric and ectacytometric analyses will be established to investigate the influence of deformation on eNOS activity in RBCs. Finally flowcytometric analysis will be

executed to determine the role of eNOS/ sGC/ RKG1 signaling with regard to ATP release via pnx1 channels. The influence of arterial hypertension and CAD will be assessed by a study comparing protein levels of sGC, PRKG and PDE5 between a group of patients who suffer from CAD and hypertension and a control group.

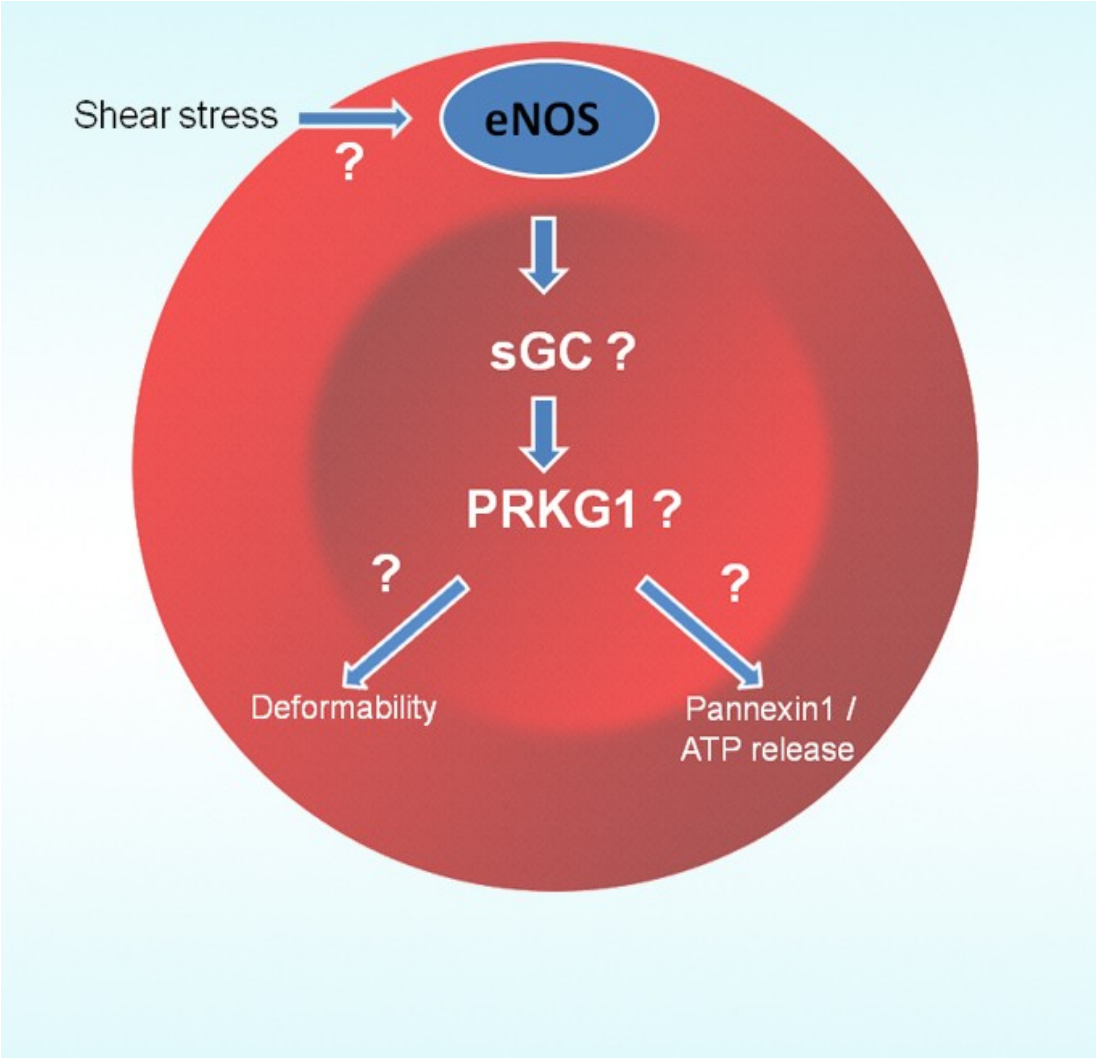

Figure 5: Potential eNOS signaling cascade in RBCs

The image illustrates the hypothesis of a full eNOS/ sGC/ PRKG1-signaling pathway within mature human RBCs. This signaling cascade is potentially activated by different levels of shear stress and influences deformability of RBCs and pannexin1, which is an ATP gating channel.

2 Materials and methods

2.1 Materials

Equipment		
Bench DGN1500(DG03)	Wesemann	Syke, DE
X Cell2 Blot Module	Invitrogen	Oslo, Norway
Centrifuge Mikro200R	Hettich	Tuttlingen, DE
Centrifuge Rotina 38R	Hettich	Tuttlingen, DE
CP225D-OCE	Sartorius	Göttingen, DE
Flowcytometer FACS Verse	BD Bioscience	SanJose, USA
Fluostar Omega	BMG Labtech GmbH	Ortenberg, DE
Heating cabinet TH15	Edmund Bühler	Tübingen, DE
Heating oven	Memmert GmbH & CO.	Schwabach, DE
ImageQuant LAS400	GE Healthcare	Buckinghamshire,UK
LORRCA laser optical rotational	Mechatronics	Zwaag, NL
Magnetic Particle Concentrator	Invitrogen	Oslo, Norway
Micro pippets	Eppendorf	Hamburg, DE
Microsyringe gastight #1710	Hamilton	Bonaduz, SUI
MiliQ	Merck	Darmstadt, DE
Minishaker MS1	IKA Labortechnik	Staufen, DE
pH Meter Lab870	Schott Instruments	Mainz, DE
Pipet boy comfort	Integra Bioscience	Biebertal, DE
PowerPac200	BioRad	California, USA
RCT Basic	IKA Labortechnik	Staufen, DE
Rotator	NeoLab	Heidelberg, DE
Scales BC BL 100 D01-09-019	Sartorius AG	Göttingen, DE
Sonyfiyer sonorexsuper	Bandelin	Berlin, DE
Testtube heater	Stuart Scientific	Staffordshire, UK
Tumbling shaker PolyMax1040	Heidolph	Schwabach, DE
Water bath GFL 1083	GFL	Burgwedel, DE
X Cell Sure Lock	Invitrogen	Oslo, Norway

Table 1: Equipment

Consumable Material		
96-well-micro-plates black, flat	Greiner Bio One	Frickenhausen, DE
96-well-micro-plates clear, flat	Greiner Bio One	Frickenhausen, DE
96-well-micro-plates white , flat	Greiner Bio One	Frickenhausen, DE
Facs-tubes 5ml, 75x12mm, PS	Sarstedt	Nümbrecht, DE
Falcons 15ml	Greiner Bio One	Frickenhausen, DE
Falcons 50ml	Greiner Bio One	Frickenhausen, DE
Gel Blot Paper GB003	Sigma Aldrich	St. Louis, USA
NuPage 3-8% Tris-Acetate Gel	Novex	California, USA
NuPage 7% Tris-Acetate Gel	Novex	California, USA
Gloves, nitril powder free	Ansell	Tamworth, UK
Nitrocellulose Membrane	GE Healthcare	Buckinghamshire, UK
Parafilm “M”	Pechiney Plastic Inc	Washington, USA
Pipette filter tip	Star Lab	Hamburg, DE
Pipette tip TipOne 10 µl	Star Lab	Hamburg, DE
Pipette tip TipOne 100 µl	Star Lab	Hamburg, DE
Pipette tip TipOne 1000 µl	Star Lab	Hamburg, DE
Safe-Lock tubes 2,0ml	Eppendorf	Hamburg, DE
Single-use Syringes 10ml	B. Braun AG	Melsungen, DE
Single-use Syringes 20ml	B. Braun AG	Melsungen, DE
Single-use Syringes 5ml	B. Braun AG	Melsungen, DE
Stripetten Costar® 10ml	Corning	NY, USA
Stripetten Costar® 25ml	Corning	NY, USA
Stripetten Costar® 5ml	Corning	NY, USA

Table 2: Consumable Material

Kits		
DC Protein Assay	BioRad	Munich, Germany
Immunoprecipitation Dynabeads Antibody Coupling Kit Cat.#: 143.11D	Invitrogen	Oslo, Norway
Silverstaining Kit Article #:P-S-2001	Proteome Factory AG	Berlin, DE
Cyclex Cyclic GMP dependent protein kinase (cGK) Assay Kit Cat.#: CY-1161	MBL International Corporation	Massachusetts, USA

Table 3: Kits

Chemicals		
10x PVP-Solution	Mecatronic	Netherlands
8-Bromo3-5cyclic GMP	Sigma Aldrich	St. Louis, USA
acetic acid	Carl Roth GmbH + Co.	Karlsruhe, Germany
Aqua bidest	Millipore	Darmstadt, Germany
Bovine serum albumin	Sigma Aldrich	St. Louis, USA
Calciumchlorid ($CaCl_2$	Sigma Aldrich	St. Louis, USA
Carbenoxolone	Sigma Aldrich	St. Louis, USA
Carboxyfluorescein diacetate	Sigma Aldrich	St. Louis, USA
CS&T beads	BD Biosciences	(Heidelberg,
8-Bromo3-5cyclic GMP	Sigma Aldrich	St. Louis, USA
DAF-FM diacetate	Invitrogen GmbH	Darmstadt, Germany
Dimethyl Sulfoxide (DMSO	Sigma Aldrich	St. Louis, USA
DT2	Sigma Aldrich	St. Louis, USA
Ethanol	Merck KGaA	Darmstadt, Germany
Glucose	Sigma Aldrich	St. Louis, USA
Heparin	Ratiopharm	Ulm, Germany
Hybond P membrane	GE healthcare	Little Chalfont, UK
Hydrochloride acid (HCl) 25%	Merck KGaA	Darmstadt, Germany
Hydrogen peroxide 30% (H_2O_2);	Carl Roth GmbH + Co.	Karlsruhe, Germany
L-Arginin	Carl Roth GmbH + Co.	Karlsruhe, Germany
L-NAME	Enzo Life Sciences	Lörrach, Germany
Magic Mark XP Western Protein	Invitrogen	Carlsbad, USA
Magnesium sulfate ($MgSO_4$	Sigma Aldrich	St. Louis, USA
Mercaptoethanol	Sigma Aldrich	St. Louis, USA
Methanol	Merck	New York, USA
Methanol, β-Nicotinamide	Sigma Aldrich	St. Louis, USA
Milkpowder blotting grade	Sigma	St. Louis, USA
NuPAGE LDS Sample Buffer	Invitrogen	Carlsbad, USA
NuPAGE Reducing Agent	Invitrogen	Carlsbad, USA
NuPAGE Transferbuffer	Invitrogen	Carlsbad, USA
NuPAGE Tris acetate running	Invitrogen	Carlsbad, USA
ODQ	Cayman Europe	Tallinn, Estland
Potassium chloride (PCl	Sigma Aldrich	St. Louis, USA
Potassium hydrogen phosphate	Sigma Aldrich	St. Louis, USA
Protease-Phosphatase-Inhibitor	Bio-Rad	Munich, Germany
Sildenafil citrate salt	Sigma Aldrich	St. Louis, USA
Sodium chloride (NaCl)	Sigma Aldrich	St. Louis, USA
Sodium dihydrogen phosphate	Sigma Aldrich	St. Louis, USA
Sodium hydrogencarbonat	Sigma Aldrich	St. Louis, USA
Sodium hydroxide (NaOH	Merck KGaA	Darmstadt, Germany
SpermineNONOate		
Tween20(P9416)	Sigma Aldrich	St. Louis, USA

Table 4: Chemicals

Primary Antibodies			
Name Cat.#	**Antigen**	**Species**	**Company**
Anti GUCY1A3 #H00002982-M01	sGC	Mouse monoclonal	Abnova
Anti GCUY1A3 #H00002982-D01P	sGC	Rabbit polyclonal	Abnova
Anti GUCY alpha AM05610PU-N	sGC	Mouse	Acris
Anti-PRKG1 H00005592-M01	PRKG1	Mouse monoclonal	Abnova
cGK alpha beta sc-271765	PRKG1	Mouse monoclonal	Santa Cruz Biotech
cGK alpha beta sc-271766	PRKG1	Mouse monoclonal	Santa Cruz Biotech
cGK alpha beta sc-25429	PRKG1	Rabbit polyclonal	Santa Cruz Biotech
Anti cGK1 Ab154724	PRKG1	Rabbit polyclonal	Abcam
Anti PDE5A #PAB12359	PDE5	Rabbit	Abnova
ANTI Spectrin S3396	Spectrin	Mouse	Sigma

Table 5: Primary Antibodies

Secondary Antibodies			
Name Cat.#	**Antigen**	**Species**	**Company**
HRP GAR #554021	IgG Fc Rabbit	Goat	BD Bioscience
HRP GAM #554002	IgG Fc Mouse	Goat	BD Bioscience

Table 6: Secondary Antibodies

2.2 Cells

Cells used throughout this work are rat fetal fibroblast lung cells (RFL6) and SMCs. Lysates of both cell lines were used as positive controls in western blot analyses. RFL6 and SMCs were stored in liquid nitrogen until the day of culturing. 500 ml culturing medium contained 375 ml RPMI, 100 ml of 20 % FCS and 5 ml of NAA, HEPES, pyruvat, penstrep and glutamine each. Cell culture of these cells was performed by Sivatharsini Thasian-Sivarajah. Prior to cell lysis, cells were kept in tubes at -80 °C. Cell pellets were taken out of the freezer and 150 µl of RIPA buffer were added to the tube. Before protease and phosphatase inhibitors were added to the buffer. The tubes were than vortexed and put into an ultrasonic bath three times for 30 seconds each. After that vials were centrifuged at 1300 G at 4 °C for 10 minutes. After centrifugation lysed cells were stored at -20 °C until the day of use. Prior to freezing an aliquot was taken for a protein determination according to Bradford (see § 2.5.3).

2.3 Animals

Tissues from wild type C57Black6 mice, eNOS KO mice and alpha1 sGC KO mice were used as controls for western blot analysis. Transgenetic eNOS KO mice were provided by Prof. Dr. rer. nat. A. Goedecke from the University of Düsseldorf (Goedecke et al. 1998). All animal procedures were performed in conformity with the national guidelines on animal care, as given by the German Tierschutzgesetz and were approved by the local Research Board for animal experimentation (LANUV = State Agency for Nature, Environment and Consumer Protection North-Rhine-Westphalia, Germany). Until the day of examination or euthanasia all mice were kept in groups, at 19-21 °C, in 50-60 % humidified atmosphere, in a 12 h day night rhythm. All animals were kept under the same conditions. Anesthesia, blood withdrawal and organ removal were performed by Dr. rer. nat. Thomas Krenz (Krenz, 2014). Organs were explanted by ventral incision of thoracic and abdominal cavities. Vena cava was cut and organs were perfused with ice cold phosphate buffer saline (PBS) via heart puncture. After removal of organs adventitia or blood coagulate were carefully removed. Organs were than shock

frozen in liquid nitrogen prior to storage at -80°C. (Ethics number: AZ 84-02.2011.A227)

2.4 Human blood samples

Blood for the investigations was obtained by antecubital venial puncture from healthy human subjects and from patients who suffer from arterial hypertension and CAD. Test persons were recruited from the department of Cardiology, Pulmonology and Angiology at the University Clinic Düsseldorf. All subjects were informed about the methods and investigations performed in this work and provided written informed consent before enrollment. Procedures were conducted in accordance with the Declaration of Helsinki and approved by the local ethics committee of the Heinrich-Heine University of Düsseldorf. The blood was anticoagulated with heparin [15 IU/ ml]. After anticoagulation the blood was either lysed for ELISA and western blot analysis or diluted 1:400 in PSS. (Ethics numbers 3857; 3450)

2.5 Experimental procedures

2.5.1 Preparation of stock solutions

Spermine NONOate (SperNO 1 mM in NaOH)

SperNO is a NO-donor, that spontaneously dissociates at neutral pH into NO with a first order kinetic and has a half life of 39 minutes and 230 minutes at 37 °C an 22-25 °C respectively at pH7.4 to liberate 2 mols of NO per mol of parent compound.

1H-[1,2,4]Oxadiazolo[4,3-a]quinoxalin-1-one (ODQ in DMSO)

ODQ is a competitive, irreversible and selective inhibitor of sGC. It inhibits the heme site of the protein and therefore binds the beta subunit of sGC.

L-N^G-Nitroarginine methyl ester (NAME 300 mM in PSS)

L-NAME is an inhibitor of NO synthase (NOS). It suppresses the release of NO by endothelial cells. 300 mM Stock solutions of L-NAME in double distilled water or physiological salt solution (PSS) have always been prepared on the day of use.

DT2-trifluoracetate salt (DT2 10 mM in PSS)

DT2 is a cell permeable, competitive cGMP-Protein-Kinase (PKG1Alpha) inhibitor. It consists of two parts and has a 1.000 fold higher selectivity for PKG over PKA. DT2 has been dissolved in PSS to a stock solution of 10 mM in the purchased vial. To avoid repeated freezing and thawing, DT2 has been aliquoted in small eppendorf vials.

8-Bromo3-5cyclic GMP (10 mM in PSS)

8-Bromo3-5cyclic GMP is a cell permeable cGMP analog, which has greater resistance to hydrolysis by phosphodiesterases than cGMP. 8-Bromo3-5cyclic GMP was used in order to stimulate PRKG1 in RBC. Stock solutions have always been prepared on the day of use.

Carbenoxolone (10 mM in PSS)

Carbenoxolone is a reversible inhibitor of Pannexin channels. 10 mM Stock solutions of Carbenoxolone in PSS have always been prepared on the day of use and been kept chilled on ice until use.

Fluorescent dyes

Carboxyfluorescein Diacetate (CF-DA 5 mM in DMSO)

Carboxyfluorescein diacetate (CF-DA) is a cell permeable fluorescent dye (λ_{ex} 492 nm and λ_{em} 517 nm). Once inside a cell it becomes deacetylated by esterases and hence being trapped in living cells. Fluorescence was measured with a flow cytometer. A 5 mM stock solution has been prepared in dimethyl sulfoxide (DMSO).

4-Amino-5-Methylamino-2,7-Difluorescein-Diacetate (5 mM in DMSO)

4-Amino-5-Methylamino-2,7-Difluorescein-Diacetate (DAF-FM-DA) is a probe that is used to detect and quantify low concentrations of NO (Cortese-Krott et al., 2012b). It is essentially nonfluorescent until it reacts with NO to form a fluorescent

benzotriazole. Fluorescent wavelengths of DAF-FM were measured at λ_{ex} 495 nm and λ_{emm} 515 nm in a flow cytometer. DAF-FM-DA has always been prepared prior to use. 5 µg of DAF-FM-DA have been diluted in 20 µl of DMSO to create a stock solution of 5 mM.

2.5.2 Preparation of buffers

The pH meter Lab870 by Schotts instruments was used to adjust the pH. Prior to use, the Lab870 has always been calibrated with three ready to use solutions by Merck with pH values of 4, 7 and 9. If the evaluation of the calibration, made by Lab870 itself, was worse than “double+”, the pH meter was calibrated again. Calibration was performed with titration of either 1 M HCl or 1 M NaOH.

Physiological salt solution (PSS)

For the solution 0.350 gram of potassium chloride (KCl), 0.294 gram of calcium chloride (CaCl), 0.296 gram of $MgSO^4$, 8.187 gram of NaCl, 3.310 gram of tris (hydroxymethyl-) aminomethane and 1.999 gram of dextrose were weight and filled up with 900 ml of double distilled water. The pH was than adjusted to pH 7.4 with NaOH or HCl. After the adjustment of pH the PSS solution was filled up to 1000 ml with double distilled water.

10 X physiological buffer saline (PBS)

10 X PBS is the stock buffer for 1 X PBS, which was used for western blot protocols for antibodies (ABs) from Abnova and Abcam. A 10 X stock solution of PBS is prepared as follows. 75.9 gram of NaCl, 13.8 gram of NaH_2PO_4-H_2O are diluted in 800 ml of double distilled water. When fully dissolved the pH was adjusted to pH 7.0 as described above. The solution was than filled up to a total volume of 1000 ml with double distilled water.

20 X Tris buffer saline (20 X TBS)

20 X TBS is the stock buffer for 1 X TBS, which was used in western blot protocols for Antibody from Santa Cruz biotech. A 20 X TBS stock solution is prepared as follows. 24.23 gram of Trizma Base and 116.88 gram of NaCl are diluted in 800 ml of double distilled water. When fully dissolved the pH was adjusted to pH 7.4 as described above. The solution was then filled up to a total volume of 1000 ml with double distilled water.

Buffers for SDS PAGE and western blot	
Name	**Composition**
Running buffer outer chamber	950 ml H2O
	50 ml 20X SDS running buffer
Running buffer inner chamber	200 ml Running buffer outer chamber
	500 µl NuPage Antioxidant
Transfer buffer	425 ml H2O
	50 ml MeOH
	25 ml 20 X NuPage transferbuffer
	500 µl NuPage Antioxidant
10 X PBS pH 7.0	1000 ml H2O
	NaCL 75.9 g
	NaH2PO4 H2O 13.8 g
1 X PBS pH 7.0	450 ml H2O
	50 ml 10 X PBS
1 X PBS-T 0.2% pH 7.0	900 ml H2O
	100 ml 10 X PBS
	2 ml Tween20
20 X TBS pH 7.4	1000 ml H2O
	TrizmaBase 24.23 g
	NaCL 116.88 g
1 X TBS pH 7.4	475 ml H2O
	25 ml 20 X TBS
1 X TBS-T 0.1% pH 7.4	1000 ml 1 X TBS
	500 µl Tween20
Blocking buffer milk 5%	50 ml TBS-T 0.1% or PBS-T 0.2%
	2.5 g dry milk powder
Blocking buffer BSA 5%	50 ml TBS-T 0.1% or PBS-T 0.2%
	2.5 g bovine serum albumin
Stripping buffer Stock Solution	418.57 ml H2O
	50 ml 20% SDS
	31.25 ml 1 M trisHCl pH6,7
Stripping buffer working solution	7 ml stripping buffer stock solution
	49 µl beta-Mercoptoethanol
Ponceau S	100 ml H2O
	0.2 g Ponceau S
	0.3 g Trichloracetic acid

Table 7: Buffers for SDS PAGE and Western Blot

Buffers for cell lysis	
Name	**Composition**
Lysis buffer pH 7.5 for ELISA	20 mMTrisBase
RIPA buffer	Tris HCl 50 mM pH7.4
	NP40 1%
	Na deoxcholat 0.5%
	SDS 0.1%
	NaCl 150 mM
	EDTA 2 mM
	NaF 50 mM

Table 8: Buffers for Cell Lysis

Buffer for LORRCA and flow cytometric analyses	
Name	**Composition**
PSS pH7.4	KCl 4.7 mM
	CaCl 2 mM
	MgSO4 1.2 mM
	NaCl 140.5 mM
	Dextrose 11.1 mM
	Tris(hydroxymethyl)-amoniomethane 21 mM

Table 9: Buffer for LORRCA and Flow Cytometric Analyses

2.5.3 Protein determination

A commercial kit (DC^{TM} protein assay) was used for protein determination according to Bradford (Bradford, 1976). Working solution A was prepared by mixing 20 µl “solution S” and 1 ml “solution A”. A bovine serum albumin (BSA) stock solution was prepared with a concentration of 2 mg/ ml. 9 standard dilutions, ranging from 0 mg/ ml to 2.0 mg/ ml, were prepared in different tubes. Different dilutions of cell lysates in lysis buffer were prepared to ensure they were in detection range of the standard curve.

2.5.4 Preparation of cell lysates

Prior to cell lysis, cells were kept in tubes at -80 °C. Cell pellets were taken out of the freezer and 150 µl of RIPA buffer were added to the tube. Before protease and

phosphatase inhibitors were added to the buffer. The tubes were then vortexed and put into an ultrasonic bath three times for 30 seconds each. After that vials were centrifuged at 1300 G at 4°C for 10 minutes. After centrifugation lysed cells were stored at -20 °C until the day of use. Prior to freezing an aliquot was taken for a protein determination according to Bradford (see § 2.5.3).

2.5.5 Preparation of organ lysates

Organs for cell lysates were kept in tubes at -80 °C until use. Prior to cell lysis organs were taken out of the freezer and put into a porcelain mortar, which was filled with liquid nitrogen. During the evaporation of liquid nitrogen the organs were crushed. Organ dust was transferred into 2 ml tubes and immediately diluted in 150 µl RIPA buffer and additionally 1.5 µl protease halt mix. In alternating order the dilution was vortexed and sonicated 30 seconds for three times. After the last sonication step the tubes where put onto a rotator for five minutes and then centrifuged for ten minutes at 400 X g and 4 °C. If a pellet was visible after centrifugation the tube-tubes were vortexed and sonicated again three times for 30 seconds. After centrifugation the lysate was transferred into a new tube and stored at -20 °C. Prior to freezing an aliquot was taken for a protein determination according to Bradford (see § 2.5.3).

2.5.6 Preparation of RBC lysates for western blot and ELISA

Western blot: 10 ml of anticoagulated whole blood were put into a 50 ml falcon. Blood was centrifuged for 15 minutes at 800 X g and 4 °C. After centrifugation the supernatant and buffy coat were discarded and the RBC concentrate was diluted in a 10 fold amount of chilled 0.9 % NaCl solution. The suspension was then centrifuged for 10 minutes at 300 X g and 4 °C for three times. The supernatant was discarded again and the RBC concentrate resuspended in 2 ml radio immunoprecipitation assay (RIPA) buffer, 20 µl protease halt mix and 1 ml aqua bidest. The solution was aliquoted into 2 ml tubes and centrifuged for 10 minutes at 13000 X g and 4 °C. The lysed blood was aliquoted into new tubes and kept

frozen at -20 °C until further use. Prior to freezing an aliquot was taken for a protein determination according to Bradford (see § 2.5.3.).

ELISA: 2 ml of whole blood were centrifuged at 300 X g for 10 minutes at 4 °C. Supernatant and buffy coat were removed and the RBC pellet was diluted in 1 ml of PBS. Washing in PBS was repeated three times. After the third washing step the RBC pellet was resuspended in 1ml lysis buffer, sonicated for 1 minute and vortexed for 30 seconds three times. The lysate was again centrifuged as described before. The clear lysate was put into a new tube. After lysis an aliquot was taken for a protein determination according to Bradford (see § 2.5.3).

2.5.9 SDS-PAGE and Western Blot

Sample preparation: Prior to use crude lysates were diluted in up to 16.25 µl of double distilled water, 2.5 µl sample reducing agent and 6.25 µl 4X Lithium dodecyl sulfate (LDS) to reach protein concentrations between 100 and 1000 µg. Final experiments were performed with a concentration of 500 µg. All components were put into 1.5ml tubes, gently mixed and put on a heating plate for 10 minutes at 70 °C. After denaturation, samples were taken out of the tubes and loaded to the gel. The first or last lane was always loaded with a molecular weight marker. After loading, the X Cell Sure Lock was closed and attached to the power supply.
Prior to use gels were taken out of the cooler and rinsed in double distilled water. Depending on the estimated size of the different proteins and for optimization, different gel types (3 - 8 % Tris-Acetate (TA) or 7 % TA gels) were used. For SDS-PAGE the outer chamber was filled with SDS-Running buffer. The inner chamber was filled with 200 ml of 1 X SDS-Running buffer and 500 µl of NuPage antioxidant. Gel pouches were carefully purged five times each with the inner running buffer solution. 3 - 8 % TA-gels were run at 150 volts until the running front reached to the bottom of the gel.

Western blot: Gel-cassettes from SDS-Page were opened and the gel was put onto a moist whatmann paper. A cut nitrocellulose membrane has been activated in methanol and washed in double distilled water before placing it on the other side of the gel and topped with the second whatmann paper. Following this preparation

the gel/membrane sandwich was put into the X Cell Mini Blot in between four sponges and sealed properly. The inner chamber was filled with transfer buffer while the outer box was filled with doubled distilled water as cooling system. The blots were performed for 1 hour at 30 volts.

In order to check for successful blotting, the membrane has been incubated in Ponceau S for ten minutes. Following the staining with Ponceau S the membrane was washed in double distilled water until all the red color was washed out. Prior to incubation with a primary antibody the membrane was blocked in blocking solution for one hour at room temperature on a horizontal shaker. If phosphoproteins were targeted, the membrane was blocked in 5 % BSA solutions in T-TBS. If non-phosphoproteins were targeted, the membranes were blocked in 5 % milk T-TBS.

2.5.10 Membrane Stripping

Membrane stripping was performed under a flue. 49 µl of Mercaptoethanol were added to 7 ml of stripping buffer. Western blot membrane and stripping solution were put into a glass cuvette. Incubation was performed at 70 °C for 30 minutes. After that the membrane was washed three times for 15 minutes on a shaker in TBS.

2.5.11 Detection of PRKG1 activity

An appropriate number of strips was taken out of the plate and put onto a plate holder. Unused wells were put back into a foil pouch, sealed and stored at 4 °C until further use.

All samples were diluted to a concentration of 1 mg / ml. All assays were prepared as duplicates. 10 µl of diluted RBC-lysates were added to wells. Two wells were loaded with “CycLex cGK positive control” (0.2 units / µl) and served as positive controls. Two additional wells were loaded with 10 µl of plain buffer and served as negative or “no enzyme” control. Inhibitor controls were prepared with either 10 µl of RBC lysates or 10 µl of positive control and additionally with 10 µl of 10 X K252a.

The kinase reaction was started by adding 90 µl, respectively 80 µl, of “cGMP plus” reaction buffer per well. Additional controls were loaded with 10 µl RBC lysates and 90 µl of “cGMP minus” buffer or 90 µl of “ATP minus” buffer (table 10).

Assay reagents	Lysate + cGMP	Lysate - cGMP	Lysate + Inhibitor	Lysate - ATP	Positive control	Positive control plus inhibitor	No enzyme control
cGMP plus	90 µl		80 µl		90 µl	80 µl	90 µl
cGMP minus		90 µl					
ATP minus				90 µl			
10X K252a [10 µM)			10 µl			10 µl	
CycLex positive control					10 µl	10 µl	
Buffer							10 µl
RBC lysate	10 µl	10 µl	10 µl	10 µl			
All samples were prepared as duplicates							

Table 10: ELISA assay reagents

After loading, microtiter-wells were sealed with plate sealer and incubated for 30 minutes at 30 °C. Following the incubation, all wells were washed for 5 times with 1 X washing buffer. By gentle aspiration with a vacuum pump all residual washing buffer was removed from the wells. In order to detect phosphorylated proteins,
100 µl of horse radish peroxidase (HRP) conjugated detection antibodies were added to each well. The plate was then covered with sealer again and incubated for 60 minutes at room temperature on a horizontal shaker. After incubation microtiter-wells were washed again as described before. To visualize phosphorylated substrates, 100 µl of substrate reagent were added to the microtiter-wells and the plate was incubated at room temperature for 15 minutes. When a clear, blue color turnover was visible, 100 µl of stop solution were added to each well, in the same order as samples have been treated previously. The absorbance was measured at dual wavelengths of 450 and 540 nm (Fig. 6).

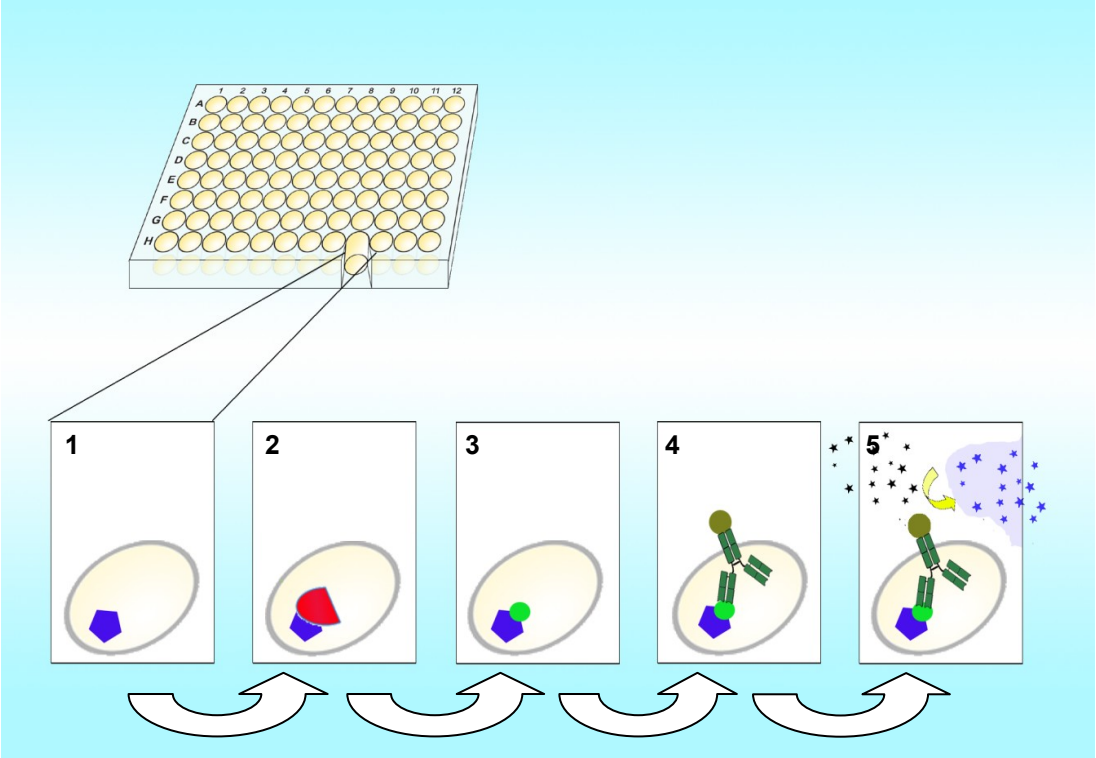

Figure 6: PRKG activity assay

The image illustrates the course of PRKG activity assay. Substrate coated micro plates (1) are being incubated with RBC lysates that potentially carry an active PRKG (2). PRKG phosphorylates target proteins (3). Horseradish peroxidase coupled ABs that specifically react to phosphorylated targets bind to the target (4) and convert a substrate reagent (5) , which can be measured in a photometer at dual wavelengths of 450 and 540 nm. The amount of fluorescence indicates phosphorylation of the substrate and therefore activity of PRKG. Red blood cell = RBC, protein kinase G = PRKG, antibody = AB, nano meter = nm.

Preparation of buffers:

Washing buffer: 100 ml 10 X washing buffer were added to 900 ml double distilled water and well mixed.

cGMP plus reaction buffer:
(For 10 assays)

Kinase reaction buffer:
(For 10 assays)

Kinase buffer	950 µl
20 X ATP	50 µl
5 mM cGMP	2 µl
Kinase buffer	950 µl
20 X ATP	50 µl

2.2.12 Laser optical rotational red cell analyzer

Deformability of RBCs was measured with LORRCA. During ectacytometric measurements RBCs are exposed to increasing levels of shear stress. In LORRCA shear forces are produced by a cup, which rotates around a stagnant cylinder. Shear stress is induced by increasing rotational speed. The gap between cup and cylinder is filled up with RBCs, which are diluted 1:200 in Polyvinylpyrrolidone (PVP). In contrast to plasma, PVP is a solution, which maintains the same viscosity at all levels of shear stress applied. A laser beam is directed through the PVP/RBC solution to measure deformability (Fig. 7). The created diffraction pattern is being transformed into an elongation index (EI), which describes the ratio between length and width of RBCs. RBC (EI = $(L - W)/(L + W)$; L=length, W=width). It is proportional to deformability at applied shear stresses. The EI constantly rises as shear stress increases (Fig. 8). 30 diffraction patterns were analyzed at every level of shear stress and their means were translated into an elongation index. Increased or decreased EIs at a given shear stress indicate changes in deformability due to intracellular adaptations. All measurements were performed at 37 °C.

Preparation of RBCs: RBCs were diluted 1:500 in 15 ml PSS, treated with inhibitors and activators belonging to the eNOS signaling pathway. Incubation was performed at room temperature for 30 minutes on a roller. After incubation RBC dilutions were centrifuged at 300 X g for 10 minutes at 4 °C and the supernatant was removed. 25 µl of RBC pellet were gently diluted in 5 ml preheated PVP solution. The PVP solution was preheated in a water bath to 37 °C. For every measurement 1ml of the solution was pipetted into the gap between cup and bob. Different shear rates ranging from 0.3 to 30 Pascal were applied for 30 seconds. After each measurement the RBC-PVP solution was removed either automatically by a vacuum pump or taken out from the cup using a pipette. Samples regained by pipetting were used for flow cytometric investigations.

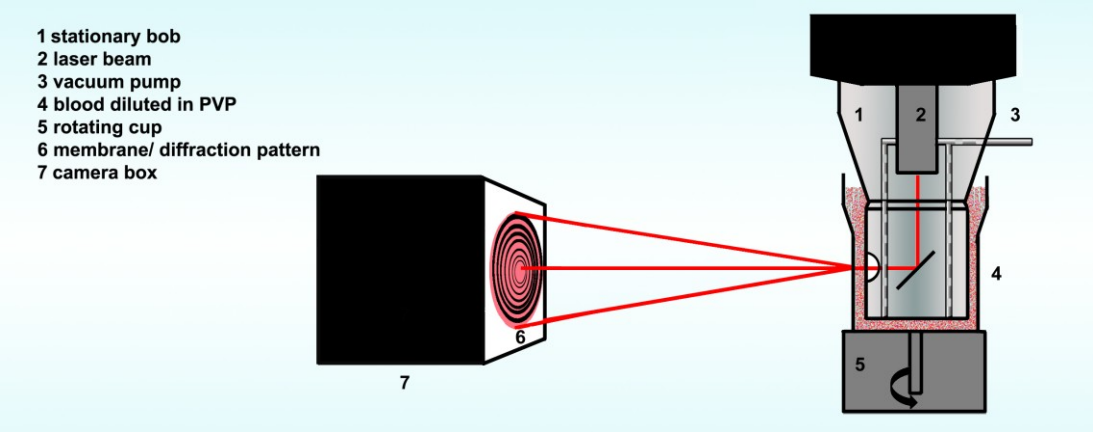

Figure 7: Principle of LORRCA

The modified image from the LORRCA manual illustrates the operating mode of the ectacytometer LORRCA. RBCs are being diluted in a PVP solution with known viscosity (4). The outer cup (5) rotates around a stationary bob (1) at a chosen pace and creates shear forces. The diffraction pattern (6) , which is caused by a laser beam (2) that is directed through the PVP/RBC solution allows the analysis of RBC deformability. The diffraction pattern is captured with a video camera (7) and analyzed with special software. A vacuum pump (3) allows easy removal of used PVP/RBC solutions.

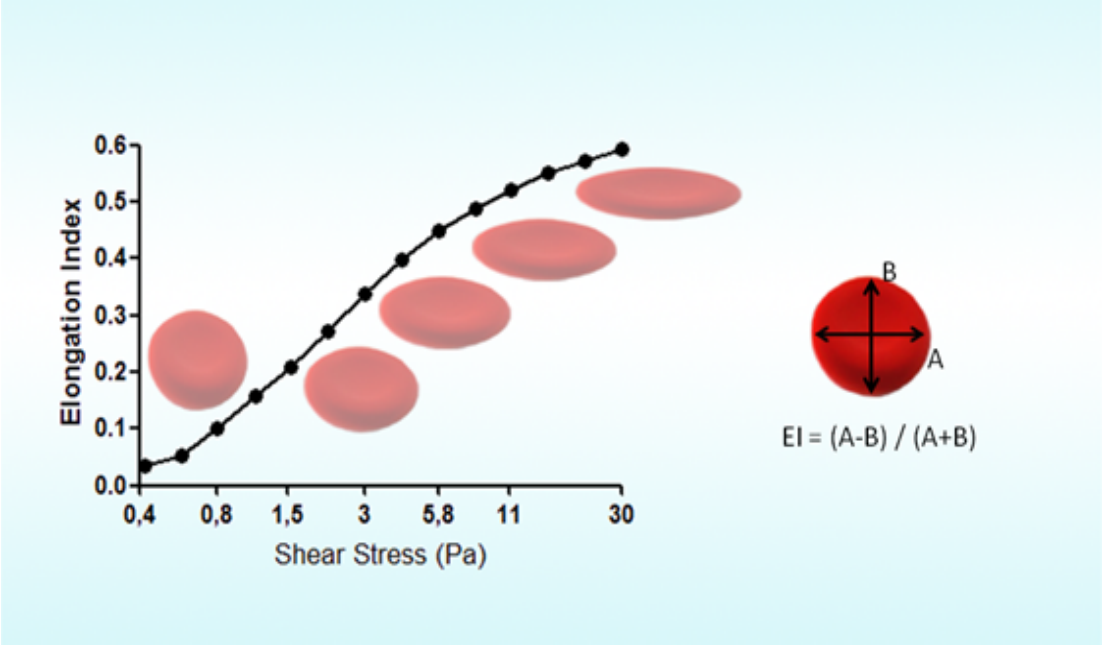

Figure 8: Elongation index

The modified image from the LORRCA manual illustrates the calculation of elongation indexes, which can be described as ratio between length and width of RBCs. The graphic displays the proportion of EI values and applied shear stresses. The EI constantly rises as shear stress increases. Increased or decreased EIs at a given shear stress indicate changes

in deformability. Elongation index = EI, pascal = Pa, transverse diameter = A, longitudinal diameter = B.

2.2.13 Flow cytometric analyses

Loading of RBCs with DAF-FM-DA

This procedure was carried out according to Cortese-Krott et al. (FRBM 2012) with small modifications. 75 µl of RBC pellet were diluted 1:400 in 30 ml PSS. Diluted blood was divided on different aliquots of 6 ml. Then falcons were incubated for 60 minutes at 37 °C on a roller. After 60 minutes all samples but the unloaded control, were loaded with 12 µl DAF-FM-DA. Samples were then incubated for 30 minutes at room temperature in the dark. Following the incubation with DAF-FM-DA, samples were washed at 300 X g for 10 minutes at 4 °C and resuspended in 6 ml PSS. The samples were again incubated for 15 minutes at room temperature. After incubation all samples were washed and resuspended in 3 ml of PVP solution. One ml of each sample was exposed to shear forces for 30 seconds ranging from 0.3 - 30 Pa using the ektacytometer LORRCA. Fluorescent signals created by DAF-FM-DA were measured with flowcytometric analysis.
NOS inhibition was carried out by incubation with 3 mM L-NAME. SperNO was used as a positive control at a final concentration of [0.05 µM]. Samples were incubated with SperNO during the 15 minute incubation period.

Loading RBCs with carboxyfluorescein diacetate

37.5 µl blood were than diluted 1:400 in 15 ml PSS. Aliquots of 500 µl were prepared in 2 ml tubes and all tubes but one were incubated with CF-DA [0.05 mM] for 30 minutes at 37 °C. One aliquot was not incubated with CF-DA in order to measure autofluorescence of RBCs. After incubation all samples were washed at 300 X g for 10 minutes at 4 °C and resuspended in the same amount of PSS in order to remove extracellular CF-DA. After resuspension samples were treated with different agents, in order to activate or inhibit proteins known to be part of eNOS signaling pathway. The first sample always served as a control and therefore was not incubated with an activator or inhibitor.

Tubes were incubated for 30 minutes at room temperature on a roller. After incubation all samples were washed again and resuspended in the 1500 µl PSS. Following the washing, all samples were subjected to flowcytometric analyses.

2.6 Statistical analyses

All values are reported as means + / - SEM or as box whiskers (tukey). Comparisons between groups were made using either two-tailed Student's T-test or ANOVA followed by Bonferroni post hoc test for multiple comparisons. Differences were deemed significant when $p < 0.05$. Statistical analyses were performed using GraphPad Prism 5.00 (GraphPad).

3 Results

3.1 sGC and PRKG1 can be detected in RBCs

To find out whether mature human RBCs carry proteins of the eNOS signaling pathway, western blot analyses were performed. Human RBC lysates from healthy donors and patients with hypertonic and cardiovascular disease were used for western blot analyses.

3.1.1 Detection of an alpha subunit of sGC in RBCs

The detection of an alpha subunit of sGC can be seen on three western blots in Figure 9 A. Control lanes were loaded with crude human red cell lysates from age matched controls. The other lanes were loaded with crude human red cell lysates from patients with hypertension and cardiovascular disease. The molecular weight marker, which indicates 80 kDa, can be seen in the first lane. The western blots show the detection of an alpha subunit of sGC in different crude RBC lysates at the expected size of 77 kDa. This reveals that mature human RBCs carry an alpha subunit of sGC. The alpha subunit of sGC can be detected in RBCs from healthy test persons and in RBCs from patients who suffer from cardiovascular disease and hypertension.

The visualization of the alpha subunit of sGC was followed by a study, which examined the amounts of the alpha subunit in mature RBCs from healthy test persons and patients suffering from cardiovascular disease and hypertension.

Figure 9 B shows the amounts of sGC in RBC lysates, which were calculated from band intensities that can be seen in Figure 9 A. Amounts of the alpha subunit of

each lane, were set up to spectrin of the same lane. The results of this examination do not show significant differences between both groups.

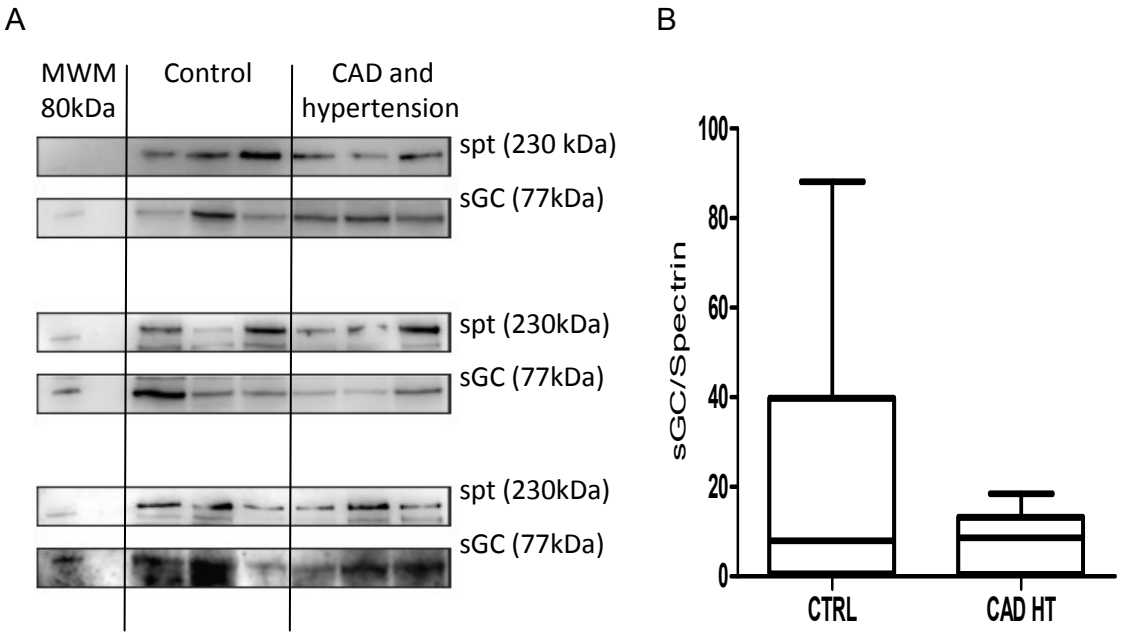

Figure 9: sGC in RBCs

The alpha subunit of sGC can be detected in mature human RBCs. The western blots (Fig 9 A) show the detection of an alpha subunit of sGC in different crude RBC lysates at the expected size of 77 kDa. Controls were loaded with 500 µg of crude RBC lysates from aged matched controls. The other lanes were loaded with 500 µg of crude human RBC lysates from patients who suffer from hypertension and cardiovascular disease. Spectrin was used as a loading control. Figure 9 B compares spectrin dependent amounts of sGC between aged matched controls and the patient group. Amounts were calculated from band intensities (Fig 9 A). n=9; p=0.217 (paired students t-test); CTRL = control; CAD + HT = coronary artery disease and hypertension; RBCs = red blood cells; spt = spectrin; sGC = soluble guanylate cyclase.

3.1.2 Detection of PRKG1in RBCs

The detection of PRKG1 can be seen on three western blots in Figure 10 A. Control lanes were loaded with crude human red cell lysates from aged matched controls. The other lanes were loaded with crude human red cell lysates from patients with hypertension and cardiovascular disease. The molecular weight marker, which indicates 80 kDa, can be seen in the first lane. The antibody detected bands at 76 kDa and thus reveals that mature human RBCs from aged matched test persons and from patients who suffer from cardiovascular disease and hypertension carry a PRKG1.

The visualization of PRKG1 was followed by a study, which examined the amounts of PRKG1 in mature RBCs from aged matched controls and patients suffering from cardiovascular disease and hypertension. The study was performed with 10 % BisTris gels. Figure 10 B shows the amounts of PRKG1 in RBC lysates, which were calculated from band intensities that can be seen in Figure 10 A. Volumes of PRKG1 of each lane were set up to spectrin of the same lane. The results of this examination do not show significant differences between both groups. Western blot results show that PRKG1 can be detected in RBCs from aged matched controls and in RBCs from patients who suffer from hypertension and cardiovascular disease.

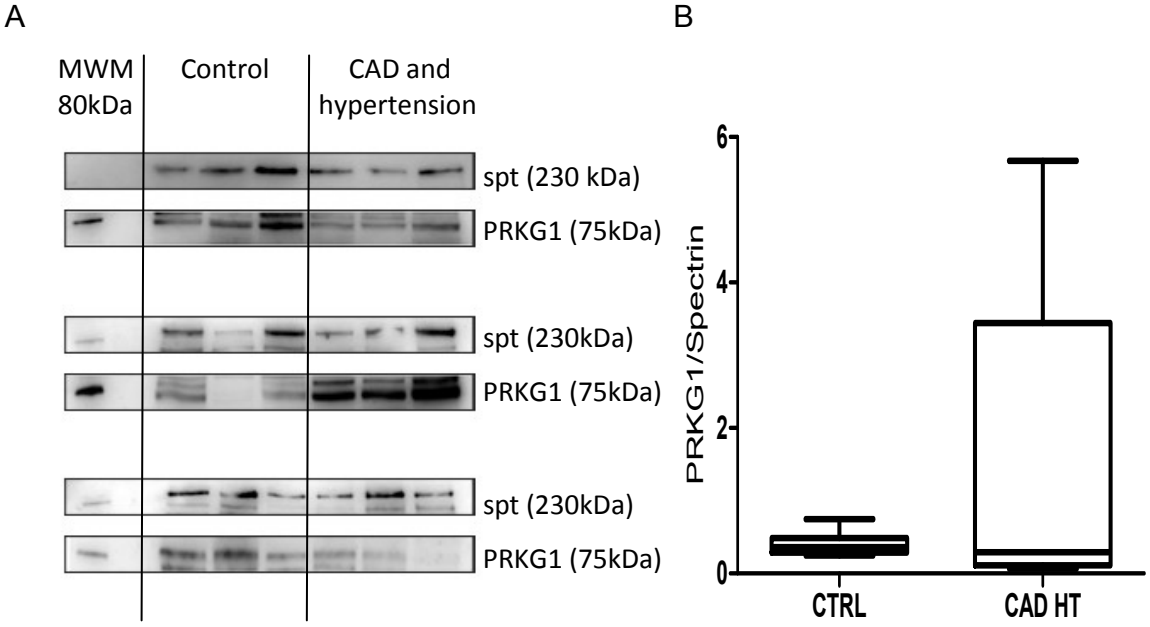

Figure 10: PRKG1 in RBCs

PRKG1 can be detected in mature human RBCs. The western blots (Fig 10 A) show the detection of PRKG1 in different crude RBC lysates at the expected size of around 75 kDa. Controls were loaded with crude RBC lysates from aged matched test persons. The other lanes were loaded with crude human RBC lysates from patients who suffer from hypertension and cardiovascular disease. Spectrin was used as a loading control. Figure 10 B compares spectrin dependent amounts of PRKG1 between healthy test persons and the patient group. Amounts were calculated from band intensities (Fig 10 A). n=9; p=0.136; (paired students t-test); CTRL = control; CAD + HT; coronary artery disease and hypertension; PRKG1 = protein kinase G1; RBCs = red blood cells; spt = spectrin.

3.1.3 Detection of PDE5A in RBCs

The detection of PDE5 can be seen on three western blots in Figure 11 A. Control lanes were loaded with crude human red blood cell lysates from age matched test persons. The other lanes were loaded with crude human red cell lysates from patients with hypertension and CAD. The molecular weight marker, which indicates 100 kDa, can be seen in the first lane. The antibody detected bands at 99 kDa and thus reveals that mature human RBCs from healthy test persons and from patients who suffer from cardiovascular disease and hypertension carry a PDE5.

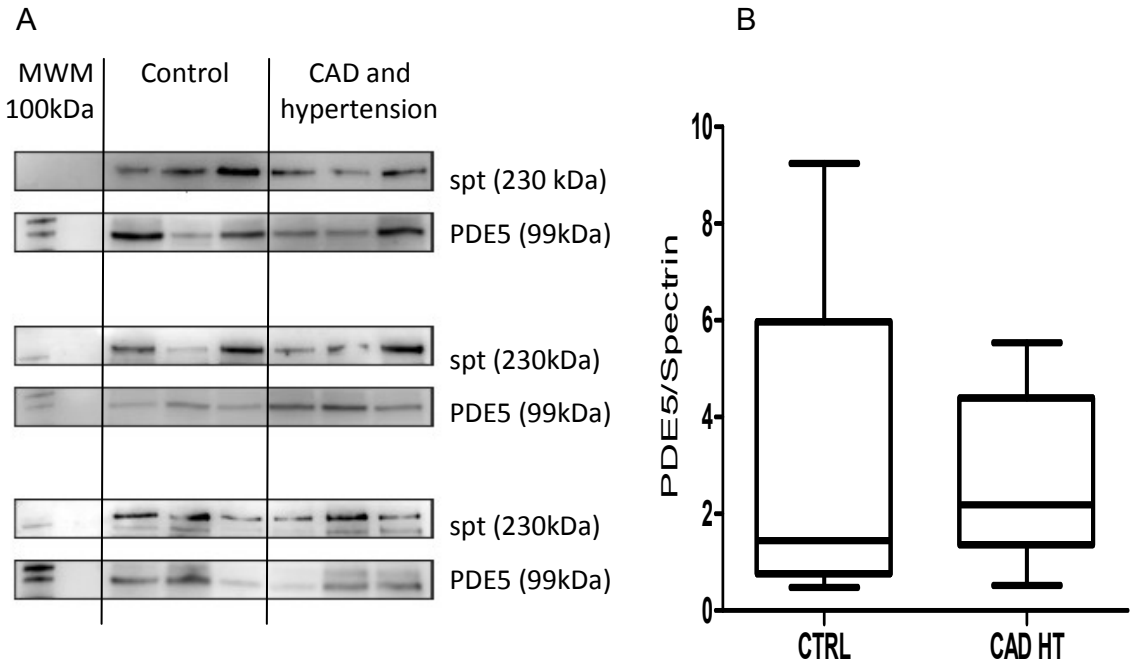

Figure 11: PDE5 in RBCs

PDE5 can be detected in mature human RBCs. The western blots (Fig 11 A) show the detection of PDE5 in different crude RBC lysates at the expected size of 99 kDa. Controls were loaded with crude RBC lysates from healthy test persons. The other lanes were loaded with crude human RBC lysates from patients with hypertension and cardiovascular disease. Spectrin was used as a loading control. Figure 11 B compares spectrin dependent amounts of PDE5 between healthy test persons and the patient group. Amounts were calculated from band intensities (Fig 11 A). n=9; p = 0.705; CTRL = control; CAD + HT = coronary artery disease and hypertension; PDE5 = phosphodiesterase 5; RBCs = red blood cells; spt = spectrin.

The visualization of PDE5 was followed by a study, which examined the amounts of PDE5 in mature RBCs from healthy test persons and patients suffering from CAD and hypertension. Figure 11 B shows the amounts of PDE5 in RBC lysates,

which were calculated from band intensities that can be seen in Figure 11 A. Volumes of PDE5 of each lane were set up to spectrin of the same lane. The results of this examination do not show significant differences between both groups. Western blot results show that PDE5 can be detected in RBCs from healthy test persons and in RBCs from patients who suffer from hypertension and CAD.

3.2 PRKG activity in RBCs

The western blot analysis revealed that PRKG1 can be detected in mature human RBCs. To analyze possible PRKG1 activity in mature human RBCs a PRKG1 assay kit was used. The establishment of the protocol was performed with lysed RBCs from young and healthy donors.

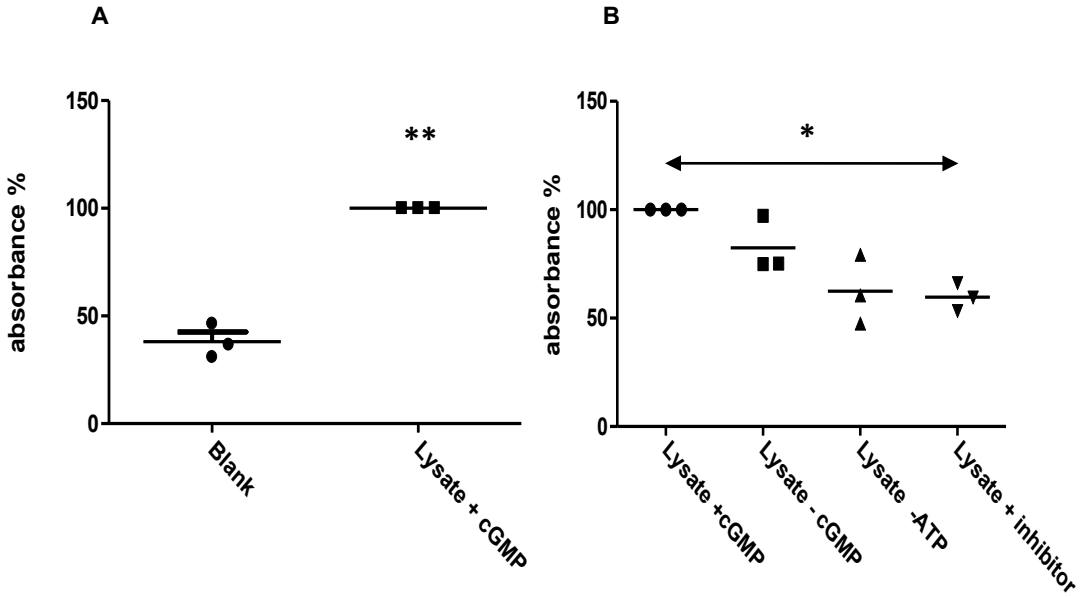

Figure 12: Activity of PRKG

An active PRKG can be detected in mature human RBCs. A PRKG assay Kit, which bases on an ELISA, coupled to an enzymatic assay, was used to measure PRKG activity in RBCs. Relative activity of PRKG was calculated from absorbance, measured with a photometer. The results indicate that mature human RBCs contain a functional PRKG. Compared to blank samples that were treated with the incubational solution but without RBC lysates, the incubation with RBC lysates causes a significant increase of absorbance. Inhibition of PRKG causes a significant decrease in absorbance. Fig 12 A: n=3; ** $p = 0.0053$; Fig 12 B: n=3; ANOVA $p < 0.05$; Bonferroni vs CTRL * $p < 0.05$; ATP = adenosine triphosphate; cGMP = cyclic guanosine monophosphate; ELISA = enzyme linked immunosorband assay; PRKG = protein kinase G; RBCs = red blood cells.

Pre coated plates used for the ELISA contained target molecules that can be phosphorylated by PRKG family members. The level of phosphorylation is measured as absorbance in a photospectrometer. Lysed RBCs from young and healthy donors were used as a substrate to catalyze the phosphorylation of target molecules.

Incubation with lysed RBCs causes a significant increase in absorption (Fig. 12 A). Incubation with a control solution did not increase absorption. Increased absorption can also be seen when lysed RBCs are not co incubated with cGMP or ATP (Fig. 12 A). These results did not reach significance. To ensure that the increase of absorbance was not caused by a different member of the PRK family, a specific inhibitor of PRKG, K252a, was added to the lysates (Fig. 12 B, fourth column). Compared to the untreated lysate (Fig. 12 B first column) a significant decrease of absorbance can be observed (Fig. 12 A).These are unreported novel findings, which indicate that mature human RBCs contain a functional PRKG.

3.3 Regulation of eNOS in RBCs

In order to investigate the influence of shear stress on eNOS activity in RBCs, ectacytometric and flowcytometric measurements were performed in parallel on the same sample. To fit with the other experiments, shear rates between 0.3 and 30 Pa were applied for 30 s. Compared to controls, which have not been exposed to shear stress, an increase of fluorescent signal can be observed. The fluorescent signal significantly peaks at 0.3 Pa. At 1.5 Pa and 3 Pa values also reached significance. At 10 Pa the fluorescent signal was increased but did not reach significance (Fig. 13). Results represent mean fluorescent signal measured in 30.000 cells ± SD. Increased signals are equivalent to increased activation of eNOS. To take into account autofluorescence of RBCs, all experiments were performed in parallel without incubation with DAF-FM-DA. Basal fluorescent signals were subtracted from data obtained in flowcytometry.

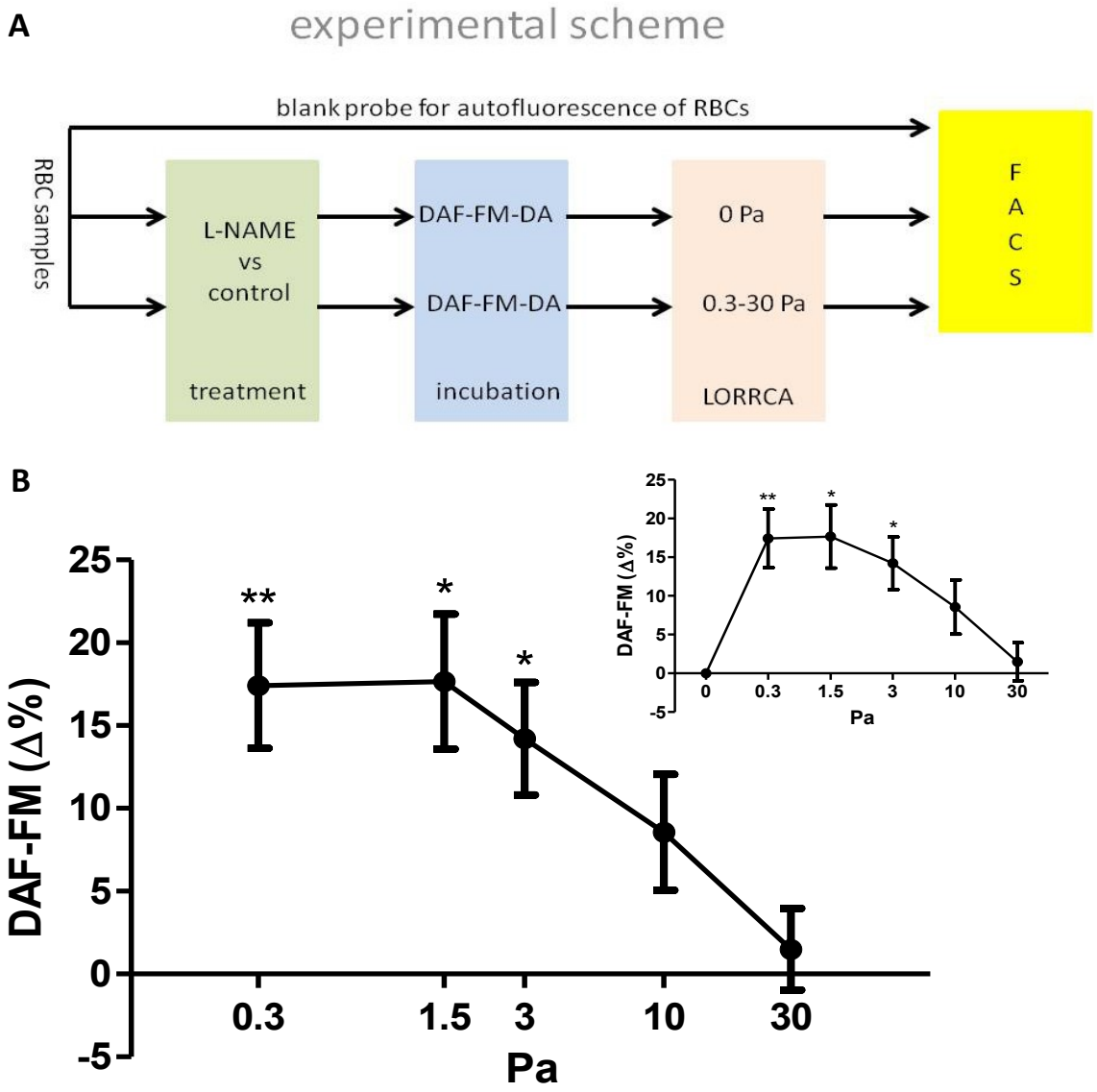

Figure 13: Shear stress induces intracellular fluorescence

Figure A illustrates the experimental setup, which combines LORRCA and flowcytometric analysis. RBCs were first treated with or without L-NAME and then incubated with DAF-FM-DA. Aliquots of every sample were then either not exposed to shear stress or to different levels of shear stress ranging between 0.3 and 30 Pa. Then flowcytometric analyses were performed to measure fluorescent levels. Figure B illustrates the fluorescent signal of DAF-FM versus shear stress on log scale. It reveals different fluorescent levels depending on the degree of shear stress. Shear stress significantly induces increased levels of NO within RBCs at 0.3, 1.5 and 3 Pa. In order to exclude autofluorescence signals of RBCs, one aliquot of every blood sample served as blank sample. The inset also illustrates the control at 0 Pa on a non-log scale. Data represent the blank corrected delta mean ± SEM in %; n=6; ANOVA $p < 0.0001$; Bonferroni vs. CTRL * $p < 0.05$; ** $p < 0.001$; DAF-FM-DA = 4-Amino-5-methylamino-2.7-difluorescein-diacetat; L-NAME = N^G-Nitro-L-arginine-methyl ester. HCl; LORRCA = Laser assisted optical rotational red cell analyzer; NO = nitric oxide; Pa = pascal; RBCs = red blood cells.

The treatment with L-NAME causes significant lower fluorescent signals at all levels of shear stress (Fig. 14). The result indicates that fluorescent signals, which have been measured in flowcytometric analyses, were due to increased eNOS activity.

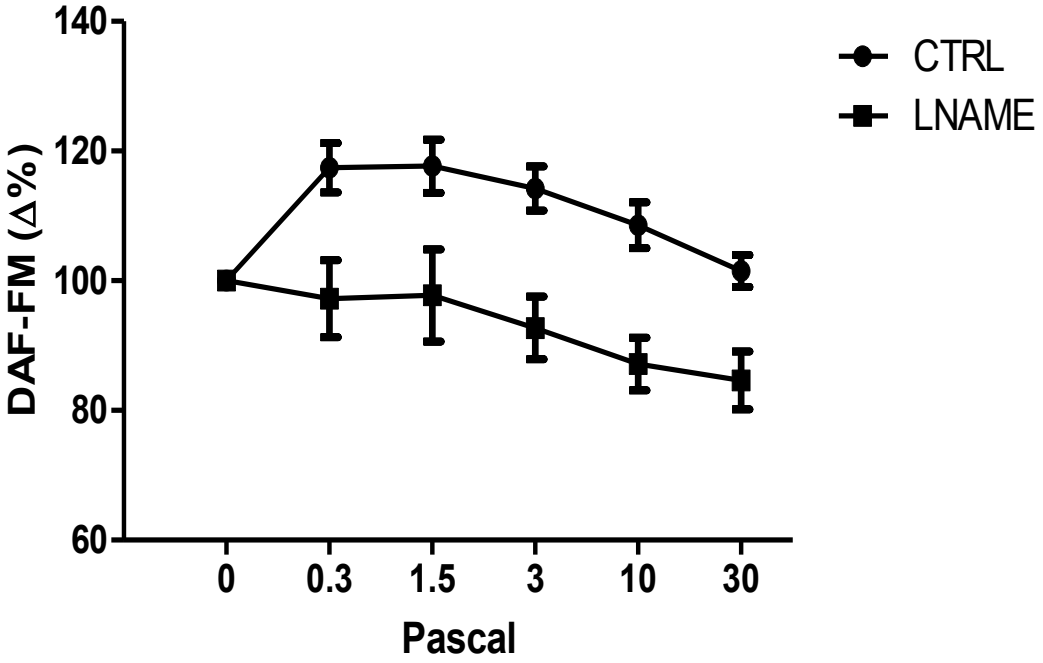

Figure 14: L-NAME significantly reduces DAF dependent fluorescence

Inhibition of endothelial eNOS within RBCs significantly reduces the formation of NO at all levels of shear stress. RBCs have been incubated with or without LNAME [3 mM]. Subsequently RBCs were treated with DAF-FM DA. Following the incubation RBC were exposed to different levels of shear stress for 30 seconds. The results indicate that changes in fluorescent signals of DAF-FM were due to changed activation of eNOS at different levels of shear stress. Data represent the blank corrected mean. n=6; Paired ANOVA $p < 0.0001$; Bonferroni vs. CTRL *$p < 0.05$; ** $p < 0.001$; DAF-FM-DA = 4-Amino-5-methylamino-2,7-difluorescein-diacetate; eNOS = endothelial nitric oxide synthase; L-NAME = N^G-Nitro-L-arginine-methyl ester. HCl; NO = nitric oxide; RBCs = red blood cells.

3.4 Effects of eNOS signaling on RBC deformability

The eNOS signaling pathway, which is known from the vasculature, consists of eNOS, sGC and PRKG1. Western blot analyses shown before illustrate that

mature human RBCs contain the same proteins, which are part of this classic eNOS signaling pathway.

To analyze the role of eNOS/ sGC/ PRKG1 signaling with regard to deformability of RBCs, ectacytometric measurements were performed. This work demonstrates the effects of eNOS, sGC and PRKG1 were at rising levels of shear stress. As expected for the controls, deformation increases with increasing levels of shear stress. Different EI values at given share rates illustrate changes in deformability due to treatment.

3.4.1 eNOS modulates deformability of RBCs

In a first step SperNO, a NO donor, was used to mimic the role of RBC-eNOS. RBCs from five healthy individuals were treated with SperNO. The deformability curve in figure 15 illustrates that SperNO increases deformability of RBCs compared to untreated controls. The strongest effect can be seen at low levels of shear stress (Fig. 15).

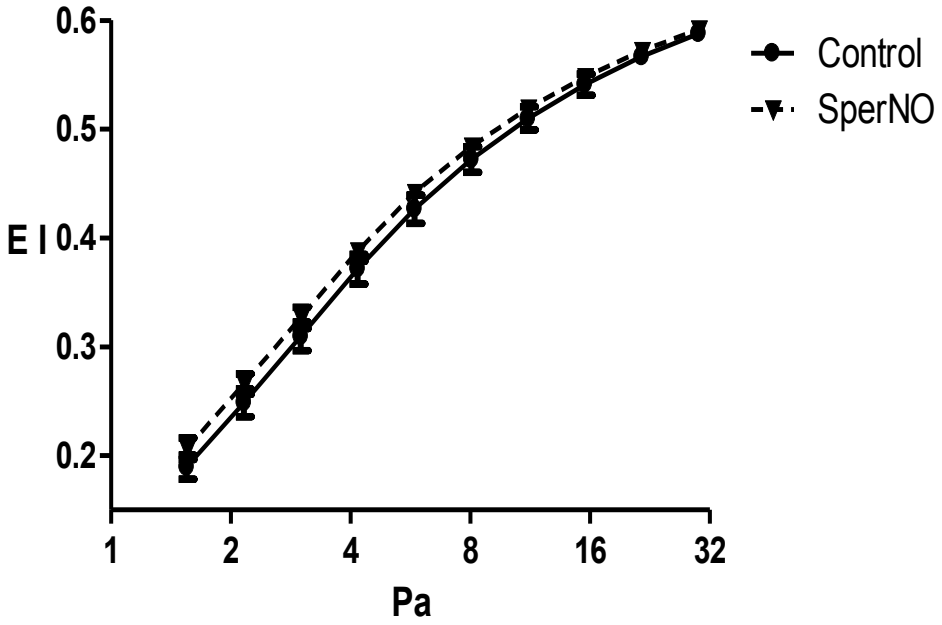

Figure 15: SperNO increases deformability of RBCs

The figure illustrates the EI with regard to shear stress. The EI of control RBCs were measured at different levels of shear stress and compared to SperNO [1 µM] treated RBCs. SperNO increases deformability of RBCs. Symbols are means ± SEM; n=5; EI = Elongation index; Pa = pascal; RBCs = red blood cells; SperNO = Spermine NONOate.

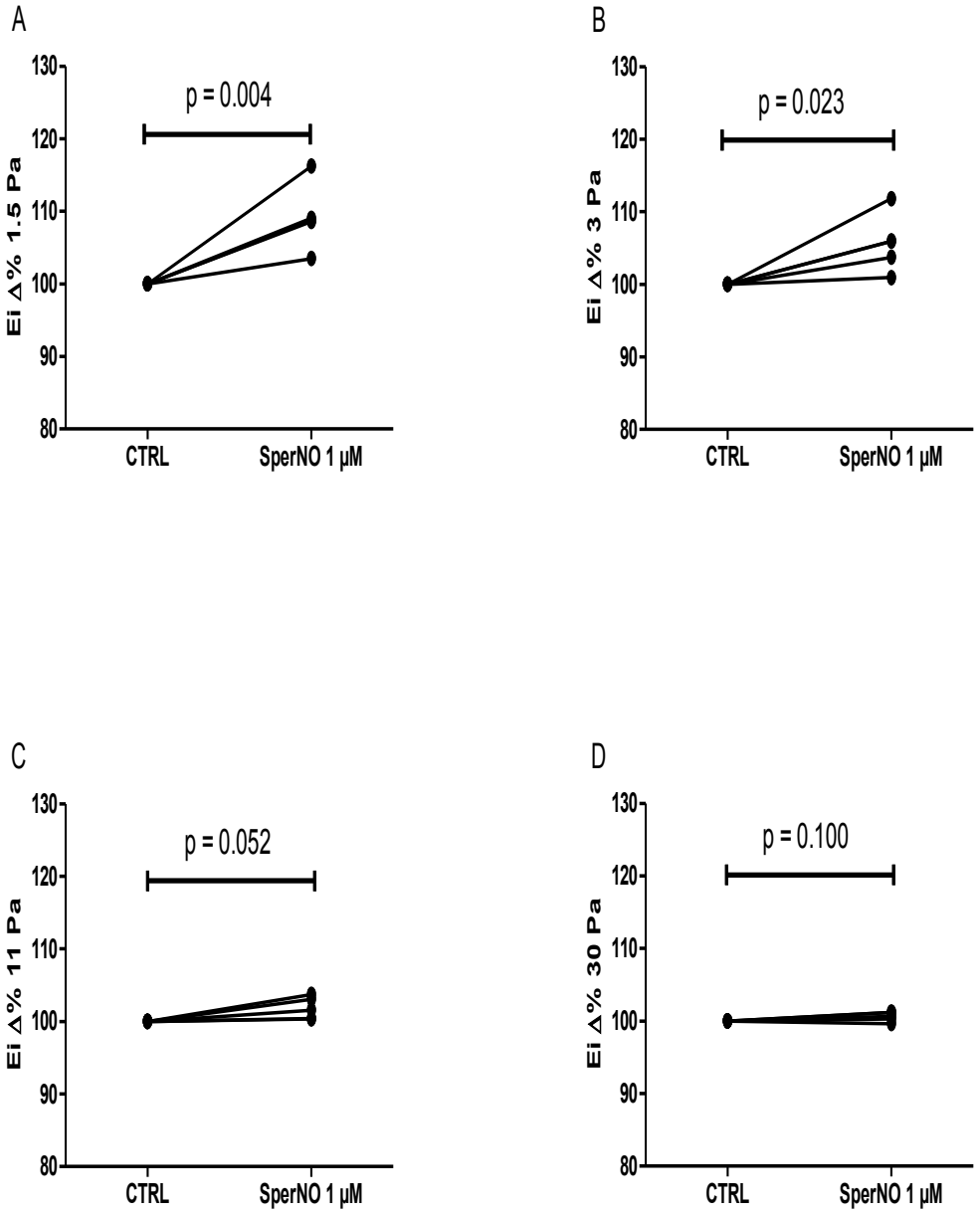

Figure 16: Deformability SperNO

SperNO [1 µM] significantly increases deformability of RBCs at low levels of shear stress (A, B). RBCs from young and healthy test persons were treated with SperNO. Deformability was measured at different levels of shear stress. Relative changes in the EI represent changes in deformability. A significant increase in deformability can be observed at 1.55 Pa and 3 Pa. SperNO does not increase deformability of RBCs significantly at high levels of shear stress. A: paired T-test; n=5; p = 0.004; B: paired T-test; n=5; p = 0.023; C: paired T-test; n=5; p = 0.052; D: paired T-test; n=5; p = 0.100; EI = elongation index; Pa =pascal; RBCs = red blood cells; SperNO = Spermine NONOate.

SperNO increases RBC deformability significantly with the greatest effect at 1.5 Pa (P=0.0044). At 3 Pa SperNO also causes a significant increase in deformability (P=0.023). At 11 Pa and 30 Pa deformability of RBCs was not affected significantly by SperNO (Fig. 16). The results show that increased levels of NO improve deformability.

3.4.2 Effects of sGC on deformability of RBCs

To investigate the effect of sGC on deformability, RBCs were treated with ODQ [1 µM]. The deformability curve illustrates that ODQ decreases deformability of RBCs compared to untreated controls (Fig. 17).

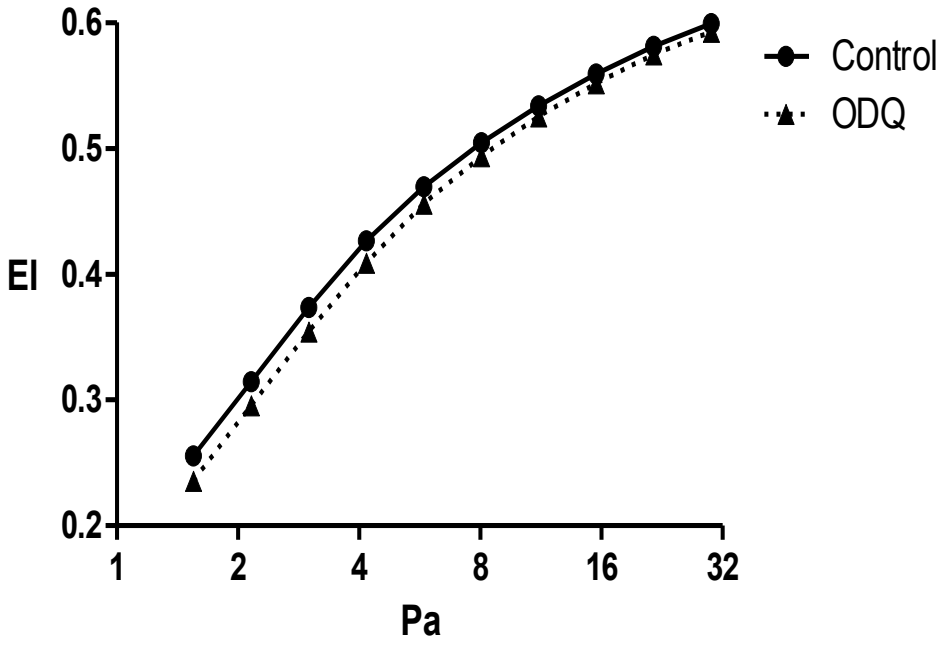

Figure 17: ODQ reduces deformability of RBCs

The figure illustrates the EI with regard to shear stress. The EI of control RBCs were measured at different levels of shear stress and compared to ODQ [1 µM] treated RBCs. ODQ decreases deformability of RBCs. Symbols are means ± SEM (not visible); n=5; EI = Elongation index; ODQ = 1H-[1,2,4]oxadiazolo[4,3-a] quinoxalin-1-one; Pa = pascal; RBCs = red blood cells.

ODQ shows the strongest effect on deformability at 1.5 Pa followed by 3 Pa (Fig. 18). At those shear rates ODQ significantly reduces deformability of RBCs. At 11

Pa and 30 Pa treatment with ODQ did not significantly reduce deformability. Yet a tendency of lowered deformability can be observed (Fig. 18).

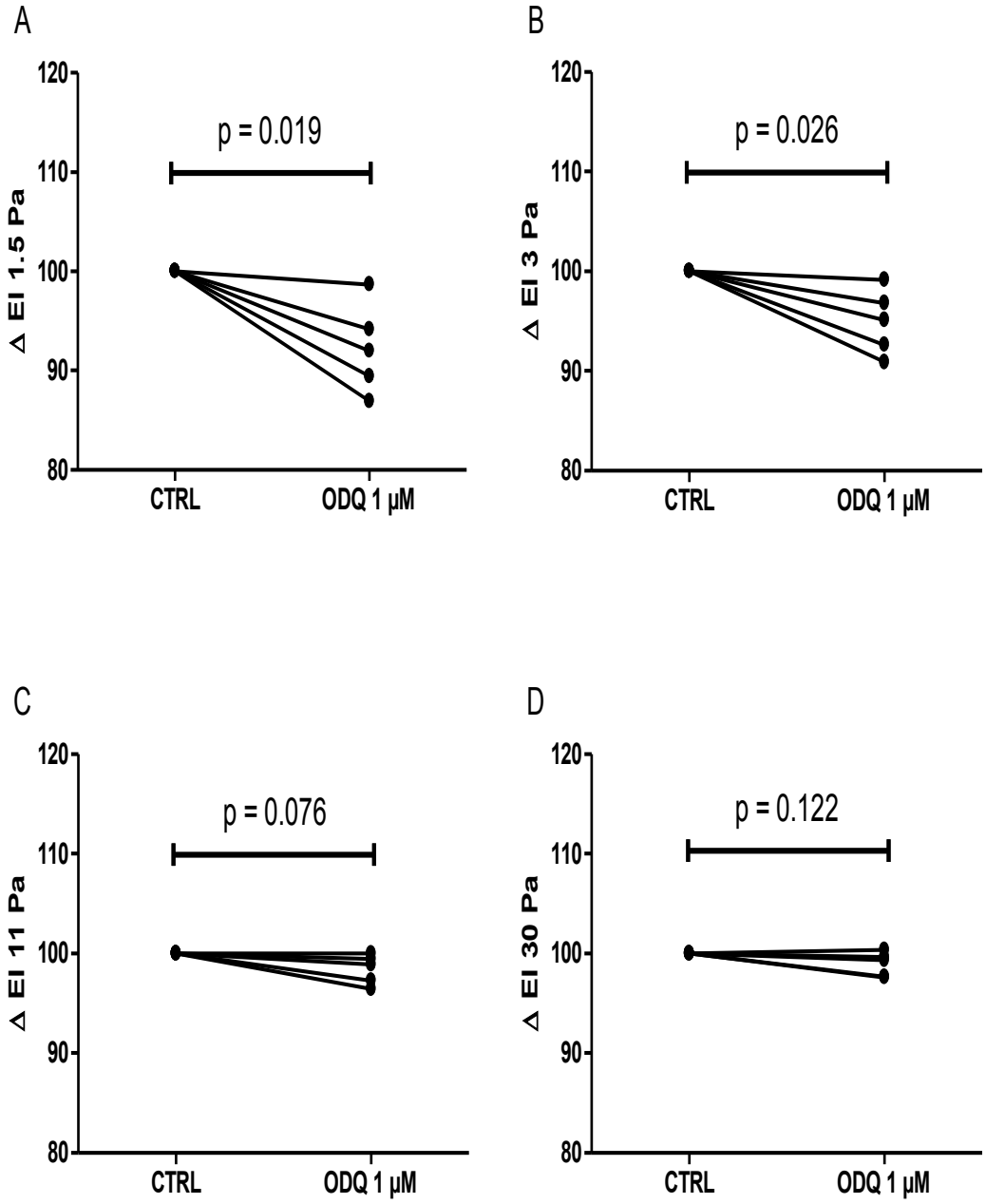

Figure 18: Deformability ODQ

ODQ [1 µM] significantly decreases deformability at low levels of shear stress. RBCs from young and healthy test persons were treated with ODQ. Deformability was measured at different levels of shear stress. Relative changes in the EI represent changes in deformability. A significant increase in deformability can be observed at 1.55 Pa and 3 Pa. A: paired T-test; n=5; p = 0.0190; B: paired T-test; n=5; p = 0.0255; C: paired T-test; n=5; p = 0.076; D: paired T-test; n=5; p = 0.122; EI = Elongation index; ODQ = 1H-[1,2,4]oxadiazolo[4,3-a] quinoxalin-1-one; Pa = pascal; RBCs = red blood cells.

3.4.3 Effects of cGMP on deformability of RBCs

This work for the first time shows that cGMP affects deformability of RBCs. RBCs were treated with 8-bromo-cGMP for 10 minutes. 8-bromo-cGMP is a cell permeable cGMP analog, which amongst other things activates PRKG1. Treatment with 8-bromo-cGMP causes an increase in deformability at all levels of shear stress that were applied (Fig. 19).

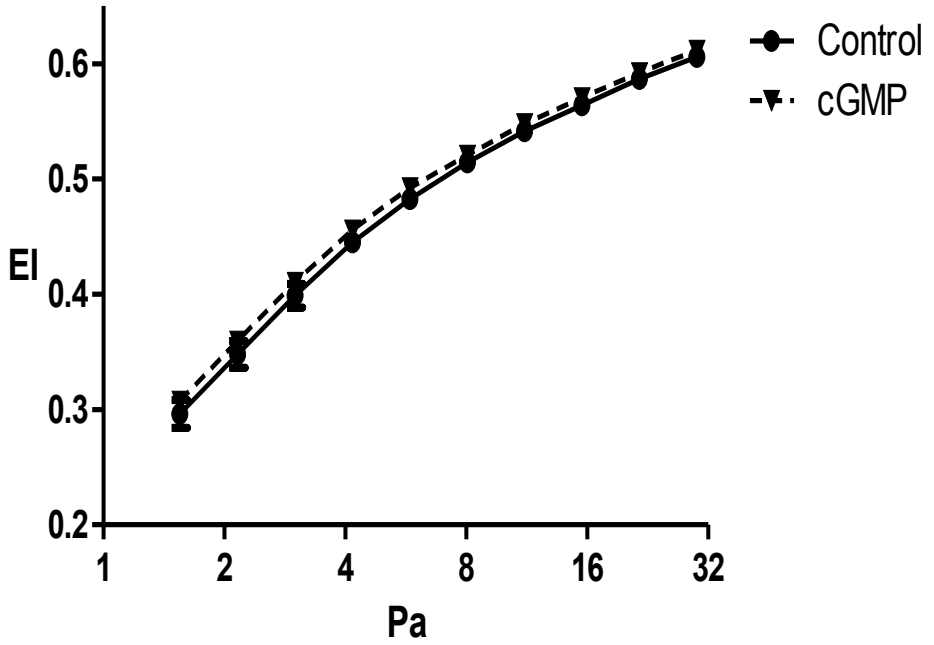

Figure 19: cGMP increases deformability

The figure illustrates the EI with regard to shear stress. The EI of control RBCs were measured at different levels of shear stress and compared to cGMP [100 µM] treated RBCs cGMP increases deformability of RBCs. Symbols are means ± SEM; n=5; cGMP = cyclic guanosine monophosphate; EI = Elongation index; Pa = pascal; RBCs = red blood cells.

cGMP shows the strongest effect on deformability at 3 Pa followed by 1,5 Pa. In contrast to SperNo and ODQ, the treatment with cGMP also caused significant changes in deformability at 11 Pa and 30 Pa (Fig. 20). RBCs that were treated with DT2, a competitive PRKG1 inhibitor, verifies the role of PRKG1 concerning deformability. The results show significantly lower EI-values at 1.55 Pa, 3 Pa and 11 Pa (Figs. 20,Figure 21). Taken together the results indicate that PRKG1 affects deformability of RBCs.

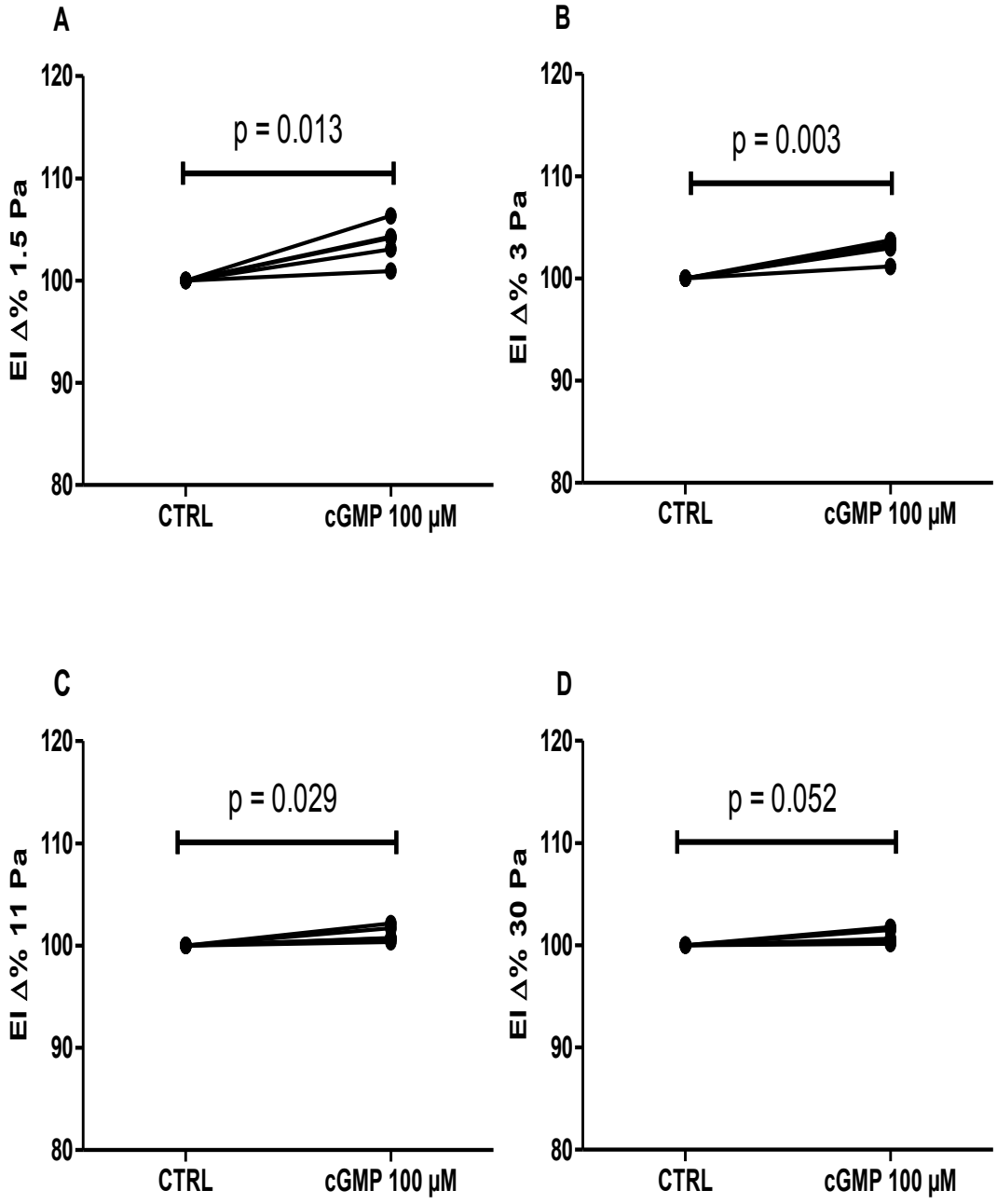

Figure 20: Deformability cGMP

8-bromo-cGMP significantly increases deformability at different levels of shear stress. RBCs from young and healthy test persons were treated with 8-bromo-cGMP. Deformability was measured at different levels of shear stress. Relative changes in the EI represent changes in deformability. A significant increase in deformability can be observed at all levels of shear stress. A: paired T-test; n=5; p=0.013, B: paired T-test; n=5; p=0.003; C: paired T-test; n=5; p=0.029; D: paired T-test; n=5; p=0.052; cGMP = Cyclic guanosine monophosphate; CTRL = control; EI = Elongation index; Pa = pascal; RBCs = red blood cells.

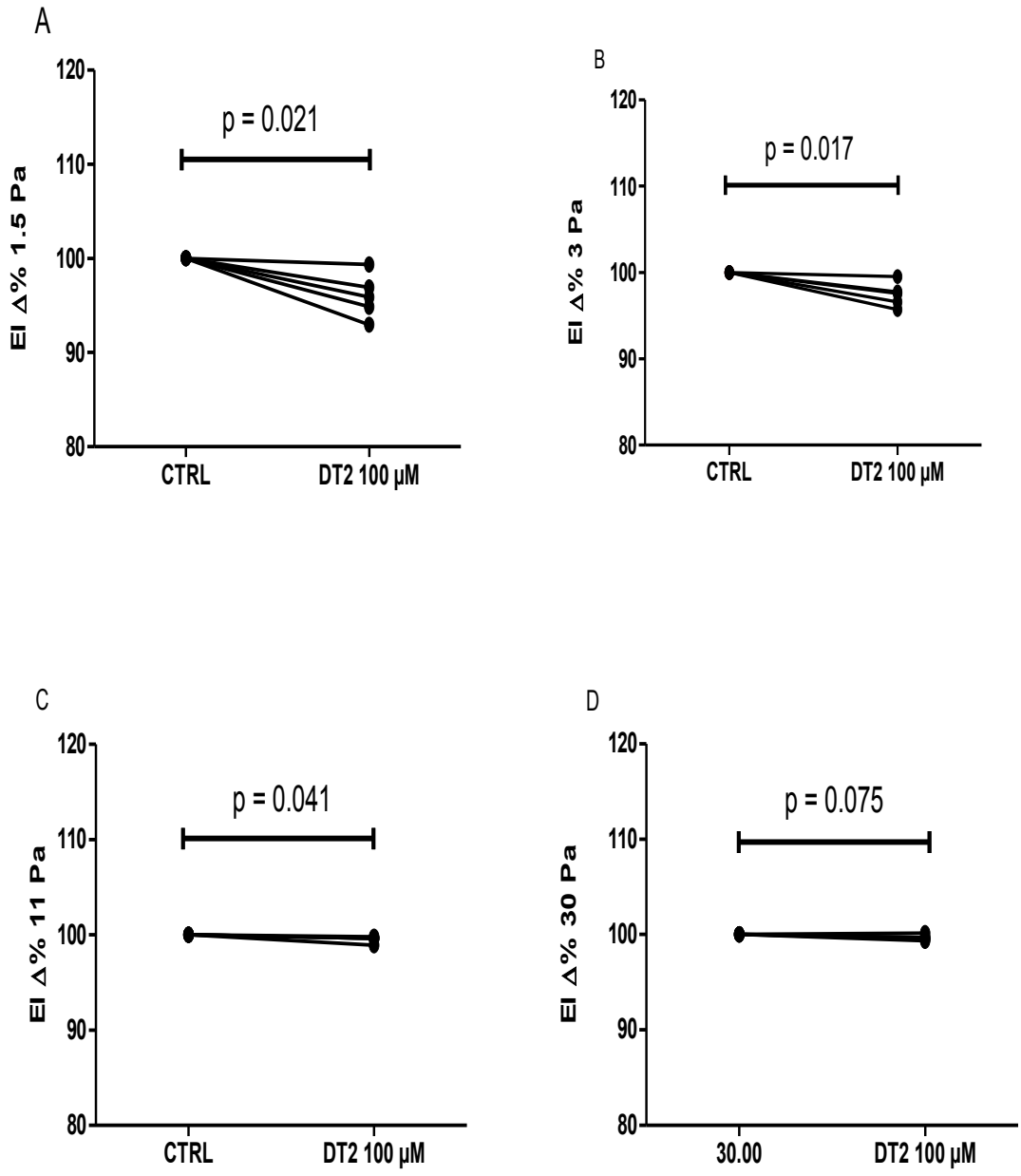

Figure 21: Deformability DT2

DT2 significantly reduces deformability of RBCs. RBCs from young and healthy test persons were treated with DT2 [100 µM]. Deformability was measured at different levels of shear stress. Relative changes in the EI represent changes in deformability. A significant increase in deformability can be observed at all levels of shear stress. A: paired T-test; n=5; p=0.021; B: paired T-test; n=5; p=0.017; C: paired T-test; n=5; p=0.041; D: paired T-test; n=5; p=0.075; CTRL = control; DT2 = DT2-trifluoracetate salt; EI = Elongation index; Pa = pascal; RBCs = red blood cells.

3.5 eNOS Signaling Regulates Pannexin1 in RBCs

3.5.1 Proof of concept

Pnx1 is a transmembrane pore, which allows ATP efflux from cells. Flowcytometric measurements were performed in order to investigate effects of eNOS signaling on Pannexin1 in RBCs. CF-DA was tested in combination with carbenoxolone, an inhibitor of pnx1, to validate the experimental setup. Obtained results reveal a significant correlation between increased fluorescence signal within RBCs and carbenoxolone concentrations. This correlation reassures the experimental setup and allows the interpretation of results (Figs. 22, 23).

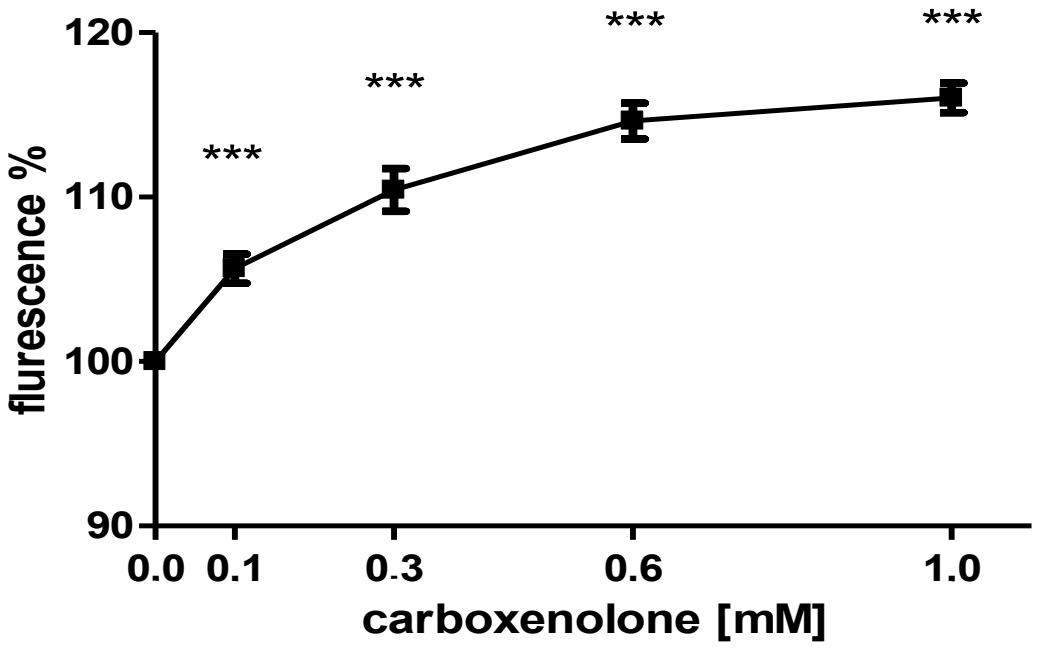

Figure 22: Carbenoxolone closes pnx1 in a dose dependent manner

Closure of pnx1 due to carbenoxolone causes a dose depending increase of fluorescence. Fluorescent intensity emitted by intracellular entrapped CF is measured by flowcytometric analyses. Data represent relative fluorescence after correction for autofluorescence of RBCs. Carbenoxolone is a reversible inhibitor of pannexin1. n=9; symbols are means + SEM; paired ANOVA $p < 0.0001$; Bonferroni vs CTRL *** $p < 0.0001$; CF = 5-carboxyfluorescein; pnx1 = pannexin 1; RBCs = red blood cells.

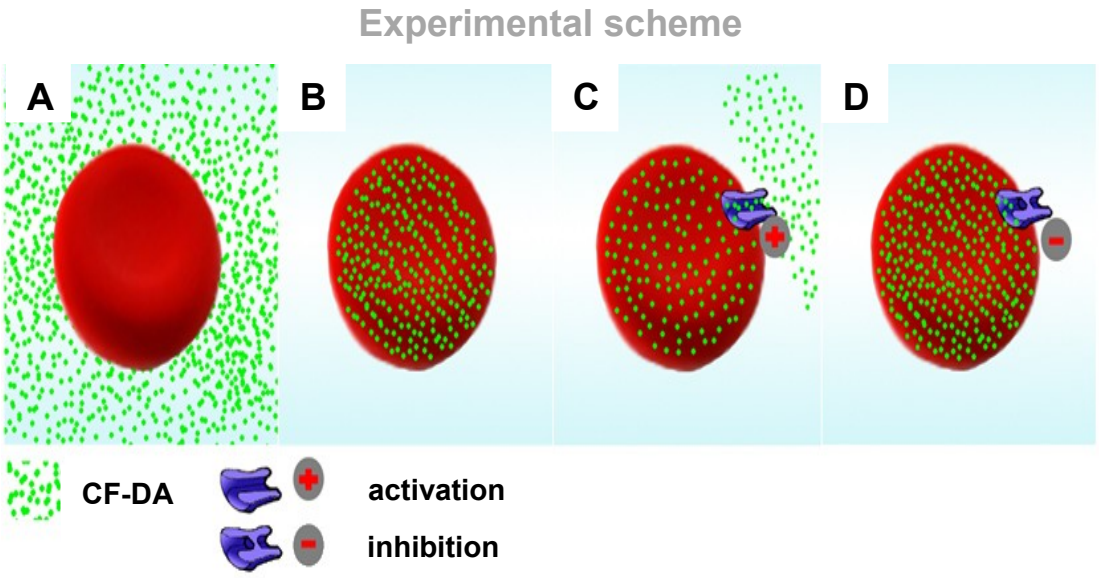

Figure 23: Experimental scheme

The figure illustrates the incubation of RBCs with CFDA (A). CFDA is able to cross the cell membrane in a concentration dependent manner. Once inside a cell (B), CFDA is only able to leave RBCs via pnx1 due to deacetylation. Activation of pnx1 causes a loss of fluorescent molecules within RBCs (C). Inhibition of pnx1 causes increased concentrations of fluorescent molecules inside RBCs (D). Flowcytometric analysis allows to measure fluorescent signals within RBCs. CF-DA = 5-carboxyfluorescein-diacetate; RBCs = red blood cells; pnx1 = pannexin 1.

3.5.2 Inhibition of eNOS closes CF-DA gating channels in RBCs

Different proteins of the eNOS signaling pathway have been activated or inhibited and the fluorescent intensity of entrapped CF was measured to investigate the effects of eNOS signaling on CF gating channels in RBCs. The treatment of RBCs with L-NAME, a competitive inhibitor of NOS, led to an increase of fluorescence intensity in a dose dependent manner (Fig. 24). The fluorescence intensity at 0,5 mM was higher than in the controls but did not reach statistical significance (P= 0.0822). Significant changes can be observed at 0.3 mM (P= 0.0442), 1 mM (P= 0.0165), 3 mM (P= 0.0004) and 5 mM (P= 0.0004). The results show that inhibition of NOS leads to closure of CF gating channels. At higher concentrations L-NAME develops an inhibitory effect comparable to the effects produced by carbenoxolone.

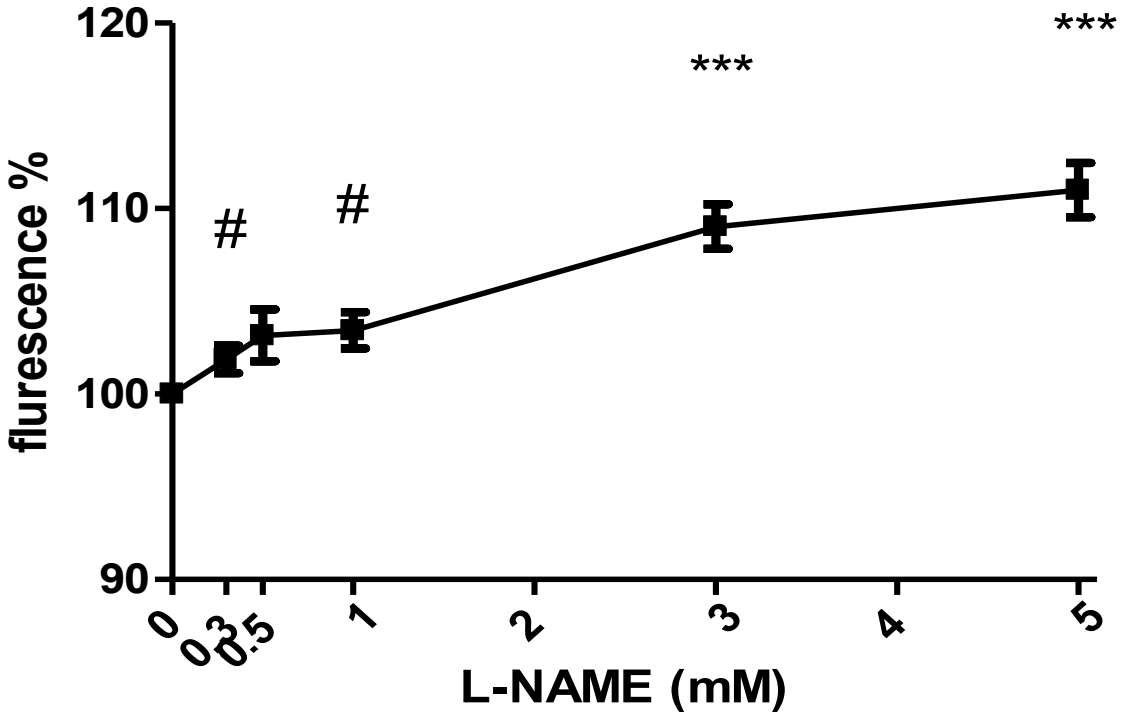

Figure 24: L-NAME closes pnx1in a dose dependent manner

L-NAME causes a dose depending increase of fluorescence. Fluorescent intensity emitted by intracellular entrapped CF is measured by flowcytometric analyses. Data represent relative fluorescence after correction for autofluorescence of RBCs. L-NAME is a competitive inhibitor of eNOS. n=7; symbols are means +SEM; paired ANOVA $p < 0.0001$; Bonferroni vs CTRL *** $p < 0.0001$; # T-Test vs CTRL $p < 0.05$. CF = 5- carboxyfluorescein; eNOS = endothelial nitric oxide synthase; L-NAME = N^G-Nitro-L-arginine-methyl ester. HCl; RBCs = red blood cells.

In the next step 8-bromo cGMP was used in order to mimic the effect of an activated sGC. A decrease of fluorescent intensity was measured in a dose dependent manner after the treatment with 8-bromo-cGMP (Fig. 25). Significant changes can be observed at 0.1 mM ($P= 0.0341$), 0.5 mM ($P < 0.0004$) and 1 mM ($P < 0.0001$). The results for the first time show that cGMP either directly or via activation of PRKG1 affects CF gating channels in RBCs.

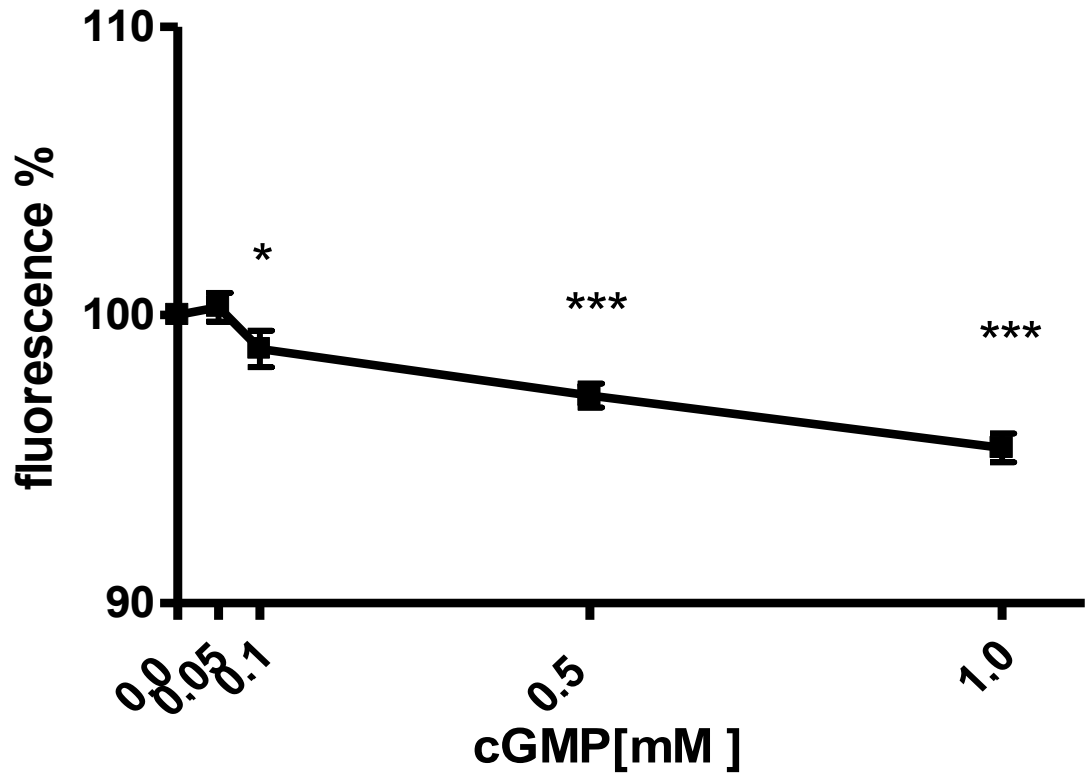

Figure 25: cGMP opens pnx1 in dose dependent manner

8-bromo-c-GMP causes a dose depending decrease of fluorescence. Fluorescent intensity emitted by intracellular entrapped CF is measured by flowcytometric analyses. Data represent relative fluorescence after correction for autofluorescence of RBCs. c-GMP is an activator of PRKG1. n=6; symbols are means + SEM; paired ANOVA $p < 0.0001$; Bonferroni vs CTRL ** $p < 0.001$; *** $p < 0.0001$; cGMP = cyclic guanosine monophosphat, CF = 5-carboxyfluorescein, RBCs = red blood cells.

DT2 was used to investigate PRKG1´s role in cell signaling. DT2 is a competitive inhibitor of PRKG1. Different concentrations of DT2 were tested. A significant increase of fluorescent intensity can be observed at 0.05 mM (n=9; P= 0.0008). Other concentrations did not cause significant changes (Fig. 26). Taken together, these results show that CF gating channels in RBCs depend on eNOS/ sGC/ PRKG1 signaling.

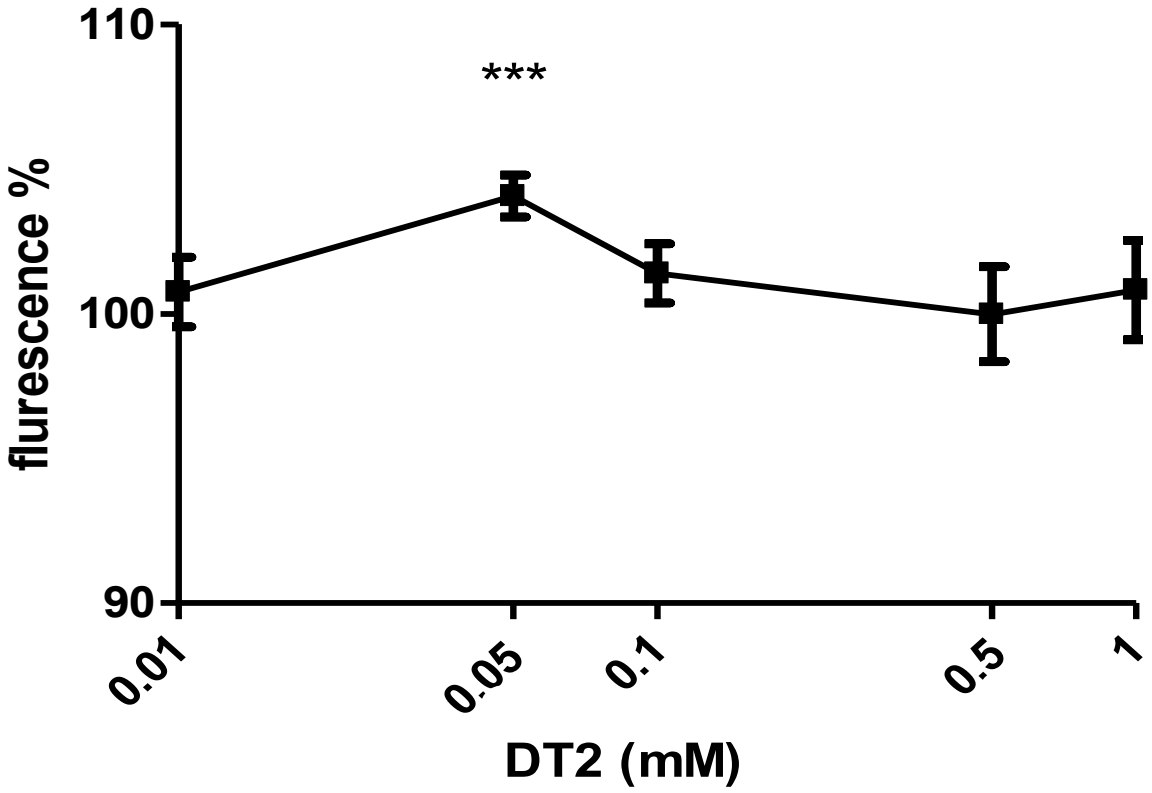

Figure 26: DT2 closes pannexin 1

DT2 causes a significant increase of fluorescence at a concentration of 0.05 mM. DT2 is an inhibitor of PRKG1. Fluorescent intensity emitted by intracellular entrapped CF is measured by flowcytometric analyses. Data represent relative fluorescence after correction for autofluorescence of RBCs. n=6, symbols are means + SEM; paired ANOVA p = 0.0004; Bonferroni vs CTRL *p < 0.05; CF = 5-carboxyfluorescein; DT2 = DT2-trifluoracetate salt; PRKG1 = protein kinase G 1; RBCs = red blood cells.

4 Discussion

This work investigated the presence of a full and functional eNOS/ sGC/ PRKG1 signaling pathway in mature human RBCs. It was driven by the hypothesis that eNOS/ sGC/ PRKG1 signaling influences RBC deformability and ATP release from RBCs.

The main findings of this work are:

1) sGC and PRKG1 can be found in mature human RBCs.
2) Shear stress induces eNOS dependent NO production.
3) eNOS/ sGC/ PRKG1 signaling modulates deformability of RBCs.
4) eNOS/ sGC/ PRKG1 signaling is involved in the control of membrane permeability of RBCs.

4.1 Mature human RBCs carry a sGC

Western blot analyzes shown in the present work provide new evidence for the presence of sGC in mature, human RBCs (Fig. 9). Using anti alpha-sGC antibodies a 77 kDa band was identified, which is the estimated size of the alpha subunit of sGC. The main technical hurdle for visualization of proteins in mature RBCs is the presence of extremely high levels of hemoglobin (Cortese-Krott et al., 2012b). High levels of hemoglobin can cause a high background after western blotting. In order to avoid these problems, the protein concentrations were optimized. All lysates were analyzed and different amounts of crude RBC lysates were used for western blot analyses. Final experiments were performed with 500 µg of crude red cell lysate. To the best of my knowledge results presented here for the first time illustrate that the alpha subunit of sGC can be found in mature human RBCs.

Previous studies used northern blot analyses to show that sGC can be found in erythroid progenitor cells. Ikuta et al. revealed the presence of both an alpha and a beta subunit of sGC in these cells (Ikuta et al., 2001). Since mature RBCs do not carry a nucleus, northern blot analyses cannot be performed on mature RBCs. Thus, these results cannot be taken as a confirmation for the presence of sGC in mature RBCs.

sGC consists of two subunits, which form a heterodimer. The presence of both subunits is crucial for a functional protein (Winger and Marletta, 2005). Western blot analyses presented in this work reveal the presence of an alpha subunit of sGC in RBCs. Results presented later in this work reveal that activators and inhibitors of sGC influence deformability and regulate pnx1. The presence of an alpha subunit of sGC in mature human RBCs together with the results presented later, provide strong evidence that mature human RBCs carry a functional sGC.

Western blot analyses were performed on mature human RBCs from healthy donors and on RBCs from patients who suffer from hypertension and CAD. The comparison of both groups was performed to detect possible differences in protein levels between the groups. In 2012 a study revealed a lower expression of eNOS in RBCs from patients who suffer from CAD and hypertension. Furthermore, this study showed an impaired function of RBC-eNOS in patients who suffer from CAD and hypertension (Cortese-Krott et al., 2012b). In pulmonary vasculature eNOS influences the gene expression of sGC. An upregulation of sGC gene expression in mice can be seen due to hypoxia. This effect is diminished in eNOS KO mice (Li et al., 2001). According to the results by Li et al. this work investigates whether an impaired function of RBC-eNOS, which can be seen in patients who suffer from CAD and hypertension, also influences the protein levels of sGC in mature human RBCs. The results presented here do not reveal significant differences between both groups. This result indicates that hypertension and CAD do not lead to lower protein levels of sGC in mature human RBCs.

4.2 Mature human RBCs carry a PRKG1 and show PRKG activity

Results presented previously showed that RBCs carry the alpha subunit of sGC. In order to understand the role of NO and cGMP signaling in RBCs, the presence of PRKG1 has been investigated. Western blot analyzes were performed to visualize PRKG1 in mature, human RBCs. The activity of PRKG has been determined with a PRKG activity assay. Taken together, both analyzes point towards the presence of an active PRKG1 in mature, human RBCs (Fig. 10, 12). The presence of an active PRKG1 in mice RBCs has been demonstrated by Feil et al. They investigated the effects of PRKG1 on the survival of RBCs in mice. In peripheral

RBCs and erythroid cells from the bone marrow of mice they were able to visualize PRKG1 by western blot analyses. They also found that the number of RBCs, hematocrit and hemoglobin were significantly reduced in PRKG1 KO mice compared to control animals. Both results provide strong evidence that an active PRKG1 can be found in mature RBCs of mice (Föller et al., 2008).

The present work tried to identify PRKG1 in mature, human RBCs. For western blot analyses different ABs have been tested to visualize PRKG1. The ABs were not specific for amino acid sequence 1-89 of the protein. It is important to note that PRKG1 alpha and beta only differ in this specific sequence. Therefore, it is not possible to distinguish between PRKG1 alpha and beta. The antibody that was finally used in western blot is directed against a recombinant fragment of the protein that corresponds to amino acids 1-686 of the human protein. It detected plain bands at 77 kDa, which is the estimated size of PRKG1 (Fig. 10). To the best of my knowledge, this is the first time that PRKG1 has been visualized in mature human RBCs. Liquid chromatography-mass spectrometry has to be performed to check for the presence of either an alpha or a beta splice variant. Both splice variants are specific for different target proteins (Butt et al., 1993).

Similar to the successful visualization of sGC, the visualization of PRKG1 in mature RBCs was followed by a study that compared the protein levels of PRKG1 in RBCs from healthy test persons and patients who suffer from CAD and hypertension. The study compared the protein levels of nine test persons in each group and revealed no significant differences between the groups (Fig 10).

The activity of PRKG in mature RBCs has been investigated with a PRKG activity assay. The results of the activity assay reveal a significant increase of phosphorylated target peptides after the incubation with RBC lysates from healthy donors (Fig. 12). In this work the assay was performed with crude RBC lysates. In order to exclude unspecific phosphorylation of the target protein different controls have been included. A specific inhibitor of PRKG has been used to ensure that increased target phosphorylation is due to PRKG. Inhibition of PRKG causes a significant decrease in target phosphorylation (Fig. 12). The PRKG family includes an alpha and beta splice variant of PRKG1 as well as the membrane bound PRKG2. The inhibitor, which has been used, does not discriminate between

PRKG1 and PRKG2. It has to be noted that PRKG2 has not yet been detected in mature human RBCs. Western blot analyses with an AB directed against PRKG2 that were performed in our group did not reveal the presence of PRKG2. Taken together the results presented in this work for the first time adduce strong evidence that mature human RBCs contain a functional PRKG1.

4.3 Expression pattern of PDE5 in RBCs

In order to get a full picture of the eNOS signaling pathway in RBCs, the volumes of PDE5, another member of the eNOS signaling pathway, has been investigated. Similar to the detection of sGC and PRKG1 in mature RBCs, PDE5 was visualized by western blot analysis. The antibody detected clear bands at 99 kDa, which is the estimated size of PDE5 (Fig.11 A**Fehler! Verweisquelle konnte nicht gefunden werden.**). These results support the data presented by Adderley et al. in 2011. They were able to show that mature RBCs carry a PDE5, which contributes to eNOS signaling (Adderley et al., 2011). It was necessary to optimize an AB directed against PDE5 in order to receive a full picture of the expression patterns of proteins of the eNOS signaling pathway in RBCs.

For this study RBC lysates from nine patients suffering from hypertension and CAD were compared to nine healthy test persons. In contrast to the expression pattern of eNOS, the results of PDE5 in this study do not indicate a difference in protein expression between both groups. Similar to the results seen in sGC and PRKG1 an impaired function of eNOS does not seem to influence the gene expression of PDE5.

4.4 Low levels of shear stress activate eNOS in RBCs

The results presented here support the idea of a shear induced NO production within RBCs. Shear forces applied to RBCs in LORRCA cause a significant increase in fluorescence of DAF-FM at 0.3 Pa, 1 Pa and 3 Pa. Shear forces of 10 Pa and 30 Pa do not cause significant changes compared to unstressed controls.
Activation of eNOS in RBCs might cause an intracellular signaling cascade similar to the eNOS signaling cascade, which is known from vasculature. eNOS activates

sGC and subsequently sGC activates PRKG1. Bor-Kucukatay et al. investigated the effects of eNOS signaling on deformability. His group showed that eNOS and sGC modulate RBC deformability at shear stress below 5 Pa.

From vasculature it is commonly known that shear forces are able to activate eNOS. Ulker et al. suggested a similar activation of eNOS within RBCs. They investigated the activation of RBC-eNOS due to shear stresses in flow chamber. In this experimental setup RBCs were loaded with DAF-FM-DA and a significant increase of the fluorescent signal was observed when exposed to shear stresses ranging from 0,013 Pa to 0.1 Pa (Ulker et al., 2011).

Physiological shear stress in vasculature ranges from 0.1 Pa in the vena cava to 5.5 Pa in arterioles and around 4.5 Pa in capillaries (Papaioannou and Stefanadis, 2005, Lipowsky et al., 1980, 1978). In this work the effect of shear stress on RBC-eNOS activity has been explored at a broader scale of shear stress in order to match shear stress, which can be found in vasculature. The detection of NO in RBCs was performed with DAF-FM-DA and flowcytometric analyses. DAF-FM-DA is a commonly used fluorescent probe for NO levels (Cortese-Krott et al., 2012a). DAF-FM-DA is able to permeate cell membranes and inside a cell esterases cause the loss of two acetate groups and DAF-FM is trapped inside the cell. The use of DAF-FM-DA for the detection of NO levels in RBCs has been validated by our group beforehand. The shear stress was applied to RBCs with LORRCA.

Comparable to earlier results, this study indicates that formation of NO can be induced by shear stress. In contrast to Ulker et al. data reveals that activation of RBC-eNOS due to shear stress depends on the degree of shear stress, which is applied. These are unreported novel findings, which indicate a complex mechanism of shear induced activation of NO production within RBCs. Interestingly lower shear forces of 0.3 Pa, 1.5 Pa and 3 Pa cause a significant increased of NO levels. Higher shear forces of 11 Pa or 30 Pa do not cause a significant increase of NO levels.

4.5 eNOS, sGC and PRKG1 modulate deformability of RBCs

Modulation of eNOS / sGC / PRKG1-signaling influences deformability of RBCs (§ 3.4.1-3.4.3). This is an important regulatory mechanism, which allows RBCs to

pass smallest capillaries (Parthasarathi and Lipowsky, 1999). As shown before, shear stress is able to induce NO formation within RBCs at certain levels of shear stress. In order to find a possible link between eNOS activity within RBCs and deformability, ectacytometric analyses were performed at 1.5 Pa, 3 Pa, 11 Pa and 30 Pa. ODQ and DT2 significantly reduce deformability at lower levels of shear stress, which have been applied. Administration of SperNO and brome-cGMP significantly increases deformability significantly at low levels of shear stress.

These findings go along with results by different groups. Earlier findings show up a link between NO bioavailability in RBCs and RBC deformability (Baskurt et al., 1998). Another group found that eNOS signaling significantly influences deformability of RBCs at a shear rate of 1.58 Pa. L-NAME and ODQ significantly decrease deformability at 1.58 Pa while administration of SNP, a NO donor, significantly increases deformability (Bor-Kucukatay et al., 2003).

The present work investigates deformability at a broader scale of shear stress. ODQ and DT2 significantly reduce deformability at 1.5 Pa. Administration of SperNO, a NO donor, increases deformability significantly at 1.5 Pa. These findings served as a proof of concept for subsequent analyses. The following results for the first time show that administration of ODQ and SperNO significantly influence deformability at 3 Pa. Yet, ODQ and SperNO did not reach significance at shear stress of 11 Pa and 30 Pa.

Furthermore, the role of another eNOS-signaling cascade member has been investigated for the first time. In the past, investigations focused on eNOS and sGC as described before. This work for the first time examined the role of PRKG1 with regard to deformability. A cGMP analog has been used to activate PRKG1. Deformability significantly increases due to cGMP at 1.5 Pa, 3 Pa and 11 Pa. At 30 Pa values did not reach significance. Inhibition of PRKG1 with DT2 causes an inverse effect with significant values at 1.5 Pa, 3 Pa, and 11 Pa. These are unreported novel findings that coincide with the results concerning RBC-eNOS and sGC signaling and indicate that PRKG1 influences deformability.

Taken together, this work links shear induced activation of RBC-eNOS at low levels of shear stress and deformability of RBCs. It also points out that PRKG1 is an integral member of the signaling cascade, which affects deformability.

4.6 eNOS/ sGC/ PRKG1 signaling regulates pnx1 in RBCs

The results presented in this work reveal that eNOS/sGC/PRKG1-signaling takes part in the regulation of pnx 1 hemichannels in RBCs (Figs. 22, 24, 25, 26). Several studies in the past analyzed the role of pnx 1 hemichannels as ATP gating pores in RBCs and provided evidence that pnx 1 is the only or at least main ATP gating channel in RBCs (Locovei et al., 2006a, Forsyth et al., 2011). Different conditions were shown to influence ATP release from RBCs. Next to shear stress, extracellular ATP and low amounts of oxygen cause ATP efflux from RBCs (Locovei et al., 2006a, Forsyth et al., 2011, Sprague et al., 1998, Sridharan et al., 2010). ATP release due to extracellular ATP works via co-expression of P2Y receptors, which can be found on the surface of RBCs (Locovei et al., 2006b).
Inhibition of pnx 1 with carbenoxolone causes a reduced ATP release from RBCs (Forsyth et al., 2011) and reduced uptake of CF (Locovei et al., 2006a). Intracellular signaling cascades that regulate pnx1 have not been illustrated yet.

As discussed before, RBCs contain a complex and functional eNOS-signaling pathway. This pathway is closely linked to RBC deformability. Different groups were able to link RBC deformation and ATP release. RBCs forced through filter paper release more ATP than RBCs at basal conditions (Sprague et al., 2001b). These data first indicated that shear stress applied to RBCs might be a reason for ATP release. The connection between ATP release from RBCs and deformation of RBCs induced the hypothesis that eNOS-signaling might also influence pnx1.

A possible way to measure the effect of eNOS-signaling on pnx1 is to evaluate the efflux of ATP from RBCs under specific conditions like inhibition or activation of eNOS, sGC or PRKG1. Higher levels of extracellular ATP would indicate the activation of pnx1 and the other way around. The measurement of ATP release from RBCs is a very complex endeavor. ATP, which has been released from RBCs, undergoes degradation by ectonucleotidases, which can be found on the membrane surface of RBCs (Jensen et al., 2009). Therefore, direct ATP measurements performed with HPLC or indirect measurements with a bioluminescent luciferin/ luciferase solution can be falsified and difficult to be interpreted. Hemolyses is yet another problem that might falsify data.

In order to avoid these problems a fluorescent indicator dye was used. Locovei et al. established carboxyfluorescein (CF) as a fluorescent dye and patch clamp techniques for pnx1 analyses (Locovei et al., 2006). In this work a new modified flowcytometric analysis has been established to analyze the role of pnx1 with regard to ATP release from RBCs in response to eNOS-signaling. As a proof of concept, RBCs were treated with carbenoxolone first. This caused significantly increased fluorescent signals within RBCs compared to untreated controls (Fig. 22). This result coincides with reduced ATP release and reduced CF uptake due carbenoxolone. The treatment with L-NAME causes a significant concentration dependent increase in fluorescence (Fig. 24). L-NAME inhibits the formation of NO by eNOS and therefore indicates that eNOS and the activation of sGC are important for the activation of pnx1 in RBCs.

Another indicator for the importance of an active sGC is the treatment of RBC with 8-bromo-cGMP. The cell permeable cGMP analog caused a significant concentration dependent decrease of fluorescence inside the cell. Hence, one can assume that an activation of sGC and increased levels of cGMP end up in opening of pnx1 (Fig. 25). DT2 was used to investigate the influence of PRKG1 on pnx1. DT2 is an inhibitor of PRKG1. At a concentration of 0.05 mM DT2 caused a significant increase of fluorescence. This result indicates that PRKG1 also plays a role in controlling of pnx1 (Fig. 26). Taken together, these results for the first time provide evidence that eNOS-signaling is involved in the intracellular mechanisms that control pnx1.

4.7 Summary

This work analyzed the role of eNOS/sGC/PRKG1 signaling in mature human RBCs. The presence of an active eNOS within mature human RBCs has been shown before but the functions of eNOS in RBCs are not fully understood.

This work for the first time illustrates the presence of sGC and PRKG1 in mature human RBCs via western blot analyses. Further investigations in this work demonstrate that sGC and PRKG1 are an active part in the eNOS signaling cascade of RBCs. Low levels of shear stress activate eNOS. Subsequently, eNOS, sGC and PRKG1 significantly influence deformability.

Moreover the eNOS/sGC/PRKG1 signaling cascade in mature human RBCs is involved in the regulation of pnx1. The influence of eNOS signaling on pnx1 has never been described before.

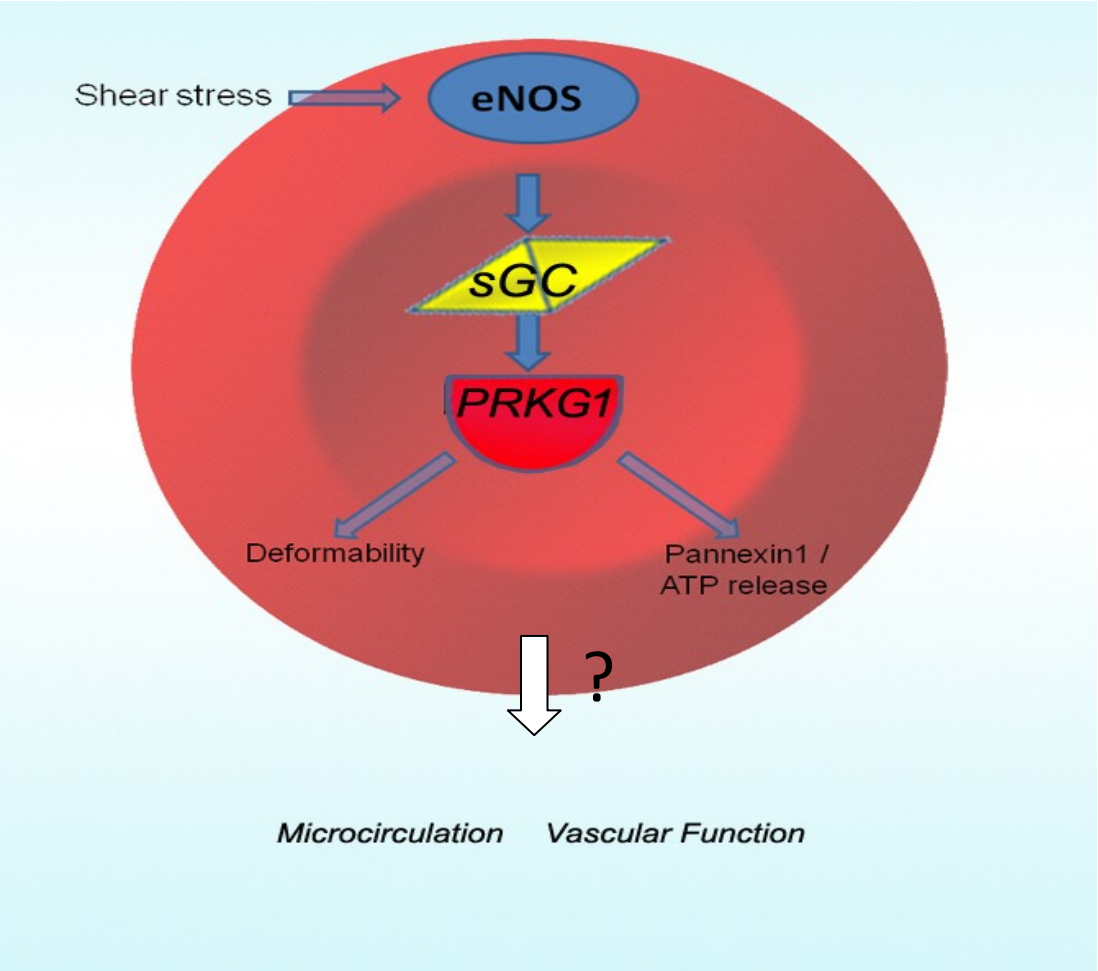

Figure 27: RBCs contain an eNOS/sGC/PRKG1 signaling cascade

The eNOS/ sGC/ PRKG1 signaling cascade in RBCs takes part in the regulation of deformability and ATP release from RBCs. Shear stress is able to induce the activation of RBC-eNOS. Activation of this signaling cascade ends up in improved deformability and increased ATP release. Further investigations need to be performed to analyze the role of eNOS signaling within RBCs with regard to microcirculation and vascular function.

5 Conclusion and outlook

This work provides significant information about the role of NO bioactivity within RBCs. It reveals that a full and functional eNOS/ sGC/ PRKG-signaling cascade can be found in mature, human RBCs. The detection of targets in this regulated signaling cascade may help to develop new strategies in the treatment of impaired deformability and ATP release.

Impaired deformability of RBCs is linked to different diseases such as diabetes, and cardiovascular disease (McMillan et al., 1978, Brown et al., 2005, Keymel et al., 2011, Cortese-Krott et al., 2012b). The investigations performed in this work reveal that eNOS/ sGC/ PRKG1-signaling in RBCs significantly influences deformability. The diameter of capillaries is significantly smaller than the diameter of RBCs. Hence, the proper ability to deform is crucial for the passage through capillaries and maintenance of microcirculation (Parthasarathi and Lipowsky, 1999, Lipowsky et al., 1993; Shiga et al., 1990). The connection between deformability and microcirculation underlines the importance of eNOS/ sGC/ PRKG1-signaling in RBCs.

The influence of eNOS/ sGC/ PRKG1-signaling on pnx1 has never been described before. Flowcytometric analyses reveal those novel findings. Inhibition of eNOS/ sGC/ PRKG1-signaling significantly closes pnx1 channels in RBCs. Activation on the other side opens pnx1 channels in RBCs. Analyses in different tissues may disclose whether eNOS/ sGC/ PRKG1-signaling in general regulates pnx1. Locovei et al. suggested that the role of pnx1 as an ATP gating channel is not restricted to RBCs. Pnx1 can also be found on the surface of endothelial cells in vessels of the heart and skeletal muscles. In those vessels pnx1 might control local blood perfusion (Locovei et al., 2006a).
Impaired ATP release from RBCs can be found in diabetes and primary pulmonary hypertension (Sprague et al., 2001b, Sprague et al., 2006). Similar to impaired deformability, it is uncertain whether impaired ATP release from RBCs is the cause or result of those diseases. However, it seems likely that restored ATP release from RBCs might improve pathological states.

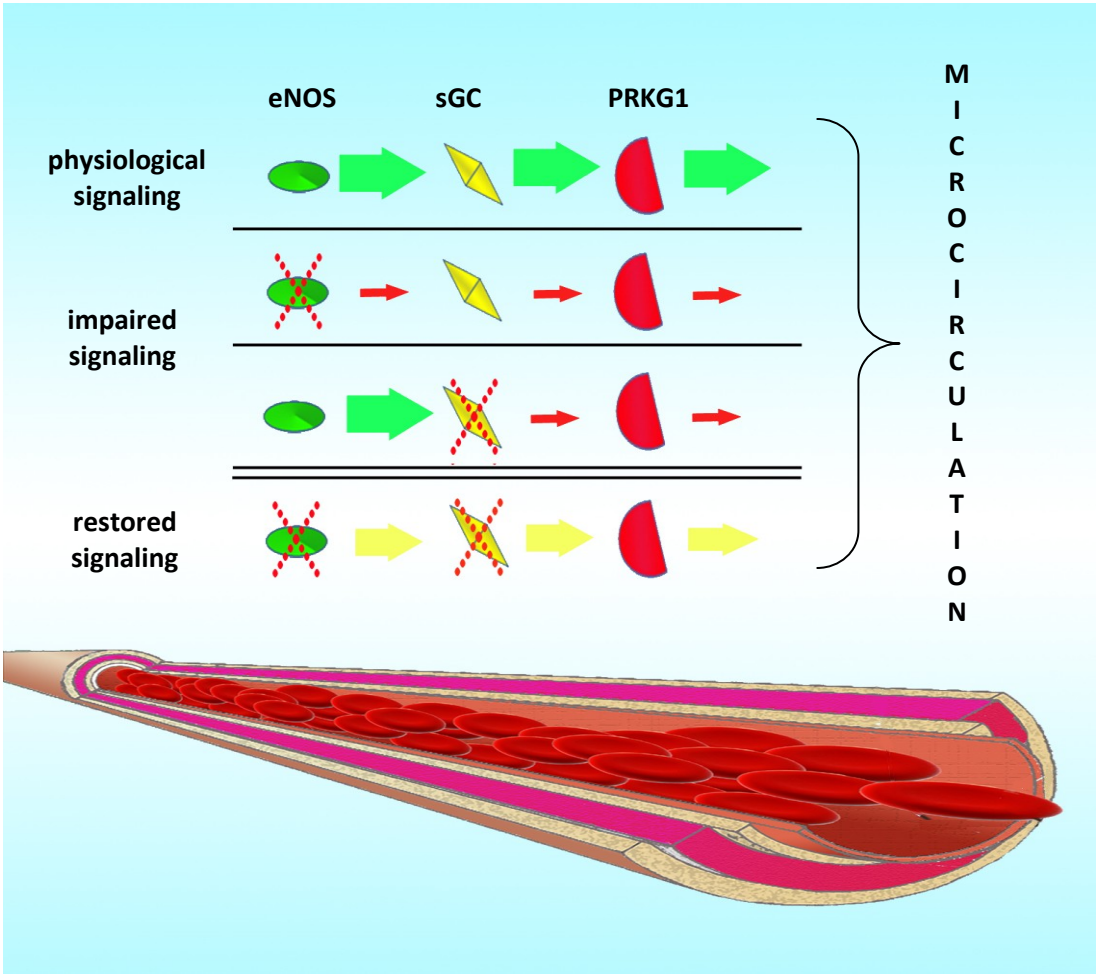

Figure 28: eNOS/ sGC/ PRKG1 signaling cascade as pharmacological target

The image illustrates the eNOS/ sGC/ PRKG1 signaling cascade as a possible pharmacological target, which is able to compensate with an impaired function of eNOS or sGC. Green arrows illustrate the physiological state of the eNOS signaling cascade. Red arrows indicate an impaired signaling cascade due to a malfunctioning eNOS or sGC (marked with a red X). Yellow arrows indicate the pharmacological treatment and restored function of the signaling cascade.

In summary this work provides new evidence for the presence of a feed forward mechanism in RBCs. It includes the activation of eNOS due to shear stress, improved deformability of RBCs and dilation of vessels due to ATP release from RBCs (Ellsworth et al., 1995; Sprague et al., 2003). This feed forward mechanism is modulated by eNOS, sGC and PRKG1 in RBCs. The identification of a signaling cascade, which influences deformability of RBCs as well as ATP release from RBCs, may motivate to develop new strategies in the therapy of impaired microcirculation and vascular function in general (Fig 28).

References

Adderley, S.P., Thuet, K.M., Sridharan, M., Bowles, E.A., Stephenson, A.H., Ellsworth, M.L., Sprague, R.S., 2011. Identification of cytosolic phosphodiesterases in the erythrocyte: a possible role for PDE5. Med. Sci. Monit. Int. Med. J. Exp. Clin. Res. 17, CR241–247.

Alderton, W.K., Cooper, C.E., Knowles, R.G., 2001. Nitric oxide synthases: structure, function and inhibition. Biochem. J. 357, 593–615.

An, X., Guo, X., Sum, H., Morrow, J., Gratzer, W., Mohandas, N., 2004. Phosphatidylserine Binding Sites in Erythroid Spectrin: Location and Implications for Membrane Stability†. Biochemistry (Mosc.) 43, 310–315. doi:10.1021/bi035653h

Arnold, W.P., Mittal, C.K., Katsuki, S., Murad, F., 1977. Nitric oxide activates guanylate cyclase and increases guanosine 3?:5?-cyclic monophosphate levels in various tissue preparations. Proc. Natl. Acad. Sci. U. S. A. 74, 3203–3207.

Ballard, S.A., Gingell, C.J., Tang, K., Turner, L.A., Price, M.E., Naylor, A.M., 1998. Effects of sildenafil on the relaxation of human corpus cavernosum tissue in vitro and on the activities of cyclic nucleotide phosphodiesterase isozymes. J. Urol. 159, 2164–2171.

Bao, L., Locovei, S., Dahl, G., 2004. Pannexin membrane channels are mechanosensitive conduits for ATP. FEBS Lett. 572, 65–68. doi:10.1016/j.febslet.2004.07.009

Barcellini, W., Bianchi, P., Fermo, E., Imperiali, F.G., Marcello, A.P., Vercellati, C., Zaninoni, A., Zanella, A., 2011. Hereditary red cell membrane defects: diagnostic and clinical aspects. Blood Transfus. 9, 274–277. doi:10.2450/2011.0086-10

Baskurt, O.K., Temiz, A., Meiselman, H.J., 1998. Effect of Superoxide Anions on Red Blood Cell Rheologic Properties. Free Radic. Biol. Med. 24, 102–110. doi:10.1016/S0891-5849(97)00169-X

Baskurt, O.K., Ulker, P., Meiselman, H.J., 2011. Nitric oxide, erythrocytes and exercise. Clin. Hemorheol. Microcirc. 49, 175–181. doi:10.3233/CH-2011-1467

Bender, A.T., Beavo, J.A., 2006. Cyclic Nucleotide Phosphodiesterases: Molecular Regulation to Clinical Use. Pharmacol. Rev. 58, 488–520. doi:10.1124/pr.58.3.5

Bergfeld, G.R., Forrester, T., 1992. Release of ATP from human erythrocytes in response to a brief period of hypoxia and hypercapnia. Cardiovasc. Res. 26, 40–47. doi:10.1093/cvr/26.1.40

B, H., M, J., P, K., E, B., B, M., 1992. Ca2+/calmodulin-dependent formation of hydrogen peroxide by brain nitric oxide synthase. [WWW Document]. URL http://www.biochemj.org/bj/281/bj2810627.htm (accessed 6.5.14).

Birk, A.V., Broekman, M.J., Gladek, E.M., Robertson, H.D., Drosopoulos, J.H.F., Marcus, A.J., Szeto, H.H., 2002. Role of extracellular ATP metabolism in regulation of platelet reactivity. J. Lab. Clin. Med. 140, 166–175. doi:10.1067/mlc.2002.126719

Boers, G.H.J., 2000. Mild Hyperhomocysteinemia is an Independent Risk Factor of Arterial Vascular Disease. Semin. Thromb. Hemost. Volume 26, 291–296. doi:10.1055/s-2000-8096

Böhme, E., Graf, H., Schultz, G., 1978. Effects of sodium nitroprusside and other smooth muscle relaxants on cyclic GMP formation in smooth muscle and platelets. Adv. Cyclic Nucleotide Res. 9, 131–143.

Bor-Kucukatay, M., Wenby, R.B., Meiselman, H.J., Baskurt, O.K., 2003. Effects of nitric oxide on red blood cell deformability. Am. J. Physiol. - Heart Circ. Physiol. 284, H1577–H1584. doi:10.1152/ajpheart.00665.2002

Bor-Küçükatay, M., Yalçin, Ö., Gökalp, O., Kipmen-Korgun, D., Yesilkaya, A., Baykal, A., Ispir, M., Senturk, Ü.K., Kaputlu, I., Başkurt, O.K., 2000. Red blood cell rheological alterations in hypertension induced by chronic inhibition of nitric oxide synthesis in rats. Clin. Hemorheol. Microcirc. 22, 267–275.

Bornfeldt, K.E., Raines, E.W., Nakano, T., Graves, L.M., Krebs, E.G., Ross, R., 1994. Insulin-like growth factor-I and platelet-derived growth factor-BB induce directed migration of human arterial smooth muscle cells via signaling pathways that are distinct from those of proliferation. J. Clin. Invest. 93, 1266–1274.

Bradford, M.M., 1976. A rapid and sensitive method for the quantitation of microgram quantities of protein utilizing the principle of protein-dye binding. Anal. Biochem. 72, 248–254.

Braunstein, G.M., Roman, R.M., Clancy, J.P., Kudlow, B.A., Taylor, A.L., Shylonsky, V.G., Jovov, B., Peter, K., Jilling, T., Ismailov, I.I., Benos, D.J., Schwiebert, L.M., Fitz, J.G., Schwiebert, E.M., 2001. Cystic Fibrosis Transmembrane Conductance Regulator Facilitates ATP Release by Stimulating a Separate ATP Release Channel for Autocrine Control of Cell Volume Regulation. J. Biol. Chem. 276, 6621–6630. doi:10.1074/jbc.M005893200

Brown, C.D., Ghali, H.S., Zhao, Z., Thomas, L.L., Friedman, E.A., 2005. Association of reduced red blood cell deformability and diabetic nephropathy. Kidney Int. 67, 295–300. doi:10.1111/j.1523-1755.2005.00082.x

Brüne, B., Schmidt, K.-U., Ullrich, V., 1990. Activation of soluble guanylate cyclase by carbon monoxide and inhibition by superoxide anion. Eur. J. Biochem. 192, 683–688. doi:10.1111/j.1432-1033.1990.tb19276.x

Brüne, B., Ullrich, V., 1987. Inhibition of platelet aggregation by carbon monoxide is mediated by activation of guanylate cyclase. Mol. Pharmacol. 32, 497–504.

Butt, E., Geiger, J., Jarchau, T., Lohmann, S.M., Walter, U., 1993. The cGMP-dependent protein kinase-gene, protein, and function. Neurochem. Res. 18, 27–42. doi:10.1007/BF00966920

Buvinic, S., Briones, R., Huidobro-Toro, J.P., 2002. P2Y1 and P2Y2 receptors are coupled to the NO/cGMP pathway to vasodilate the rat arterial mesenteric bed. Br. J. Pharmacol. 136, 847–856. doi:10.1038/sj.bjp.0704789

Byers, T.J., Branton, D., 1985. Visualization of the protein associations in the erythrocyte membrane skeleton. Proc. Natl. Acad. Sci. 82, 6153–6157.

Chabanel, A., Flamm, M., Sung, K.L., Lee, M.M., Schachter, D., Chien, S., 1983. Influence of cholesterol content on red cell membrane viscoelasticity and fluidity. Biophys. J. 44, 171–176.

Chadjichristos, C.E., Scheckenbach, K.E.L., Veen, T.A.B. van, Sarieddine, M.Z.R., Wit, C. de, Yang, Z., Roth, I., Bacchetta, M., Viswambharan, H., Foglia, B., Dudez, T., Kempen, M.J.A. van, Coenjaerts, F.E.J., Miquerol, L., Deutsch, U., Jongsma, H.J., Chanson, M., Kwak, B.R., 2010. Endothelial-Specific Deletion of Connexin40 Promotes Atherosclerosis by Increasing CD73-Dependent Leukocyte Adhesion. Circulation 121, 123–131. doi:10.1161/CIRCULATIONAHA.109.867176

Chen, C.-H., Walterscheid, J.P., 2006. Plaque Angiogenesis Versus Compensatory Arteriogenesis in Atherosclerosis. Circ. Res. 99, 787–789. doi:10.1161/01.RES.0000247758.34085.a6

Chen, L.Y., Mehta, J.L., 1998. Evidence for the presence of L-arginine-nitric oxide pathway in human red blood cells: relevance in the effects of red blood cells on platelet function. J. Cardiovasc. Pharmacol. 32, 57–61.

Conran, N., Oresco-Santos, C., Acosta, H.C., Fattori, A., Saad, S.T.O., Costa, F.F., 2004. Increased soluble guanylate cyclase activity in the red blood cells of sickle cell patients. Br. J. Haematol. 124, 547–554.

Coquil, J.F., Franks, D.J., Wells, J.N., Dupuis, M., Hamet, P., 1980. Characteristics of a new binding protein distinct from the kinase for guanosine 3':5'-monophosphate in rat platelets. Biochim. Biophys. Acta 631, 148–165.

Corbin, J.D., Turko, I.V., Beasley, A., Francis, S.H., 2000. Phosphorylation of phosphodiesterase-5 by cyclic nucleotide-dependent protein kinase alters its catalytic and allosteric cGMP-binding activities. Eur. J. Biochem. 267, 2760–2767. doi:10.1046/j.1432-1327.2000.01297.x

Cortese-Krott, M.M., Horn, P., Krenz, T., Krisp, C., Sivarajah, S., Lysaja, K., Strigl, F., Kröncke, K.-D., Heiss, C., Kelm, M., 2010. Isolation, Characterization, and Activity of an Endothelilal Nitric Oxide Sythase in Human Red Blood Cells. Free Radic. Biol. Med., SFRBM's 17th Annual Meeting: Program and Abstracts 49, Supplement, S112–S113. doi:10.1016/j.freeradbiomed.2010.10.301

Cortese-Krott, M.M., Rodriguez-Mateos, A., Kuhnle, G.G.C., Brown, G., Feelisch, M., Kelm, M., 2012a. A multilevel analytical approach for detection and visualization of intracellular NO production and nitrosation events using diaminofluoresceins. Free Radic. Biol. Med. 53, 2146–2158. doi:10.1016/j.freeradbiomed.2012.09.008

Cortese-Krott, M.M., Rodriguez-Mateos, A., Sansone, R., Kuhnle, G.G.C., Thasian-Sivarajah, S., Krenz, T., Horn, P., Krisp, C., Wolters, D., Heiß, C., Kröncke, K.-D., Hogg, N., Feelisch, M., Kelm, M., 2012b. Human red blood cells at work: identification and visualization of erythrocytic eNOS activity in health and disease. Blood blood–2012–07–442277. doi:10.1182/blood-2012-07-442277

Dort, H.M.V., Knowles, D.W., Chasis, J.A., Lee, G., Mohandas, N., Low, P.S., 2001. Analysis of Integral Membrane Protein Contributions to the Deformability and Stability of the Human Erythrocyte Membrane. J. Biol. Chem. 276, 46968–46974. doi:10.1074/jbc.M107855200

Ellsworth, M.L., Forrester, T., Ellis, C.G., Dietrich, H.H., 1995. The erythrocyte as a regulator of vascular tone. Am. J. Physiol. 269, H2155–2161.

Evans, E.A., Celle, P.L., 1975. Intrinsic material properties of the erythrocyte membrane indicated by mechanical analysis of deformation. Blood 45, 29–43.

Evans, E., Mohandas, N., Leung, A., 1984. Static and dynamic rigidities of normal and sickle erythrocytes. Major influence of cell hemoglobin concentration. J. Clin. Invest. 73, 477–488. doi:10.1172/JCI111234

Evgenov, O.V., Pacher, P., Schmidt, P.M., Hasko, G., Schmidt, H.H.H.W., Stasch, J.-P., 2006. NO-independent stimulators and activators of soluble guanylate cyclase: discovery and therapeutic potential. Nat. Rev. Drug Discov. 5, 755–768. doi:10.1038/nrd2038

Föller, M., Feil, S., Ghoreschi, K., Koka, S., Gerling, A., Thunemann, M., Hofmann, F., Schuler, B., Vogel, J., Pichler, B., Kasinathan, R.S., Nicolay, J.P., Huber, S.M., Lang, F., Feil, R., 2008. Anemia and splenomegaly in cGKI-deficient mice. Proc. Natl. Acad. Sci. 105, 6771–6776. doi:10.1073/pnas.0708940105

Forsyth, A.M., Wan, J., Owrutsky, P.D., Abkarian, M., Stone, H.A., 2011. Multiscale approach to link red blood cell dynamics, shear viscosity, and ATP release. Proc. Natl. Acad. Sci. U. S. A. 108, 10986–10991. doi:10.1073/pnas.1101315108

Francis, S.H., Bessay, E.P., Kotera, J., Grimes, K.A., Liu, L., Thompson, W.J., Corbin, J.D., 2002. Phosphorylation of Isolated Human Phosphodiesterase-5 Regulatory Domain Induces an Apparent Conformational Change and Increases cGMP Binding Affinity. J. Biol. Chem. 277, 47581–47587. doi:10.1074/jbc.M206088200

Fukushima, Y., Byers, M.G., Watkins, P.C., Winkelmann, J.C., Forget, B.G., Shows, T.B., 1990. Assignment of the gene for β-spectrin (SPTB) to chromosome 14q23→q24.2 by in situ hybridization. Cytogenet. Genome Res. 53, 232–233. doi:10.1159/000132939

Garg, U.C., Hassid, A., 1989. Nitric oxide-generating vasodilators and 8-bromo-cyclic guanosine monophosphate inhibit mitogenesis and proliferation of cultured rat vascular smooth muscle cells. J. Clin. Invest. 83, 1774–1777.

Glagov, S., Weisenberg, E., Zarins, C.K., Stankunavicius, R., Kolettis, G.J., 1987. Compensatory Enlargement of Human Atherosclerotic Coronary Arteries. N. Engl. J. Med. 316, 1371–1375. doi:10.1056/NEJM198705283162204

Goldstein, I., Lue, T.F., Padma-Nathan, H., Rosen, R.C., Steers, W.D., Wicker, P.A., 1998. Oral sildenafil in the treatment of erectile dysfunction. Sildenafil Study Group. N. Engl. J. Med. 338, 1397–1404. doi:10.1056/NEJM199805143382001

Hamet, P., Coquil, J.F., 1978. Cyclic GMP binding and cyclic GMP phosphodiesterase in rat platelets. J. Cyclic Nucleotide Res. 4, 281–290.

Heiss, C., Lauer, T., Dejam, A., Kleinbongard, P., Hamada, S., Rassaf, T., Matern, S., Feelisch, M., Kelm, M., 2006. Plasma Nitroso Compounds Are Decreased in Patients With Endothelial Dysfunction. J. Am. Coll. Cardiol. 47, 573–579. doi:10.1016/j.jacc.2005.06.089

Horn, P., Cortese-Krott, M.M., Amabile, N., Hundsdörfer, C., Kröncke, K.-D., Kelm, M., Heiss, C., 2013. Circulating Microparticles Carry a Functional Endothelial Nitric Oxide Synthase That Is Decreased in Patients With Endothelial Dysfunction. J. Am. Heart Assoc. 2, e003764. doi:10.1161/JAHA.112.003764

Horn, P., Cortese-Krott, M.M., Keymel, S., Kumara, I., Burghoff, S., Schrader, J., Kelm, M., Kleinbongard, P., 2011. Nitric oxide influences red blood cell velocity independently of changes in the vascular tone. Free Radic. Res. 45, 653–661. doi:10.3109/10715762.2011.574288

Huang, Y.-J., Maruyama, Y., Dvoryanchikov, G., Pereira, E., Chaudhari, N., Roper, S.D., 2007. The role of pannexin 1 hemichannels in ATP release and cell–cell communication in mouse taste buds. Proc. Natl. Acad. Sci. 104, 6436–6441. doi:10.1073/pnas.0611280104

Ignarro, L.J., Harbison, R.G., Wood, K.S., Kadowitz, P.J., 1986. Activation of purified soluble guanylate cyclase by endothelium-derived relaxing factor from intrapulmonary artery and vein: stimulation by acetylcholine, bradykinin and arachidonic acid. J. Pharmacol. Exp. Ther. 237, 893–900.

Ignarro, L.J., Wood, K.S., Wolin, M.S., 1982. Activation of purified soluble guanylate cyclase by protoporphyrin IX. Proc. Natl. Acad. Sci. U. S. A. 79, 2870–2873.

Ikuta, T., Ausenda, S., Cappellini, M.D., 2001. Mechanism for fetal globin gene expression: Role of the soluble guanylate cyclase–cGMP-dependent protein kinase pathway. Proc. Natl. Acad. Sci. 98, 1847–1852. doi:10.1073/pnas.98.4.1847

Inaba, M., Maede, Y., 1986. Na,K-ATPase in dog red cells. Immunological identification and maturation-associated degradation by the proteolytic system. J. Biol. Chem. 261, 16099–16105.

Johnson, C.P., Tang, H.-Y., Carag, C., Speicher, D.W., Discher, D.E., 2007. Forced Unfolding of Proteins Within Cells. Science 317, 663–666. doi:10.1126/science.1139857

Joshi, C.N., Martin, D.N., Fox, J.C., Mendelev, N.N., Brown, T.A., Tulis, D.A., 2011. The Soluble Guanylate Cyclase Stimulator BAY 41-2272 Inhibits Vascular Smooth Muscle Growth through the cAMP-Dependent Protein Kinase and cGMP-Dependent Protein Kinase Pathways. J. Pharmacol. Exp. Ther. 339, 394–402. doi:10.1124/jpet.111.183400

Kang, J., Kang, N., Lovatt, D., Torres, A., Zhao, Z., Lin, J., Nedergaard, M., 2008. Cx43 hemichannels are permeable to ATP. J. Neurosci. Off. J. Soc. Neurosci. 28, 4702–4711. doi:10.1523/JNEUROSCI.5048-07.2008

Keymel, S., Heiss, C., Kleinbongard, P., Kelm, M., Lauer, T., 2011. Impaired red blood cell deformability in patients with coronary artery disease and diabetes mellitus. Horm. Metab. Res. Horm. Stoffwechselforschung Horm. Métabolisme 43, 760–765. doi:10.1055/s-0031-1286325

Kleinbongard, P., Schulz, R., Rassaf, T., Lauer, T., Dejam, A., Jax, T., Kumara, I., Gharini, P., Kabanova, S., Ozüyaman, B., Schnürch, H.-G., Gödecke, A., Weber, A.-A., Robenek, M., Robenek, H., Bloch, W., Rösen, P., Kelm, M., 2006. Red blood cells express a functional endothelial nitric oxide synthase. Blood 107, 2943–2951. doi:10.1182/blood-2005-10-3992

Knowles, R.G., Palacios, M., Palmer, R.M., Moncada, S., 1989. Formation of nitric oxide from L-arginine in the central nervous system: a transduction mechanism for stimulation of the soluble guanylate cyclase. Proc. Natl. Acad. Sci. U. S. A. 86, 5159–5162.

Koc, B., Erten, V., Yilmaz, M.I., Sonmez, A., Kocar, I.H., 2003. The relationship between red blood cell Na/K-ATPase activities and diabetic complications in patients with type 2 diabetes mellitus. Endocrine 21, 273–278. doi:10.1385/ENDO:21:3:273

Koeppen, M., Feil, R., Siegl, D., Feil, S., Hofmann, F., Pohl, U., Wit, C. de, 2004. cGMP-Dependent Protein Kinase Mediates NO- but not Acetylcholine-Induced Dilations in Resistance Vessels In Vivo. Hypertension 44, 952–955. doi:10.1161/01.HYP.0000147661.80059.ca

Krenz, T., n.d. Role of eNOS and Nrf2 in the vascular effects of epicatechin.

Kubes, P., Suzuki, M., Granger, D.N., 1991. Nitric oxide: an endogenous modulator of leukocyte adhesion. Proc. Natl. Acad. Sci. 88, 4651–4655.

Lee, J.C., Wong, D.T., Discher, D.E., 1999. Direct measures of large, anisotropic strains in deformation of the erythrocyte cytoskeleton. Biophys. J. 77, 853–864.

Lee, J.H., Li, S., Liu, T., Hsu, S., Kim, C., Woods, V.L., Casteel, D.E., 2011. The amino terminus of cGMP-dependent protein kinase I? increases the dynamics of the protein's cGMP-binding pockets. Int. J. Mass Spectrom. 302, 44–52. doi:10.1016/j.ijms.2010.07.021

Le, K.N., Hwang, C.-W., Tzafriri, A.R., Lovich, M.A., Hayward, A., Edelman, E.R., 2009. Vascular Regeneration by Local Growth Factor Release Is Self-Limited By Microvascular Clearance. Circulation 119, 2928–2935. doi:10.1161/CIRCULATIONAHA.108.823609

Li, D., Laubach, V.E., Johns, R.A., 2001. Upregulation of lung soluble guanylate cyclase during chronic hypoxia is prevented by deletion of eNOS. Am. J. Physiol. - Lung Cell. Mol. Physiol. 281, L369–L376.

Lipowsky, H.H., Cram, L.E., Justice, W., Eppihimer, M.J., 1993. Effect of Erythrocyte Deformability on in Vivo Red Cell Transit Time and Hematocrit and Their Correlation with in Vitro Filterability. Microvasc. Res. 46, 43–64. doi:10.1006/mvre.1993.1034

Lipowsky, H.H., Kovalcheck, S., Zweifach, B.W., 1978. The distribution of blood rheological parameters in the microvasculature of cat mesentery. Circ. Res. 43, 738–749. doi:10.1161/01.RES.43.5.738

Lipowsky, H.H., Usami, S., Chien, S., 1980. In vivo measurements of "apparent viscosity" and microvessel hematocrit in the mesentery of the cat. Microvasc. Res. 19, 297–319. doi:10.1016/0026-2862(80)90050-3

Litvin, O., Tiunova, A., Connell-Alberts, Y., Panchin, Y., Baranova, A., 2006. What is hidden in the pannexin treasure trove: the sneak peek and the guesswork. J. Cell. Mol. Med. 10, 613–634. doi:10.1111/j.1582-4934.2006.tb00424.x

Locovei, S., Bao, L., Dahl, G., 2006a. Pannexin 1 in erythrocytes: Function without a gap. Proc. Natl. Acad. Sci. 103, 7655–7659. doi:10.1073/pnas.0601037103

Locovei, S., Wang, J., Dahl, G., 2006b. Activation of pannexin 1 channels by ATP through P2Y receptors and by cytoplasmic calcium. FEBS Lett. 580, 239–244. doi:10.1016/j.febslet.2005.12.004

Lux, S.E., Tse, W.T., Menninger, J.C., John, K.M., Harris, P., Shalev, O., Chilcote, R.R., Marchesi, S.L., Watkins, P.C., Bennett, V., Mclntosh, S., Collins, F.S., Francke, U., Ward, D.C., Forget, B.G., 1990. Hereditary spherocytosis associated with deletion of human erythrocyte ankyrin gene on chromosome 8. Nature 345, 736–739. doi:10.1038/345736a0

McMillan, D.E., Utterback, N.G., Puma, J.L., 1978. Reduced Erythrocyte Deformability in. Diabetes 27, 895–901. doi:10.2337/diab.27.9.895

Michael Pittilo, R., 2000. Cigarette smoking, endothelial injury and cardiovascular disease. Int. J. Exp. Pathol. 81, 219–230. doi:10.1046/j.1365-2613.2000.00162.x

Mitra, S., Goyal, T., Mehta, J.L., 2011. Oxidized LDL, LOX-1 and Atherosclerosis. Cardiovasc. Drugs Ther. 25, 419–429. doi:10.1007/s10557-011-6341-5

Moncada, S., Palmer, R.M., Higgs, E.A., 1991. Nitric oxide: physiology, pathophysiology, and pharmacology. Pharmacol. Rev. 43, 109–142.

Murakami, J., Maeda, N., Kon, K., Shiga, T., 1986. A contribution of calmodulin to cellular deformability of calcium-loaded human erythrocytes. Biochim. Biophys. Acta BBA - Biomembr. 863, 23–32. doi:10.1016/0005-2736(86)90383-4

Napoli, C., Ignarro, L.J., 2009. Nitric oxide and pathogenic mechanisms involved in the development of vascular diseases. Arch. Pharm. Res. 32, 1103–1108. doi:10.1007/s12272-009-1801-1

Neunteufl, T., Heher, S., Katzenschlager, R., Wölfl, G., Kostner, K., Maurer, G., Weidinger, F., 2000. Late prognostic value of flow-mediated dilation in the brachial artery of patients with chest pain. Am. J. Cardiol. 86, 207–210. doi:10.1016/S0002-9149(00)00857-2

Oonishi, T., Sakashita, K., Uyesaka, N., 1997. Regulation of red blood cell filterability by Ca2+ influx and cAMP-mediated signaling pathways. Am. J. Physiol. - Cell Physiol. 273, C1828–C1834.

O W Griffith, Stuehr, and D.J., 1995. Nitric Oxide Synthases: Properties and Catalytic Mechanism. Annu. Rev. Physiol. 57, 707–734. doi:10.1146/annurev.ph.57.030195.003423

Palmer, R.M.J., Moncada, S., 1989. A novel citrulline-forming enzyme implicated in the formation of nitric oxide by vascular endothelial cells. Biochem. Biophys. Res. Commun. 158, 348–352. doi:10.1016/S0006-291X(89)80219-0

Papaioannou, T.G., Stefanadis, C., 2005. Vascular wall shear stress: basic principles and methods. Hell. J. Cardiol. HJC Hellēnikē Kardiologikē Epitheōrēsē 46, 9–15.

Parthasarathi, K., Lipowsky, H.H., 1999. Capillary recruitment in response to tissue hypoxia and its dependence on red blood cell deformability. Am. J. Physiol. - Heart Circ. Physiol. 277, H2145–H2157.

Pfeifer, A., Klatt, P., Massberg, S., Ny, L., Sausbier, M., Hirneiss, C., Wang, G.X., Korth, M., Aszodi, A., Andersson, K.E., Krombach, F., Mayerhofer, A., Ruth, P., Fassler, R., Hofmann, F., 1998. Defective smooth muscle regulation in cGMP kinase I-deficient mice. EMBO J. 17, 3045–3051. doi:10.1093/emboj/17.11.3045

Prado, C.M., Ramos, S.G., Elias, J., Rossi, M.A., 2008. Turbulent blood flow plays an essential localizing role in the development of atherosclerotic lesions in experimentally induced hypercholesterolaemia in rats. Int. J. Exp. Pathol. 89, 72–80. doi:10.1111/j.1365-2613.2007.00564.x

Rajfer, J., Aronson, W.J., Bush, P.A., Dorey, F.J., Ignarro, L.J., 1992. Nitric oxide as a mediator of relaxation of the corpus cavernosum in response to nonadrenergic, noncholinergic neurotransmission. N. Engl. J. Med. 326, 90–94. doi:10.1056/NEJM199201093260203

Ramos, K.S., Lin, H., McGrath, J.J., 1989. Modulation of cyclic guanosine monophosphate levels in cultured aortic smooth muscle cells by carbon monoxide. Biochem. Pharmacol. 38, 1368–1370. doi:10.1016/0006-2952(89)90347-X

Ransford, G.A., Fregien, N., Qiu, F., Dahl, G., Conner, G.E., Salathe, M., 2009. Pannexin 1 Contributes to ATP Release in Airway Epithelia. Am. J. Respir. Cell Mol. Biol. 41, 525–534. doi:10.1165/rcmb.2008-0367OC

Robertson, B.E., Schubert, R., Hescheler, J., Nelson, M.T., 1993. cGMP-dependent protein kinase activates Ca-activated K channels in cerebral artery smooth muscle cells. Am. J. Physiol. 265, C299–303.

Ross, R., Glomset, J.A., 1973. Atherosclerosis and the arterial smooth muscle cell: Proliferation of smooth muscle is a key event in the genesis of the lesions of atherosclerosis. Science 180, 1332–1339.

Rothe, F., Langnaese, K., Wolf, G., 2005. New aspects of the location of neuronal nitric oxide synthase in the skeletal muscle: A light and electron microscopic study. Nitric Oxide 13, 21–35. doi:10.1016/j.niox.2005.04.008

Roy, B., Mo, E., Vernon, J., Garthwaite, J., 2008. Probing the presence of the ligand-binding haem in cellular nitric oxide receptors. Br. J. Pharmacol. 153, 1495–1504. doi:10.1038/sj.bjp.0707687

Rybalkin, S.D., Rybalkina, I.G., Shimizu-Albergine, M., Tang, X.-B., Beavo, J.A., 2003. PDE5 is converted to an activated state upon cGMP binding to the GAF A domain. EMBO J. 22, 469–478. doi:10.1093/emboj/cdg051

Rybicki, A.C., Heath, R., Lubin, B., Schwartz, R.S., 1988. Human erythrocyte protein 4.1 is a phosphatidylserine binding protein. J. Clin. Invest. 81, 255–260.

Saliez, J., Bouzin, C., Rath, G., Ghisdal, P., Desjardins, F., Rezzani, R., Rodella, L.F., Vriens, J., Nilius, B., Feron, O., Balligand, J.-L., Dessy, C., 2008. Role of Caveolar Compartmentation in Endothelium-Derived Hyperpolarizing Factor–Mediated Relaxation Ca2+ Signals and Gap Junction Function Are Regulated by Caveolin in Endothelial Cells. Circulation 117, 1065–1074. doi:10.1161/CIRCULATIONAHA.107.731679

Salomao, M., Zhang, X., Yang, Y., Lee, S., Hartwig, J.H., Chasis, J.A., Mohandas, N., An, X., 2008. Protein 4.1R-dependent multiprotein complex: New insights into the structural organization of the red blood cell membrane. Proc. Natl. Acad. Sci. U. S. A. 105, 8026–8031. doi:10.1073/pnas.0803225105

Sausbier, M., Schubert, R., Voigt, V., Hirneiss, C., Pfeifer, A., Korth, M., Kleppisch, T., Ruth, P., Hofmann, F., 2000. Mechanisms of NO/cGMP-Dependent Vasorelaxation. Circ. Res. 87, 825–830. doi:10.1161/01.RES.87.9.825

Sawada, K., Echigo, N., Juge, N., Miyaji, T., Otsuka, M., Omote, H., Yamamoto, A., Moriyama, Y., 2008. Identification of a vesicular nucleotide transporter. Proc. Natl. Acad. Sci. 105, 5683–5686. doi:10.1073/pnas.0800141105

Schächinger, V., Britten, M.B., Zeiher, A.M., 2000. Prognostic Impact of Coronary Vasodilator Dysfunction on Adverse Long-Term Outcome of Coronary Heart Disease. Circulation 101, 1899–1906. doi:10.1161/01.CIR.101.16.1899

Schmidt, P., Schramm, M., Schröder, H., Stasch, J.-P., 2003. Mechanisms of nitric oxide independent activation of soluble guanylyl cyclase. Eur. J. Pharmacol. 468, 167–174. doi:10.1016/S0014-2999(03)01674-1

Schultz, K., Schultz, K., Schultz, G., 1977. Sodium nitroprusside and other smooth muscle-relaxants increase cyclic GMP levels in rat ductus deferens. Nature 265, 750–751.

Seigneuret, M., Devaux, P.F., 1984. ATP-dependent asymmetric distribution of spin-labeled phospholipids in the erythrocyte membrane: relation to shape changes. Proc. Natl. Acad. Sci. 81, 3751–3755.

Shiga, T., Maeda, N., Kon, K., 1990. Erythrocyte rheology. Crit. Rev. Oncol. Hematol. 10, 9–48. doi:10.1016/1040-8428(90)90020-S

Shimizu-Albergine, M., Rybalkin, S.D., Rybalkina, I.G., Feil, R., Wolfsgruber, W., Hofmann, F., Beavo, J.A., 2003. Individual Cerebellar Purkinje Cells Express Different cGMP Phosphodiesterases (PDEs): In Vivo Phosphorylation of cGMP-Specific PDE (PDE5) as an Indicator of cGMP-dependent protein kinase (PKG) Activation. J. Neurosci. 23, 6452–6459.

Siedlar, M., Mytar, B., Krzeszowiak, A., Baran, J., Hyszko, M., Ruggiero, I., Wieckiewicz, J., Stachura, J., Zembala, M., 1999. Demonstration of iNOS-mRNA and iNOS in human monocytes stimulated with cancer cells in vitro. J. Leukoc. Biol. 65, 597–604.

Sowers, J.R., Epstein, M., Frohlich, E.D., 2001. Diabetes, Hypertension, and Cardiovascular Disease An Update. Hypertension 37, 1053–1059. doi:10.1161/01.HYP.37.4.1053

Sprague, R., Bowles, E., Stumpf, M., Ricketts, G., Freidman, A., Hou, W.-H., Stephenson, A., Lonigro, A., 2005. Rabbit erythrocytes possess adenylyl cyclase type II that is activated by the heterotrimeric G proteins Gs and Gi. Pharmacol. Rep. PR 57 Suppl, 222–228.

Sprague, R.S., Bowles, E.A., Hanson, M.S., Dufaux, E.A., Sridharan, M., Adderley, S., Ellsworth, M.L., Stephenson, A.H., 2008. Prostacyclin Analogs Stimulate Receptor-Mediated cAMP Synthesis and ATP Release from Rabbit and Human Erythrocytes. Microcirculation 15, 461–471. doi:10.1080/10739680701833804

Sprague, R.S., Ellsworth, M.L., Stephenson, A.H., Kleinhenz, M.E., Lonigro, A.J., 1998. Deformation-induced ATP release from red blood cells requires CFTR activity. Am. J. Physiol. - Heart Circ. Physiol. 275, H1726–H1732.

Sprague, R.S., Ellsworth, M.L., Stephenson, A.H., Lonigro, A.J., 2001a. Participation of cAMP in a signal-transduction pathway relating erythrocyte deformation to ATP release. Am. J. Physiol. - Cell Physiol. 281, C1158–C1164.

Sprague, R.S., Olearczyk, J.J., Spence, D.M., Stephenson, A.H., Sprung, R.W., Lonigro, A.J., 2003. Extracellular ATP signaling in the rabbit lung: erythrocytes as determinants of vascular resistance. Am. J. Physiol. - Heart Circ. Physiol. 285, H693–H700. doi:10.1152/ajpheart.01026.2002

Sprague, R.S., Stephenson, A.H., Bowles, E.A., Stumpf, M.S., Lonigro, A.J., 2006. Reduced Expression of Gi in Erythrocytes of Humans With Type 2 Diabetes Is Associated With Impairment of Both cAMP Generation and ATP Release. Diabetes 55, 3588–3593. doi:10.2337/db06-0555

Sprague, R.S., Stephenson, A.H., Ellsworth, M.L., Keller, C., Lonigro, A.J., 2001b. Impaired Release of ATP from Red Blood Cells of Humans with Primary Pulmonary Hypertension. Exp. Biol. Med. 226, 434–439.

Springer, T., Cybulsky, M., 1995. Traffic signals on endothelium for leukocytes in health, inflammation, and atherosclerosis., in: Arteriosclerosis and Coronary Artery Disease, 29. Philadelphia: Lippincott-Raven, pp. 511–537.

Sridharan, M., Adderley, S.P., Bowles, E.A., Egan, T.M., Stephenson, A.H., Ellsworth, M.L., Sprague, R.S., 2010. Pannexin 1 is the conduit for low oxygen tension-induced ATP release from human erythrocytes. Am. J. Physiol. Heart Circ. Physiol. 299, H1146–1152. doi:10.1152/ajpheart.00301.2010

Stasch, J.-P., Alonso-Alija, C., Apeler, H., Dembowsky, K., Feurer, A., Minuth, T., Perzborn, E., Schramm, M., Straub, A., 2002. Pharmacological actions of a novel NO-independent guanylyl cyclase stimulator, BAY 41-8543: in vitro studies. Br. J. Pharmacol. 135, 333–343. doi:10.1038/sj.bjp.0704484

Stasch, J.-P., Pacher, P., Evgenov, O.V., 2011. Soluble Guanylate Cyclase as an Emerging Therapeutic Target in Cardiopulmonary Disease. Circulation 123, 2263–2273. doi:10.1161/CIRCULATIONAHA.110.981738

Stengelin, M.K., Hoffman, J.F., 1997. Na,K-ATPase subunit isoforms in human reticulocytes: Evidence from reverse transcription-PCR for the presence of ?1, ?3, ?2, ?3, and ? Proc. Natl. Acad. Sci. U. S. A. 94, 5943–5948.

Tamura, N., Itoh, H., Ogawa, Y., Nakagawa, O., Harada, M., Chun, T.-H., Suga, S., Yoshimasa, T., Nakao, K., 1996. cDNA Cloning and Gene Expression of Human Type Iα cGMP-Dependent Protein Kinase. Hypertension 27, 552–557. doi:10.1161/01.HYP.27.3.552

Taraschi, T.F., O'Donnell, M., Martinez, S., Schneider, T., Trelka, D., Fowler, V.M., Tilley, L., Moriyama, Y., 2003. Generation of an erythrocyte vesicle transport system by Plasmodium falciparum malaria parasites. Blood 102, 3420–3426. doi:10.1182/blood-2003-05-1448

Tsuda, K., Iwahashi, H., Minatogawa, Y., Nishio, I., Kido, R., Masuyama, Y., 1987. Electron spin resonance studies of erythrocytes from spontaneously hypertensive rats and humans with essential hypertension. Hypertension 9, III19. doi:10.1161/01.HYP.9.6_Pt_2.III19

Tsuda, K., Kimura, K., Nishio, I., Masuyama, Y., 2000. Nitric Oxide Improves Membrane Fluidity of Erythrocytes in Essential Hypertension: An Electron Paramagnetic Resonance Investigation. Biochem. Biophys. Res. Commun. 275, 946–954. doi:10.1006/bbrc.2000.3408

Tsuda, K., Kinoshita, Y., Nishio, I., Masuyama, Y., 2000. Role of insulin in the regulation of membrane fluidity of erythrocytes in essential hypertension: an electron paramagnetic resonance investigation. Am. J. Hypertens. 13, 376–382.

Ulker, P., Yaras, N., Yalcin, O., Celik-Ozenci, C., Johnson, P.C., Meiselman, H.J., Baskurt, O.K., 2011. Shear stress activation of nitric oxide synthase and increased nitric oxide levels in human red blood cells. Nitric Oxide Biol. Chem. Off. J. Nitric Oxide Soc. 24, 184–191. doi:10.1016/j.niox.2011.03.003

Vasquez-Vivar, J., Kalyanaraman, B., Martasek, P., Hogg, N., Masters, B.S.S., Karoui, H., Tordo, P., Pritchard, K.A., 1998. Superoxide generation by endothelial nitric oxide synthase: The influence of cofactors. Proc. Natl. Acad. Sci. U. S. A. 95, 9220–9225.

Vennemann, P., Lindken, R., Westerweel, J., 2007. In vivo whole-field blood velocity measurement techniques. Exp. Fluids 42, 495–511. doi:10.1007/s00348-007-0276-4

Weimann, J., Ullrich, R., Hromi, J., Fujino, Y., Clark, M.W., Bloch, K.D., Zapol, W.M., 2000. Sildenafil is a pulmonary vasodilator in awake lambs with acute pulmonary hypertension. Anesthesiology 92, 1702–1712.

WHO | Global status report on noncommunicable diseases 2010 [WWW Document], n.d. . WHO. URL http://www.who.int/nmh/publications/ncd_report2010/en/ (accessed 3.4.14).

WHO | Global status report on noncommunicable diseases 2014 [WWW Document], n.d. . WHO. URL http://www.who.int/nmh/publications/ncd-status-report-2014/en/ (accessed 10.27.15).

Wierzbicki, A.S., 2007. Homocysteine and cardiovascular disease: a review of the evidence. Diab. Vasc. Dis. Res. 4, 143–149. doi:10.3132/dvdr.2007.033

Winger, J.A., Marletta, M.A., 2005. Expression and characterization of the catalytic domains of soluble guanylate cyclase: interaction with the heme domain. Biochemistry (Mosc.) 44, 4083–4090. doi:10.1021/bi047601d

Wooldridge, A.A., MacDonald, J.A., Erdodi, F., Ma, C., Borman, M.A., Hartshorne, D.J., Haystead, T.A.J., 2004. Smooth Muscle Phosphatase Is Regulated in Vivo by Exclusion of Phosphorylation of Threonine 696 of MYPT1 by Phosphorylation of Serine 695 in Response to Cyclic Nucleotides. J. Biol. Chem. 279, 34496–34504. doi:10.1074/jbc.M405957200

Zabel, U., Weeger, M., La, M., Schmidt, H.H., 1998. Human soluble guanylate cyclase: functional expression and revised isoenzyme family. Biochem. J. 335, 51–57.

Acknowledgments

In 2011 I started this work in order to learn about scientific research and contribute to new scientific findings. Retrospective this work is the result of years of interesting, challenging and sometimes hard scientific work that was performed next to my medical studies. It never would have been possible without the help and support of persons I would like to thank.

First I would like to thank Prof. Dr. med. Malte Kelm, director of the Department of Cardiology, Pneumology and Angiology, for the opportunity to work in a great environment for basic and translational research.

A special thank is dedicated to PD Dr. rer. nat. Miriam M. Cortese-Krott for the supervision during my time in the laboratory. She gave me great insight into the field of basic research that medical students usually don't deal with. She supported me in the establishment of new methods and taught me how to deal with success and disappointment in the laboratory work. I want to thank her for interesting discussions that often led to new ideas and thoughts what could be done next. Finally I thank her for reviewing this dissertation and for the help in preparation of the final examination.

I honestly thank all the members of the cardiology lab. This team made it easy to find and spend "free time" in the laboratory, which is a rare good in the life of a medical student. In particular I would like to thank Sivatharsini Thasian-Sivarajah. In her calm way she helped me with words and deeds throughout my entire laboratory time. I would like to thank her for culturing and preparation of cells that were essential for my experiments and for all the discussions we had in order to optimize different experiments. Without her help this dissertation would hardly have been possible.

Finally I want to thank my wife, my family and my friends. They always supported me and believed in me on the long run to my medical studies and this dissertation.

Eidesstattliche Versicherung

Ich versichere an Eides statt, dass die Dissertation selbständig und ohne unzulässige fremde Hilfe erstellt worden ist und die hier vorgelegte Dissertation nicht von einer anderen medizinischen Fakultät abgelehnt worden ist.